THE EXPERIMENTAL DETERMINATION OF DIELECTRIC PROPERTIES AT FREQUENCIES BETWEEN 50 c/s AND 5000 Mc/s

F. C. DE VOS

THE EXPERIMENTAL DETERMINATION OF DIELECTRIC PROPERTIES AT FREQUENCIES BETWEEN 50 c/s AND 5000 Mc/s

Bijlage academisch proefschrift
F.C.de Vos Leiden 1958

29/1'58

STELLINGEN

1

Het door Halverstadt en Kumler, door Kwestroo en door Cohen-Fernandes experimenteel gevonden verschil tussen de waarden van de diëlectrische constante van een oplosmiddel, verkregen enerzijds door rechtstreekse meting en anderzijds door extrapolatie naar concentratie nul van metingen aan verdunde oplossingen, is te wijten aan tekortkomingen van de gebruikte meetmethode.

I. F. Halverstadt and W.D. Kumler J.A.C.S. 64. 2988.(1942)
W. Kwestroo, Proefschrift Leiden 1954
P. Cohen-Fernandes, Proefschrift Leiden 1957
Dit proefschrift, hoofdstuk III, pag. 101.

2

De door Mecke en Rosswog voorgestelde constructie van een meetcel voor diëlectrische metingen aan vloeistoffen, waarbij met één ijkvloeistof zou kunnen worden volstaan, is aan bedenkingen onderhevig.

R. Mecke und K. Rosswog, Arch. für techn. Messen:
ATM-blatt, V, 942-5, Aug. 1955
V, 942-6, Oct. 1955.

3

Zowel op grond van theoretische overwegingen, als op grond van experimentele gegevens, blijkt het door Reynolds gevonden lineaire verband tussen de resonantie-frequentie van een „re-entrant cavity" en de capaciteit van een over een deel der trilholte aangebrachte variabele condensator, onjuist te zijn.

S. J. Reynolds, Gen. El. Rev., 50. 34. (1947)
Dit proefschrift, hoofdstuk II. F, pag. 83.

4

De door Lynch gepubliceerde methode, voor de bepaling van de diëlectrische eigenschappen van vaste stoffen, is alleen toepasbaar op materialen met zeer geringe verliezen.

A. C. Lynch, Proc. I. E. E., 104. B. 359. (1957).

5

Het is te verwachten, dat, door gebruik te maken van permanente magneten, bij het onderzoek van kernmagnetische resonantiespectra minstens even goede resultaten kunnen worden bereikt, als thans verkregen worden met gestabiliseerde electromagneten. De permanente magneten zullen dan echter voorzien moeten worden van extra Helmholtz-spoelen, teneinde een kleine verandering in de veldsterkte van het permanente magnetische veld mogelijk te maken.

6

De door Poley gegeven verklaring voor het experimenteel gevonden verschil tussen ε_∞ en n^2_∞ bij mono-gesubstitueerde benzeen derivaten is aanvechtbaar. Een keuze tussen de verschillende mogelijke verklaringen kan wellicht gemaakt worden op grond van metingen van de temperatuur-afhankelijkheid van het gevonden verschil.

J. Ph. Poley, J. Chem. Phys., 23. 405. (1955)
J. Ph. Poley, Proefschrift Delft 1955.

7

De door Kirson voorgestelde interpretatie van het absorptiespectrum van het koper-tetraethyleenpentamine-complex is, in verband met het resultaat van de onderzoekingen van Bjerrum, Ballhausen en Jørgensen aan koper-ammoniak-complexen, zeer onwaarschijnlijk.

B. Kirson, Bull. Soc. Chim. France, p. 1178. (1957)
J. Bjerrum e.a. Acta Chem. Scand. 8. 1275. (1954).

8

De argumenten, welke door Smith worden aangevoerd ter verklaring van de door hem gevonden intra-moleculaire cyclisering van glycyl-dl-prolyl-glycine, zijn aan bedenkingen onderhevig.

P. W. G. Smith, J. Chem. Soc., p. 3985 (1957).

9

Ten onrechte veronderstelt Sinclair een verband tussen een tekort aan essentiele vetzuren in de voeding en athero-sclerose.

H. M. Sinclair, Lancet 270. 381. (1956).

10

Het verdient aanbeveling aan artikel 30. 5. van het wedstrijdreglement der „International Yacht Racing Union" een nadere precisering van de term „proper way" toe te voegen. De in 1950 vastgestelde algemene definitie van deze term, in artikel 27. 6., blijkt speciaal in verband met artikel 30.5. tot moeilijkheden aanleiding te geven.

International Yacht Racing Union; Racing rules.
G. Sambrooke Sturgess: Yacht Racing, Iliffe 1955.

THE EXPERIMENTAL DETERMINATION OF DIELECTRIC PROPERTIES AT FREQUENCIES BETWEEN 50 c/s AND 5000 Mc/s

PROEFSCHRIFT

TER VERKRIJGING VAN DE GRAAD VAN DOCTOR IN DE WIS- EN NATUURKUNDE AAN DE RIJKSUNIVERSITEIT TE LEIDEN, OP GEZAG VAN DE RECTOR MAGNIFICUS DR. S. E. DE JONGH, HOOGLERAAR IN DE FACULTEIT DER GENEESKUNDE, TEGEN DE BEDENKINGEN VAN DE FACULTEIT DER WIS- EN NATUURKUNDE TE VERDEDIGEN OP WOENSDAG 29 JANUARI 1958 TE 16 UUR

DOOR

FRANSISCUS CORNELIS DE VOS

GEBOREN TE 'S-GRAVENHAGE IN 1924

UITGEVERIJ EXCELSIOR - ORANJEPLEIN 96 - 'S-GRAVENHAGE

Promotor: Prof.Dr. C.J.F.Böttcher

CONTENTS

LIST OF SYMBOLS

B	susceptance, equals ωC.
C	capacitance.
C_o	capacity in vacuo or cellconstant of measuringcell.
C_{xs}	unknown capacitance, as series equivalent.
C_{xp}	unknown capacitance, as parallel equivalent.
c	velocity of light.
D	loss-tangent (= tan δ).
f	frequency.
G	Conductance.
i	electric current.
j	$\sqrt{-1}$.
L	inductance.
n_D	refractive index, for sodium D line.
n_∞	extrapolated refractive index, related to total polarisability.
r	reflection-coefficient.
R	resistance.
S	voltage standing wave ratio, E_{max}/E_{min}
s	inverse vswr, E_{min}/E_{max}.
x_o	distance between sample and first min. in standingwave pattern.
Y	admittance.
Z	impedance.
γ	complex propagation factor, equals $\alpha + j\beta$.
δ	loss angle.
$\hat{\varepsilon}$	complex permittivity, relative to vacuum.
ε_o	relative permittivity of dry air.
ε_s	relative permittivity at zero frequency.
ε_∞	relative permittivity at infinite frequency.
λ	wavelength.
μ	permanent dipolemoment.
τ	relaxation time.
t	time.
ω	circular frequency.

INTRODUCTION

In chemistry, physics and technology, there is an increasing demand for experimental methods suitable for the accurate determination of the dielectric properties of matter at various frequencies. The frequencies of interest may range from the lowest radio frequencies up to the highest frequencies attainable. A separation must be made between the so-called optical measurements, up to wavelengths of about 0.1 mm in the far infra-red, and the so-called dielectric measurements, down to a wavelength of a few millimetres. In the wavelength-range around these limits entirely different sources of radiation are used. The radiation sources used in the far infra-red, e.g. heated strips of metal, give a rapid decrease of radiated power with increasing wavelength. For the sources used in the micro wave region, e.g. klystrons or magnetrons, a marked decrease of radiated power with decreasing wavelength is found. A remarkable minimum in the radiated power of the various sources occurs in the intermediate range from about 0.1 - 1 millimetres, which therefore is hardly accessible for measurements.
Also in this thesis the use of the term "dielectric measurements", as mentioned above, will be restricted to wavelengths larger than 1 mm.

In physics dielectric measurements are of interest in relation to the general theory of dielectrics. In molecular physics the study of dielectric phenomena may contribute, in combination with other methods, to the knowledge of the charge distribution in molecules and of the molecular interactions. As far as dielectric relaxation is concerned, the great importance of the study of dielectrics for the general theory of relaxation phenomena must be recalled. It is an important example of linear relaxational behaviour [1], with the additional characteristic that a wide frequency range can be covered in the measurements. Better than several other relaxation phenomena it enables a molecular interpretation.

A chemist may be interested in the relation between dielectric phenomena and chemical constitution and behaviour. Though dipole moment determinations will not reveal the structure of a molecule as such, the results are sometimes decisive in the choice between several possible isomers. Dielectric measurements are also useful in relation to the study of adsorption and cohesion phenomena.

In technology the determination of the dielectric properties of materials is of paramount importance for the development of new insulating materials and the testing of materials for various applications. Furthermore in some cases convenient moisture determinations can be based on dielectric measurements [40-43].

The first dielectric measurements, though of rather limited accuracy, were published in the last decades of the nineteenth century. They were mainly carried out at audiofrequencies. By that time the formulae for the capacitance-values of capacitors of different shape were already known with considerable accuracy [2, 3]. Owing to the impurity of the materials and the difficulty to fill a capacitor completely with the material under investigation, the accuracy of the dielectric measurements was considerably inferior to that of the capacity measurements, particularly in the case of solids [4, 10]. Even today high accuracy is only obtainable for liquids or, with extreme precautions, for solids that can be introduced into a capacitor in the molten state and then be solidified [11].

Special mention must be made of the measurements carried out by Drude [12] in 1897. He succeeded in measuring the dielectric constants of a great number of liquids at a frequency of about 400 Mc/s with errors amounting to a few per cents. Investigating the dielectric properties of alcohols he also gave experimental evidence for the dispersion (frequency dependence) of the real part of the permittivity.

Around 1919 a number of measurements on the dielectric dispersion of water and ethyl alcohol were carried out by Möbius [13], with very primitive but ingenious means, at wavelengths between 7 and 35 millimetres. Up to 1929 no reliable measurements of the dielectric constant of liquids were known. In that year the first determination of the dielectric constant of a highly purified material with modern precision, with the object of providing a standard value, was published by Hartshorn and Oliver [14] on benzene.

After 1925 many experimental methods were devised for the determination of permanent dipole moments from measurements on liquids and gases, on the basis of an equation published by Debye [15] in 1912. On account of the limited accuracy of various measuring results and the theoretical complications, the interest in the dipole moment determinations gradually subdued, though many interesting results were obtained e. g. by Smith [16], Errera [17] and Sutton [18].

The first universal method for dielectric measurements with reasonable accuracy up to 100 Mc/s is the reactance variation method, now generally known as Hartshorn-Ward method [19] and published by these authors in 1936.

The enormous advances in measuring techniques after 1945, particularly at high frequencies, are mainly due to the development of electronic apparatus for various purposes in the war years. This development, partly necessitated by immediate need for insulating materials at very high frequencies, did not only provide new approaches for the determination of dielectric properties of materials, but also made the necessary instruments, such as high frequency generators and detectors, currently available in later years.

In the present thesis an account is given of work carried out

in the period of 1949-1957, aiming at the construction of a complete set of instruments suitable for dielectric measurements in a frequency range between audio frequencies and the highest radio frequencies. This wide frequency range was considered to be necessary for a general study of dielectric phenomena, since measurements carried out over a limited frequency range, even in combination with a wide temperature range, can only be expected to give incomplete information about the molecular mechanisms, responsible for the dielectric behaviour.

To this end experimental methods were devised in our laboratory for measurements in a frequency range between 50 c/s and 30 000 MC/s with the possibility of varying the temperature over a limited range.

The measuring equipment and measuring cells, for frequencies between 50 c/s and 5000 Mc/s will be described in this thesis. In chapter I a survey will be given of the relationships between the instrumental and theoretical quantities involved and the precision required for the measurements.

The experimental methods will be described in chapter II, which also deals with the preliminary measurements carried out as a check on the accuracy obtainable in the various frequency ranges. Measurements were carried out for the selection of compounds suitable for the calibration of measuring cells, considering the purification, the influence of impurities on the results and the stability of the permittivity values over prolonged periods. In the development of measuring cells a number of measurements were necessary for the determination of the variation of the cell constants with the permittivity of the liquid under investigation. During and after the calibrations of the instruments many measurements were carried out as a check on the consistancy of the results obtained on the same material over the whole frequency range.

Moreover, as an example of the results obtainable with these instruments, some measurements of the complex permittivity and relaxation time of pure liquids and solutions are presented in chapter III and a comparison is made with the data obtained by other investigators.

Chapter I

RELATIONS BETWEEN THE INSTRUMENTAL AND THEORETICAL QUANTITIES

For the description of the dielectric properties of materials the term "specific inductive capacity" was introduced by Faraday and defined as the ratio of the capacitance of a capacitor filled with material and the capacitance of the empty capacitor.

This definition soon turned out to be insufficiently precise. A completely empty capacitor, though never realised in practice, has a fixed capacity value; in a capacitor filled with material, however, changes in capacitance occur with the duration of charge and discharge. Hence, in the case of alternating electric fields, the capacitance changes with the variation of the frequency. More precisely the property defined by the capacity-ratio must therefore be defined with respect to steady state sinusoïdal voltage and be recognised as variable with frequency. For this reason, in the description of dielectric properties, the term "permittivity" is to be preferred to the terms "specific inductive capacity" or "dielectric constant".

The permittivity introduced above and related to the energy storage in a material, is always associated with a second specific property which determines the energy dissipation in the material and is therefore closely related to conductivity. This dissipation may be described in terms of a phase difference between the applied electric field E and the dielectric displacement D. Thus the dielectric behaviour of matter requires for its precise representation a complex permittivity $\hat{\varepsilon} = \varepsilon' - j\,\varepsilon''$, where ε' is the real permittivity given by the capacity ratio defined above and ε'' is the loss factor. For a more complete definition of the complex permittivity we can refer to the textbooks on dielectrics [20, 21, 22]. In this thesis $\hat{\varepsilon}$, ε' and ε'' refer to the values of the complex permittivity relative to vacuum.

If dissipation in the material, due to the migration of charge-carriers is left out of account the dielectric loss may be considered to be due to a relaxation effect. In its simplest form this relaxation effect can be described in terms of a dispersion or loss curve characterised by one "relaxation time" τ. By dividing the total polarisation of the material into two parts:

$$P = P_{\infty} + (P_s)_{dip},$$

where $(P_s)_{dip}$ is the part of P due to the permanent dipoles and P_{∞} is the part due to the electronic and atomic polarisability of

the particles, the following relation between the dielectric displacement and an applied field $\hat{E} = E_o e^{j\omega t}$, may be derived [20]:

$$\hat{D} = \hat{E} + 4\pi\hat{P} = \left[\varepsilon_\infty + \frac{\varepsilon_s - \varepsilon_\infty}{1 + j\omega\tau}\right] E_o e^{j\omega t}, \qquad (I.1)$$

where ε_s is the static permittivity, ε_∞ is the permittivity at infinite frequency and τ is the relaxation time. Thus the complex permittivity, defined as the ratio of $\hat{D}$ and $\hat{E}$ is given by:

$$\varepsilon' - j\,\varepsilon'' = \varepsilon_\infty + \frac{\varepsilon_s - \varepsilon_\infty}{1 + j\omega\tau} \qquad (I.2)$$

or

$$\varepsilon' = \varepsilon_\infty + \frac{\varepsilon_s - \varepsilon_\infty}{1 + \omega^2\tau^2} \qquad \varepsilon'' = (\varepsilon_s - \varepsilon_\infty)\frac{\omega t}{1 + \omega^2\tau^2} \qquad (I.3)$$

By plotting $\frac{\varepsilon' - \varepsilon_\infty}{\varepsilon_s - \varepsilon_\infty}$ and $\frac{\varepsilon''}{\varepsilon_s - \varepsilon_\infty}$ against $\log\omega\tau$ the well known symmetrical dispersion curves are obtained. The circular frequency $\omega_{max} = \frac{1}{\tau}$, at which the maximum in the curve for ε'', with a value $(\varepsilon'')_{max} = \frac{\varepsilon_s - \varepsilon_\infty}{2}$, occurs is generally called the "critical frequency".

The experimental results satisfy these equations only in the case of one macroscopic relaxation time. Deviations are due to the fact that the behaviour of a dielectric cannot always be described in terms of only one relaxation time. Whether the experimental data satisfy the equations for one relaxation time can be checked by determining the experimental values of ε_s, ε_∞ and ω_{max} and examining whether the measured values of ε' and ε'' are in accordance with the ideal dispersion curves based on the values of ε_s, ε_∞ and $\tau = \frac{1}{\omega_{max}}$.

Two other methods of checking the experimental results with the equations (I.3) were proposed by Cole [23, 24]. First the equations (I.3) may be written in the form:

$$\left(\varepsilon' - \frac{\varepsilon_s + \varepsilon_\infty}{2}\right)^2 + (\varepsilon'')^2 = \left(\frac{\varepsilon_s - \varepsilon_\infty}{2}\right)^2 \qquad (I.4)$$

Thus the well known Cole-Cole plot, a semicircle with radius $\frac{\varepsilon_s - \varepsilon_\infty}{2}$, is obtained by plotting ε'' vs. ε', the centre of the circle being on the abscissa at a distance $\frac{\varepsilon_s + \varepsilon_\infty}{2}$ from the origin.
The equations (I.3) may also be rewritten in the form:

$$\varepsilon' = -\omega\varepsilon''\tau + \varepsilon_s \qquad (I.5)$$

In this way a linear plot of ε' vs. $\omega\varepsilon''$ is obtained, its slope being equal to the relaxation time τ.

Both methods are convenient for the presentation of experimental data, on systems with one relaxation time. Owing to a distribution of relaxation times the dispersion curves are often flatter and extend over a wider frequency range, with a resulting lower value for $(\varepsilon'')_{max}$, than is predicted by the above equations. For the corresponding ε', ε'' curve Cole and Cole [23] showed that the experimental curve is still an almost circular arc, but with its centre lying under the abscissa. Since no satisfactory general theory has been given for the dependence of ε' and ε'' on the frequency, nor for the distribution function of the relaxation times, several authors approached the problem from the semi-empirical side [23, 25, 27].

It seems a disadvantage that in the plots, presented by the equations (I. 4) and (I. 5), one important experimental datum, viz. the frequency dependence of ε' and ε'', does not appear in a simply predictable way. This does not mean however that they contain less information than any other set of curves based on the same equations, but renders it advisable to investigate further possibilities for the graphical interpretation of relaxation data, which in addition leave more scope for the description of the distribution of relaxation times, like the one proposed by Gorter et al. [26] for the analysis of paramagnetic relaxation data.

The study of dielectric absorption in liquids also allows the determination of dipole moments in the liquid without the necessity of making approximations regarding the value of the atomic- and electronic-polarisation, as is required in the determination of dipole moments from low frequency measurements with the Debye- [15] or Onsager-Böttcher [20] equations. Since these equations have been extensively dealt with by Böttcher [20], they will be cited as such:

For a dilute solution of a polar compound in a non polar solvent the Debye equation reads:

$$\frac{\varepsilon-1}{\varepsilon+2} = \frac{4}{3}\pi\left[N_0\alpha_0 + N_1\left(\alpha_1 + \frac{\mu^2}{3kT}\right)\right] \qquad (I.6)$$

where α_0 is the polarisability of the solvent molecule and α_1 and μ are the polarisability and the permanent dipole moment of the solute respectively.

Various procedures for the determination of dipole moments from measurements on dilute solutions, by extrapolation to infinite dilution, are based on this equation [28-31].

While the approximations used in the derivation of the Debye equation may be considered of minor consequence for very dilute solutions, the use of this equation introduces considerable deviations for pure dipole liquids. The Onsager-Böttcher equation, resulting from the consideration of the difference between the reaction field of the dipoles and their directing field, reads for a solution:

$$\frac{(\varepsilon_s - 1)(2\varepsilon_s + 1)}{12\pi\varepsilon_s} = N_0\frac{\alpha_0}{1-f_0\alpha_0} + N_1\frac{\alpha_1}{1-f_1\alpha_1} + N_1\frac{\mu^2}{3kT(1-f_1\alpha_1)^2} \qquad (I.7)$$

where the suffices 0 and 1 refer to the solvent and the solute respectively and f is given by the equation:

$$f = \frac{1}{a^3} \times \frac{2\varepsilon_s - 2}{2\varepsilon_s + 1}.$$

For a pure dipole liquid Debye's equation (I. 6) is simplified to:

$$\frac{\varepsilon_s - 1}{\varepsilon_s + 2} = \frac{4}{3} \pi N(\alpha + \frac{\mu^2}{3kT})$$

or with the aid of the Lorenz-Lorentz equation:

$$\mu^2 = \frac{9kT}{4\pi N} \frac{(\varepsilon_s - n^2_\infty)\ 3}{(\varepsilon_s + 2)\ (n^2_\infty + 2)} \qquad (I.8)$$

In the same way the Onsager-Böttcher equation may be simplified to:

$$\mu^2 = \frac{9kT}{4\pi N} \frac{(\varepsilon_s - n^2_\infty)\ (2\varepsilon_s + n^2_\infty)}{\varepsilon_s (n^2_\infty + 2)^2} \qquad (I.9)$$

In each of the above equations the polarisabilities α_0 and α_1 of solvent and solute (which include both electronic and atomic polarisation) or the resulting refractive index at infinite wave length, n_∞, must be known in the evaluation of the dipole moments. Although it might be possible to determine n_∞ by extrapolation from refractive index measurements in the far infrared, several attempts have been made to obtain approximate values of n_∞ with simpler means by extrapolation from refractive index measurements in the visible region and introduction of an approximate value for the atomic polarisation [20, 34, 35].

These difficulties can be avoided by measuring the dispersion of the permittivity or the dielectric loss, i. e. by determining the value of ε_∞, which may be inserted in the above equations instead of n^2_∞.

For liquids with one relaxation time the variation of ε'' with frequency must only be determined as far as the maximum in the curve. The value of ε_∞ when ε_s is known from a low frequency measurement, will then be given according to (I. 3) by the equation:

$$\varepsilon_s - \varepsilon_\infty = 2(\varepsilon'')_{max.}$$

For liquids with a distribution of relaxation times it is still possible to obtain the dispersion $\varepsilon_s - \varepsilon_\infty$ from the area under the absorption-curve [20, 33, 36] using the more general equation (I. 11), of which (I. 10) is a special example in the case of one relaxation time:

$$\varepsilon_s - \varepsilon_\infty = \frac{2}{\pi} \int \varepsilon'' \omega\, d(\ln\omega) \qquad (I.11)$$

The determination of dipole moments from high frequency measurements on very dilute solutions is also possible, when the difference between ε_s and ε_∞ is very small, by making use of an equation originally derived by Debye [37]:

$$\varepsilon'' = (\varepsilon_o + 2)^2 \frac{4\pi N\mu^2}{27\,kT} \frac{\omega\tau}{1+\omega^2\tau^2} \qquad (I.12)$$

Apart from the approximations introduced in the Debye equation (I. 6) the difference between the values of ε_s and ε_∞ is neglected in the derivation of (I. 12) and both ε_s and ε_∞ are taken equal to ε_0, the permittivity of the non polar solvent.

Although the Onsager-Böttcher equations may be expected to give more reliable results in the determination of permanent dipole moments, than the Debye equations, the values obtained with equ. (I. 9) are still quite different from the values of the dipole moment obtained from measurements in the gas-phase. If n^2_∞ or ε_∞ in equ. (I. 9) is replaced by n^2_D the differences are smaller, but still evident in some cases. Böttcher showed that it is even preferable to use n^2_D in equ. (I. 9) since thus the approximations used in the derivation of this equation would tend to cancel each other. It therefore should be borne in mind that values of permanent dipole moments, obtained from measurements on pure dipole liquids using the value of ε_∞ in the Onsager-Böttcher equation, may not be compared directly with the values obtained from measurements on gases or even on dilute solutions.

For the evaluation of dielectric measurements it is necessary to relate the dielectric properties ε' and ε'' introduced above to the measured quantities, viz. capacitance and resistance.

A capacitor, which has a capacitance C_o in vacuo, will in first approximation have a capacitance $C = C_o \frac{\varepsilon}{\varepsilon_o}$, when a material with a relative permittivity $\frac{\varepsilon}{\varepsilon_o}$ is inserted between the plates. The current through this capacitor, in quadrature with the applied sinusoidal voltage V, is given by:

$$i_c = \frac{\partial Q}{\partial t} = j\omega C V = I_o e^{j(\omega t + \frac{\pi}{2})}$$

For a capacitor containing a dielectric with loss an additional loss-current, $i_{loss} = GV$, will flow which is in phase with the applied voltage. The phase relationships between these currents are indicated in fig. I. 1. a. and the total current through the capacitor will be given by:

$$I_T = (G + j\omega C)\, V.$$

The current vector is inclined by a power factor angle $\theta < 90^o$ against the applied voltage and hence by a loss angle δ against the + j-axis.

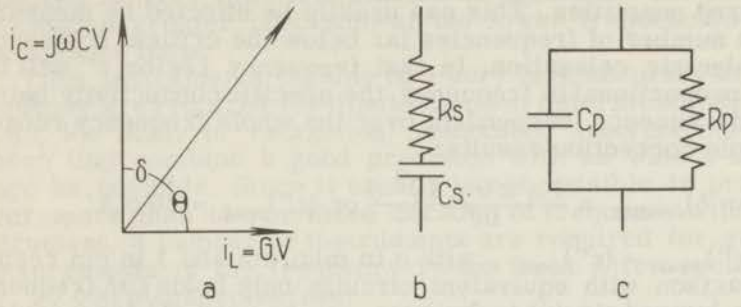

Fig. I.1. Equ. circuits of a capacitor with loss.

From this we may not conclude that the dielectric material corresponds in its electrical behaviour to a parallel circuit of a frequency independent capacitance C and a frequency independent resistance 1/G. The current-voltage diagram of fig. I.1.a., measured for a capacitor with dielectric at one frequency only, allows any number of equivalent networks. The simplest equivalent circuits are those consisting of an ideal capacitor C and a resistor R in a series- or parallel-combination [21, 32] (fig. I.1.b and c).

The frequency dependences of these two elementary circuits have completely different trends, but at one frequency either may be used for the evaluation of the data obtained, depending on the measuring technique employed. How well either one of these circuits, or combinations of them, simulates the behaviour of the actual dielectric can only be established by calculating the frequency responses of a number of networks and comparing them with the dielectric response observed.

By inserting the complex permittivity in the equations for the current through a lossy capacitor, the equation for the total current may be rewritten:

$$I_T = (\omega\varepsilon'' + j\omega\varepsilon') \frac{C_o}{\varepsilon_o} V$$

The product $\omega\varepsilon''$ is equivalent to a dielectric conductivity and sums over all dissipative effects in the material. The value of ε' is obtained directly from capacitance readings, whereas the value of ε'' can be evaluated from conductance readings, either in terms of resistance or loss tangent:

$$\varepsilon' = C \frac{\varepsilon_o}{C_o}$$

$$\frac{\varepsilon''}{\varepsilon'} = \tan\delta = \frac{1}{\omega R_p C_p} = \omega R_s C_s$$

In dealing with dielectric relaxation processes the contribution of

the migration of charge carriers to ε' must be substracted from the measured quantities. This can usually be effected by measuring ε'' at a number of frequencies far below the critical frequency for the dielectric relaxation. In that frequency region ε'' will be inversely proportional to frequency, the specific conductivity being considered frequency independent over the whole frequency range, and a simple correction results:

$$(\tan \delta)_{\text{conduct.}} = \frac{4 \pi \times 9 \times 10^9 \sigma}{\omega \varepsilon'} \text{ or } (\varepsilon'')_{\text{cond.}} = 60 \sigma \lambda$$

and $\varepsilon'' = (\varepsilon'')_{\text{meas.}} - (\varepsilon'')_{\text{cond.}}$, with σ in mhq/cm and λ in cm resp. The comparison with equivalent circuits only holds for frequencies where lumped circuit techniques may be used. At frequencies above a few hundred megacycles/sec. the dielectric properties must be evaluated from transmission line measurements, with reference to the field equations. The equations for the calculation of the complex permittivity from the measuring data at these frequencies will be given in section II. F.

For the specification of the instrumental requirements for dielectric measurements, two points must be considered. First the frequency ranges and the accuracies, necessary in each of these ranges, must be fixed in connection with the problems to be studied. Second measuring techniques must be chosen in each frequency range that can be adapted to dielectric measurements with sufficient accuracy.

The problems to be studied by dielectric measurements can roughly be divided into two groups:

a. the determination of polarisabilities, including the determination of dipole moments.
b. the study of relaxation phenomena.

For the determination of permanent dipole moments from measurements on pure liquids or dilute solutions of polar substances and, even more so, for the determination of polarisabilities [37, 38] a very high accuracy of measurement is required at one frequency, which must be chosen far below the relaxation frequency of the polar substance. Various procedures, starting from the Debye-equation (I. 6), have been proposed for the calculation of dipole moments from measurements of the temperature- or concentration-dependence of the permittivity of dilute solutions [28-31, 34]. When e.g. the equations derived by Hedestrand [28] or Halverstadt-Kumler [30] are used, an error of about 1% in the value of the dipole moment will result from a relative error of 3 units in the fourth decimal place in the permittivity values.

In the study of relaxation phenomena measurements are required over a wide frequency range, which must include the critical frequency or frequencies of the relaxation and a few decades below and above this frequency. Hence a number of different measuring techniques will usually be involved in the determination of the relaxation curves. Since it hardly seems possible at present to reduce the errors in the complex-permittivity meas-

urements at very high frequencies to less than one or even two per cent, a greater precision at the lower frequencies is of no consequence here.

Thus instruments capable of a very high accuracy at a single frequency are required for dipole moment determinations, whereas for the study of relaxation phenomena instruments will be chosen that combine a good precision with as wide a frequency range as possible. Since it usually is not possible in practice to cover more than two or three decades of frequency with a single instrument, a number of instruments are required for relaxation measurements in the frequency range from a few cycles/sec to e.g. 30 000 Megacycles/sec.

At very low frequencies dielectric measurements may be carried out by delineating the current-time curves of a measuring-cell filled with the material under investigation [45, 46] or by using special low frequency bridge-circuits [47].

Above a few cycles bridge circuits are in general use, most bridges for dielectric measurements being derived from the Schering-bridge [48, 49]. At frequencies in excess of 1 Mc/s the parasitic impedances in the bridge-arms tend to decrease the overall accuracy. This can be partly overcome by the use of correction curves or special circuits, of which the Twin-T circuit [50] and the bridges with inductively coupled ratio-arms [51, 52] are good examples. For frequencies between 50 c/s and 0.5 Mc/s however, Schering-bridges can be constructed to give a very high accuracy, the errors being mainly due to imperfections in the calibration of the precision condensers and measuring cells or to impurities in the calibrating compounds.

A very high accuracy over a limited frequency range can also be obtained with the heterodyne-beat method [53, 54], with the additional advantage that very small capacitances can be measured, but the disadvantage that the method can only be used for low-loss substances. This method is most suitable for dipole moment determinations, since accurate measurements may be carried out on small samples and the samples usually have very low loss factors at the measuring frequency of e.g. 1.5 Mc/s. The measuring cells present a major problem, which will be considered in detail in Chapter II.

In the frequency range between 1 Mc/s and 300 Mc/s several methods may be used with moderate accuracy. It appears that resonance methods are not very well suited for dielectric measurements, since the many sources of error involved greatly reduce the overall accuracy. By very careful design and thorough mathematical analysis bridge-circuits have been developed with errors of less than 0.2% up to 200 Mc/s [55]. Owing to uncertainties in the properties of the measuring cells, the errors of the dielectric measurements at these frequencies will increase to about 1%, with a subsequent simplification of the mathematical analysis of the bridge circuits.

Above 300 Mc/s transmission line methods are in general use. The coaxial systems are well suited for dielectric meas-

urements, since a large frequency range may be covered by one instrument with sufficient accuracy. For low-loss samples resonance methods may be used to advantage [56, 57], whereas for medium loss samples standing wave methods are to be preferred [21]. Very interesting combinations of these two methods in a single instrument, by the use of a non-slotted coaxial line, were recently introduced by Eichacker [58] and Huber [59].

The special problem of high-loss substances can best be approached by the application of travelling-wave methods [60, 61].

Owing to the dimensions of the coaxial systems, the risk of introducing unwanted modes imposes a high-frequency limit on the measurements. Above this frequency wave guide systems must be used, with the disadvantage that each system can only be used over a very limited frequency range.

Our apparatus was chosen according to the above considerations. Since the coaxial systems described, can be used up to 5000 Mc/s a reasonable overlap is established with the waveguide systems, to be described by Bos [44], for frequencies between 3 000 and 30 000 Mc/s.

Chapter II

DESCRIPTION OF THE APPARATUS

II.A. Low Frequency Bridge (30 c/s-350 kc/s)

In the low-frequency range several bridge-circuits for dielectric measurements are used [49, 62, 63]. The Schering-bridge circuit, with its modifications, are to be preferred however for wide range applications. Fig. II.A.1 shows a modified Schering bridge, suitable for the measurement of complex impedances, i.e. permittivity and loss. In this case the series equivalent of the unknown impedance (Chapter I) is measured in terms of a capacity C_{xs} having a loss tangent D_x. As will be derived later, the value of the condenser C_N is proportional to C_{xs} and the value of C_2 is proportional to D_x.

Thus the only variables in the bridge are condensers, which can be calibrated accurately and have low and constant parasitic impedances.

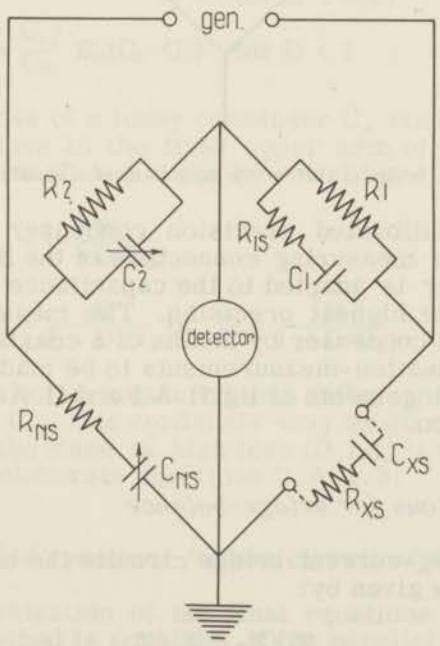

Fig. II.A.I. Circuit of modified Schering-bridge.

A bridge constructed according to the diagram given in fig. II.A.1, gave very accurate results up to 20 000 c/s. Above this frequency difficulties arose, as a result of parasitic impedances in the resistors and the bridge transformer. It was possible however to check the importance of the various possible parasitic effects and to calculate the possibilities of the method for our purposes. On account of these experiences it was decided to use a commercial bridge (General Radio type 716 C), working on the same principle in the frequency range of 30 c/s to 350 kc/s and capable, after suitable corrections, of the required accuracy of 0.1% for capacity – and 1% for loss – measurements.

In order to maintain the same accuracy for the low capacitance of the measuring cells, a modified arrangement of the measuring-circuit was used, as shown in fig. II.A.II.

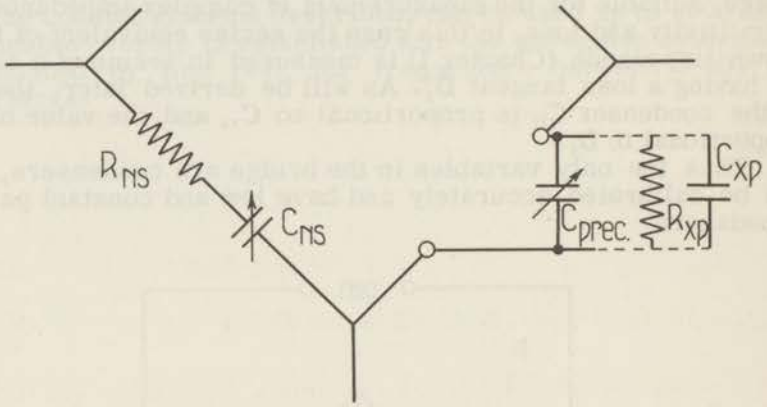

Fig. II.A.II. Bridge circuit for the measurement of small capacitances.

An accurately calibrated precision condenser is connected in parallel with the measuring connectors of the bridge. The range of this condenser is adapted to the capacitance of the measuring cell to obtain the highest precision. The measuring cell can be connected to this condenser by means of a coaxial connector, thus enabling compensation-measurements to be made. Suitable equations for the arrangements of fig. II.A.I and II.A.II will be derived in the next section.

II.A.1.1. *Equations for bridge-balance*

In alternating-current bridge circuits the basic condition for bridge balance is given by:

$$Z_1/Z_2 = Z_x/Z_N \qquad \text{(II.A.1.1)}$$

For the circuit of fig. II.A.I, taking R_1 equal to R_2, this results in the balance condition:

$$\frac{\frac{1}{R} + j\omega C_2}{\frac{1}{R} + \frac{1}{R_{ls} + \frac{1}{j\omega C_1}}} = \frac{R_{xs} + \frac{1}{j\omega C_{xs}}}{R_{Ns} + \frac{1}{j\omega C_{Ns}}} \qquad \text{(II.A.1.2)}$$

A rearrangement of this equation, followed by separation of the real and imaginary parts leads to:

$$\frac{C_{xs}}{C_{Ns}} = \frac{(R_1 + R_{ls})^2 + \frac{1}{\omega^2 C_1^2}}{R_1 R_{ls} + R_{ls}^2 + \frac{C_2}{C_1} R_1^2 + \frac{1}{\omega^2 C_1^2}} \quad (1+\omega^2 C_{xs} C_{Ns} R_{xs} R_{Ns})$$

$$(R_{Ns} C_{Ns} - R_{xs} C_{xs}) \left\{ \omega^2 C_1^2 (R_1 + R_{ls})^2 + 1 \right\} = \frac{C_{xs}}{C_{Ns}} R_1 (C_1 - C_2) \qquad \text{(II.A.1.3)}$$

Taking into account the accuracy required for C_{xs} and D_x, and limiting the frequency to 350 kc/s, these equations can be greatly simplified:

$$\frac{C_{Ns}}{C_{xs}} = 1 + \omega^2 R_1 R_{ls} C_1 (C_2 - C_1) \qquad \text{for } D < 1 \qquad \text{(II.A.1.4)}$$

$$\text{or} \quad C_{xs} = C_N \qquad \text{for } D < 0.01 \qquad \text{(II.A.1.5)}$$

$$(R_{xs} C_{xs} - R_{Ns} C_{Ns}) = \frac{C_{xs}}{C_{Ns}} R_1 (C_2 - C_1) \qquad \text{for } D < 1 \qquad \text{(II.A.1.6)}$$

For the series loss of a lossy condenser C, $\tan \delta = D = \omega R_s C_s$; so, when D_o is the loss in the fixed upper arm of the bridge, equations II.A.1.4. and II.A.1.6 can be rewritten:

$$C_{xs} = \frac{C_{Ns}}{1 + D D_o} \qquad \text{(II.A.1.7)}$$

$$(D_x - D_s) = \frac{D}{1 + D D_o} \quad \text{or} \quad D_x = \frac{D}{1 + D D_o} \qquad \text{(II.A.1.8)}$$

Since D_x is always measured as a difference of two readings of the condenser C_2, this condenser may be directly calibrated in terms of D_x. In the case of high loss ($D > 1$) it will be necessary to use the more elaborate equations II.A.1.3.

II.A.1.2. *Modified equations for the circuit of fig. II.A.II*

A simple evaluation of the final equations for this parallel compensation method is possible, if the parallel-equivalent of the unknown impedance is used in the various equations. In this case we have two balance conditions:

a. unknown impedance not connected to the circuit:

$$C_N = C_p + C'_{prec.} \qquad \text{(II.A.1.9)}$$

$$D = D'$$

in this case D' will be very small.

b. unknown impedance connected to the circuit:

$$(C_p)_{total} = C_p + C_{prec.} + C_{xp}$$

$$D_{total} = \frac{1}{\omega R_{xp}(C_p + C_{prec.} + C_{xp})} \qquad \text{(II.A.1.10)}$$

In case b. C_N no longer equals $(C_p)_{total}$ according to equ. II.A.1.7.

$$C_N = (C_p)_{total}\ (1+D^2)\ (1+D\ D_o) \qquad \text{(II.A.1.11)}$$

$$D_T = \frac{D}{1+D\ D_o} = \frac{1}{\omega R_{xp}(C_p)_{total}} \qquad \text{(II.A.1.12)}$$

The factor $(1+D^2)$ in equ. (II.A.1.11) results from the change-over from the series equivalent C_{xs} in (II.A.1.7) to the parallel equivalent in this case. As we leave the value of C_N unchanged during the measurement, the foregoing equations can be recombined:

$$C_N - \frac{C_N}{(1+D^2)\ (1+D\ D_o)} = (C'_{prec} - C_{prec}) - C_{xp}$$

or

$$C_{xp} = \Delta C_{prec} - \left\{ C_N - \frac{C_N}{(1+D^2)\ (1+D\ D_o)} \right\} \qquad \text{(II.A.1.13)}$$

$$R_{xp} = \frac{(1+D^2)\ (1+D\ D_o)}{\omega D\ C_N} \qquad \text{(II.A.1.14)}$$

$$D_x = \frac{D\ C_N}{(1+D^2)\ (1+D\ D_o)}\ \frac{1}{C_{xp}} \qquad \text{(II.A.1.15)}$$

The equations (II.A.1.13 and II.A.1.14) were checked by measuring a number of well defined parallel combinations of R and C at various frequencies. An accuracy of better than 0.5% in R_{xp} was obtained for values of $D < 1$.

II.A.2. Description of the bridge circuit

The bridge-circuit and its subsidiary apparatus are shown in fig. II.A.III.

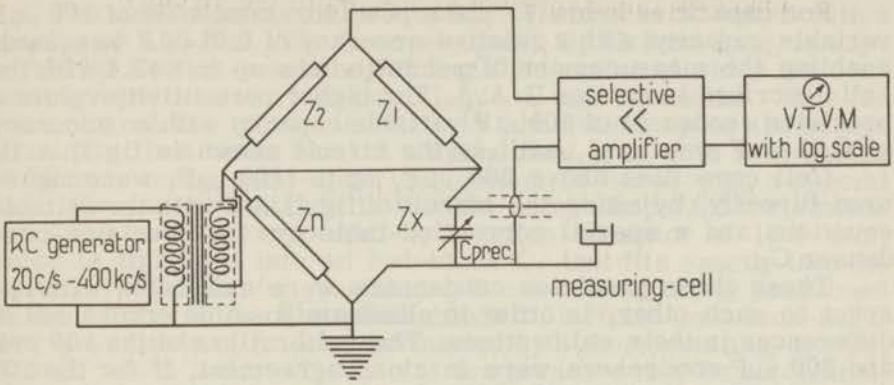

Fig. II.A.III. Low-frequency bridge and subsidiary apparatus.

A stable RC oscillator, with a frequency range of 20 c/s to 400 kc/s supplies an a.c. voltage of about 10 Volts to the bridge. The bridge-detector terminals D_1 and D_2 are connected to a highly selective amplifier through a well shielded separating transformer. In the selective amplifier a vacuumtube voltmeter is incorporated, the logarithmic scale of which greatly facilitates the balancing of the bridge. The input sensitivity of this bridge detector is about 5 μV at a bandwidth of 2%, the equivalent noise level at the input terminals being ca. 2 μV.

Considering the impedances in the bridge circuit, we can evaluate the minimum increments of C and D, that can be detected with this arrangement [65], by using equation II.A.2.1.

$$V_{det} = V_{gen} \left(\frac{Z_x}{Z_1+Z_x} - \frac{Z_N}{Z_2+Z_N}\right) \qquad \text{(II.A.2.1)}$$

Inserting V_{gen}=10 Volts and $V_{det}=5\times10^{-6}$ Volts in this equation and differentiating the result, we obtain the minimum increments $(\Delta C)_{min}$ and $(\Delta D)_{min}$ that can be detected:

$(\Delta C)_{min}=10^{-3}$ $\mu\mu$F.
$(\Delta D)_{min}\approx 1\times10^{-4}$.

So the measuring accuracy will be entirely determined by the calibration-accuracy of C_{prec} and the range of validity of equ. (II.A.1.13), (II.A.1.14) and (II.A.1.15).

The various precision condensers used were calibrated to be accurate and reproducible within $\pm$0.02 $\mu\mu$F. As a result the overall accuracy for values of $D < 1$ will be $\pm$ 0.5% for the measurement of D_x and $\pm$ 0.1% for the capacity-measurement. The accuracy of 0.1% for the capacity measurement will only be obtained, however, for capacities of 20 $\mu\mu$F and above, because of the possible deviations of $\pm$ 0.02 $\mu\mu$F in the precision condensers: the accuracy of the loss-measurement is limited by the minimum detectable increment of 1×10^{-4}.

For capacities below 75 μμF a precision condenser of 100 μμF variable capacity with a relative accuracy of 0.01 μμF was used, enabling the measurement of permittivities up to ε=2.4 with the cell described in section II. A. 3. For higher permittivity values a precision condenser of 300μμF variable capacity with an accuracy of 0.02 μμF was used, still in the circuit shown in fig. II. A. II.

Cell capacities above 300 μμF, up to 1100 μμF, were measured directly, by using the circuit of fig. II. A. I with the suitable equations and a special correction-table for the precision-condenser C_N.

These three precision condensers were calibrated with respect to each other, in order to eliminate possible errors due to differences in their calibrations. The calibrations of the 100 μμF and 300 μμF condensers were in close agreement, if for the 100 μμF condenser the first 25 μμF were left out of account. The 1100 μμF condenser was recalibrated in terms of the other two, necessitating only minor corrections at the ends of the scale.

II.A.3. Measuring cells and evaluation of results

For the bridge described above special measuring cells were developed. Fig. II. A. IV shows the details of the cell, for measurements on liquids, which has a cellconstant C_o of about 60 μμF, and a further parallel capacity of about 10 μμF. As will be shown below, the value of this parallel capacity does not enter into the results.

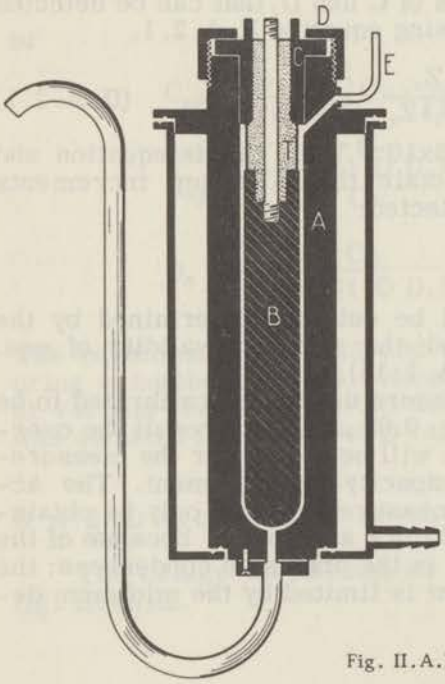

Fig. II.A.IV. Cell for dielectric measurements on liquids.

The cell consists of two coaxial electrodes A and B with a spacing of 1.25 mm. The inner electrode B, 12.5 cm long, is supported by a teflon-insulator, through the center of which the connecting wire leads to a coaxial L-piece and connector. Thus the screening of the inner electrode is maintained up to the bridge terminals. In a brass block A a cylindrical hole with a diameter of 20 mm and a semi-spherical bottom is bored with a special tool. The inner-electrode B has the same shape and a diameter of 17.5 mm. It is supported by a teflon-insulator of 12.5 mm, which is tightened into an end-block C, that fits exactly into the top of A. With careful machiening B can be accurately positioned in the centre of A. The slidingblock C is fixed by a lock-nut D over the outside of A. A is surrounded by a thermostating-mantle, through which water of constant temperature may be circulated. The cell is filled through a platinum tube E and a small hole in the bottom of the cell. A glass tube, fixed with araldite into a brass block is screwed onto the cell opposite this hole with a teflon washer. Thus the liquid level in the cell can be checked and the glass tube can easily be renewed when necessary. All parts of the cell, that are in contact with the liquid are rhodium-plated.

The cell has a very small edge-effect, since the spacing between the electrodes is small compared with their length and the connecting wire is very thin in proportion to the diameter of the insulator. Thus within the measuring accuracy a virtually linear relation exists between the capacity of the cell and the relative dielectric constant of the liquid in it:
$C_x = \varepsilon C_o + C_p$, where C_p is the wiring capacity of the cell.
During the measurements the cell is always connected to the bridge and the differences in the bridge-readings for the empty cell and the cell filled with liquid are used for the evaluation of the results.
Since the equations II.A.1.13 and II.A.1.14 give the parallel equivalent of the unknown impedance in terms of the bridge readings a very simple calculation results. We only have to bear in mind that for the first readings a loss-free capacity C_o', the capacity of the airfilled cell, is already in the circuit. So a capacity C_o' must be added to the value of C_{xp} calculated with equ. II.A.1.13.

$$C_{xp} = \varepsilon' C_o = C_{prec} + C_o' - \{corr.\} \qquad (II.A.3.1)$$

The value of D_x has to be changed accordingly, whereas the equation for R_{xp} is not affected.

For low-loss liquids the correction term may be neglected and the permittivity of the liquid is given by the simple equation:

$$\Delta C_{prec} = \varepsilon C_o - C_o' \qquad (II.A.3.2)$$

The constants C_o and C_o' were determined by measuring three pure liquids for which reliable data were known in the literature

[63, 64] and four liquids, the permittivity of which was determined by the absolute method described in section II.B.2. From these data the average values of C_o and C_o' were evaluated statistically, as with the first method small discrepancies result from the fact that the purity of the liquids used may be different from the purity of the ones cited in the literature and with the second method the accuracy is limited by the precision of the absolute method.
The values thus obtained, are $C_o = 62.55 \pm 0.01$ $\mu\mu$F
$C_o = 62.85 \pm 0.01$ $\mu\mu$F
For a temperature range of 20-40°C no change in these values can be detected within the measuring accuracy. A calculation based on the equation for the capacity of a coaxial capacitor and the expansion coefficients of the materials used, leads to the same result.

By inserting these values and the results of the measurements in equ. II.A.3.2 the value of the permittivity obtained for each liquid may be compared with the literature value and the value obtained with the absolute cell. These results are summarized in table I; it will be seen that the overall accuracy of this bridge-method is ca. 0.1% for permittivity values between 2 and 6.

Table I

	ΔC_{prec}	ε_{bridge}	$\varepsilon_{abs.}$	$\varepsilon_{lit.}$
cyclohexane (30°C)	63.05	2.0127	2.013	2.010
benzene (30°C)	79.28	2.270	2.269	2.265
diethyl ether (25°C)	201.81	4.247		4.26
mixture C_6H_5Cl/C_6H_6 (30°C)	162.97	3.610	3.613	
chloro benzene (25°C)	289.54	5.634	5.636	

If for special applications a cell with a lower cell-constant is wanted, the inner electrode is replaced by a thinner one. Since with this bridge, as with most of the instruments described in this thesis, essentially capacity-measurements are performed, any type of cell can be used within the ranges of the bridge. It should be borne in mind, however, that as a result of this the final accuracy of the dielectric measurements depends entirely on the precision with which the cell constant and the parasitic impedances of the respective cells are known.

II.B. HETERODYNE METHOD (1-2.5 Mc/s)

For the determination of dipole moments in dilute solutions (see chapter I) a relative accuracy of 2 units in the fourth decimal place is desirable. A further consideration in the construction of a measuring-set for this purpose is the fact that often only small amounts of the pure compounds to be investigated are available.

This necessitates the use of very. small measuring cells and hence the measurement of small capacities.

The apparatus constructed for this purpose is also useful for the determination of the dielectric constant of low-loss liquids at one frequency with an accuracy not readily obtainable with other methods e.g. of the liquids necessary for the calibration of measuring cells.

II.B.1. Description of the apparatus

This apparatus was constructed on the basis of the heterodyne-method, used in various forms by other authors [53, 54]. In a preceding paper [38] it was pointed out that the stability of the oscillators was raised to such an extent that their relative shift did not impair the precision of the results. A general diagram of the apparatus is shown in fig. II.B.I.

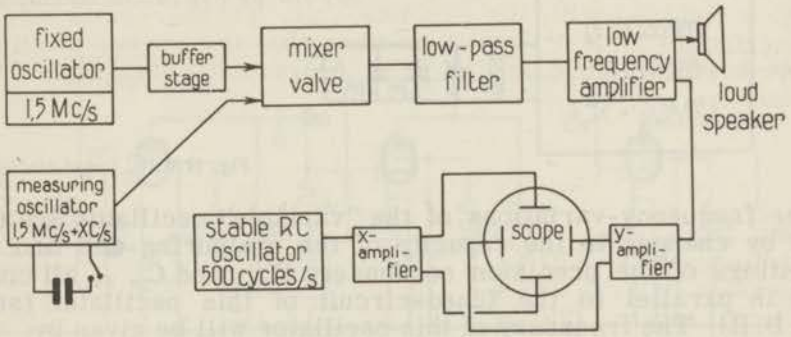

Fig. II.B.I. Block-diagram of the heterodyne method.

In a heterodyne method the frequency variation of one oscillator is measured accurately from the difference between it and the constant frequency of another oscillator of roughly the same frequency. The beat-frequency of the two oscillators being directly proportional to the variation of the frequency of the first oscillator, a determination of this variation, and hence of capacity-changes in the tuned circuit of the first oscillator, is possible with much higher relative accuracy.

The frequencies of two H.F. oscillators are fed into a mixer-amplifier, where the difference – or beat – frequency is amplified and fed onto the vertical deflection plates of a cathode-ray tube. The beat-frequency of the two H. F. oscillators is also amplified and supplied to a loudspeaker for quick tuning of the oscillators to roughly the right frequency.

The horizontal deflection plates of the cathode-ray tube are connected to a sine-wave generator with a stable frequency of e.g. 500 c/s.

For a difference of 500 c/s between the frequencies of the two H. F. oscillators the beat-frequency will be 500 c/s and a

simple Lissajous figure will appear on the screen of the tube. Thus the frequency of one oscillator can be set within a cycle, with respect to the other. The whole measurement is based on this setting of the frequency of the "variable" oscillator. During the measurement the other or "fixed" oscillator is maintained at the same frequency of e.g. 1.5 Mc/s.

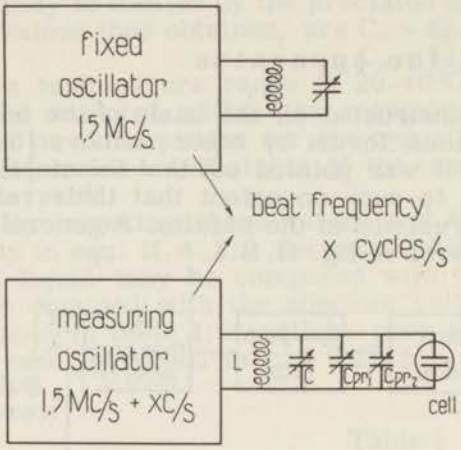

Fig. II.B.II. Tuned circuits.

The frequency-variations of the "variable" oscillator are effected by changes in the capacity of the measuring-cell and in the settings of the precision condensers $C_{pr.1}$ and $C_{pr.2}$, all connected in parallel to the tuned-circuit of this oscillator (see fig. II.B.II). The frequency of this oscillator will be given by:

$$f = \frac{1}{2\pi\sqrt{L(C+C_{pr.1}+C_{pr.2}+C_{cell})}} \qquad \text{(II.B.1.1)}$$

During a measurement the oscillator is first tuned to a frequency 500 c/s above the frequency of the fixed oscillator, the measuring-cell being disconnected. Coarse tuning is effected with $C_{pr.1}$, after which exact tuning with $C_{pr.2}$ follows. After switching the cell into the circuit, the same frequency is reestablished by changing the settings of $C_{pr.1}$ and $C_{pr.2}$. The capacity of the measuring-cell is found directly from the differences in the readings of the precision condensers in the two cases.

II.B.1.1. *High stability oscillators*

For the accurate measurement of small capacities high stability of the oscillators is a necessity. For the fixed oscillator this stability can easily be achieved by using a crystal-controlled circuit. Since, however, this is not possible for the variable oscillator anyhow, the use of two electronically stabilised oscillators was preferred. This has the additional advantage that a small

shift in the frequencies of the two oscillators, provided this takes place in the same way, does not affect the beat-frequency. By constructing the two oscillators in exactly the same way this advantage was fully realised.

After experiments with various circuits, e.g. Collpitts-, Hartley-, Franklin- [65, 66, 67] and Clapp-oscillators [68], it was decided to use the Franklin-circuit, since it combined easy tuning with great stability over the tuning-range. It might be possible to reach even better results with a modified Clapp-circuit, published by Shulman [69] after our apparatus was completed. With elaborate stabilisation of the supply-voltages a frequency-stability of ± 10 cycles was reached at a frequency of 1.5 Mc/s after a warming-up period of several hours. During a measurement the beat-frequency varies less than 2 cycles. This stability is more than adequate, since the frequency-shift of the variable oscillator is 3 cycles per scale-division of the fine tuning capacitor $C_{pr.2}$ and a deviation of 1-2 scale-divisions is allowable with regard to the required accuracy of 0.01%.

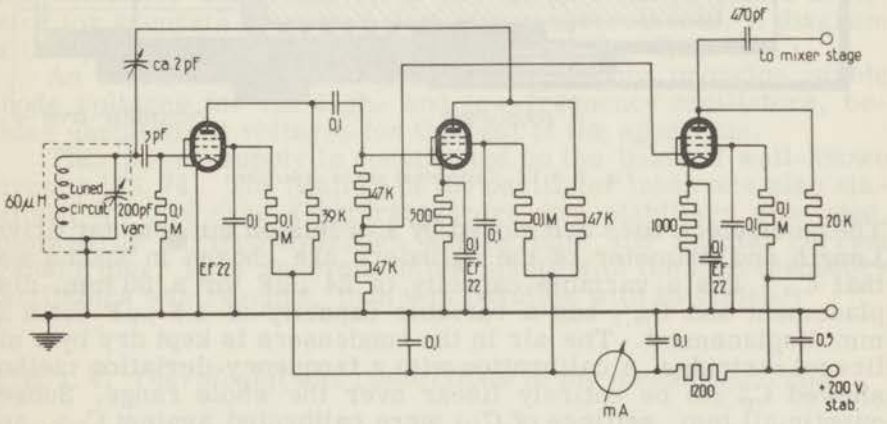

Fig. II.B.III. Diagram of Franklin oscillator with buffer stage.

The main advantage of the Franklin-oscillator is the very loose coupling between the tuned circuit and the electronic part. As a result the frequency-stability is mainly determined by the stability of the components in the tuned circuit. The diagram of these oscillators is reproduced in fig. II.B.III. The whole apparatus, including the power-supplies and a thermostat for the measuring-cells is built into a steel enclosure with sliding chassis. Thus a large heat-inertia is obtained, as a result of which quick temperature changes in the surroundings do not affect the frequency of the oscillators.

II.B.1.2. *Tuned circuits and precision condensers*

The tuned circuits of the two oscillators comprise the same selfinductances and tuning-condensers. The coils are wound from

solid copper wire on an open ceramic core. The condensers are 200 $\mu\mu$F linear variable capacitors, cut from solid aluminum blocks, with quartz insulators. Coil and condenser are mounted in a heat-insulating box, and the condenser-shaft, also made from heat insulating material, is driven from a slow-motion dial on the front panel. In addition to these components, the tuned circuit of the variable – or measuring – oscillator comprises two precision condensers $C_{pr.1}$ and $C_{pr.2}$. These are cylindrical piston-capacitors, the capacity of which varies linearly with the displacement of the inner electrode. The design of these condensers is shown in fig. II.B.IV.

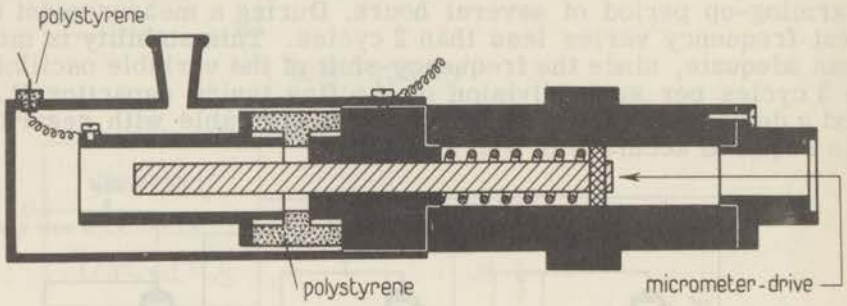

Fig. II.B.IV. Cylindrical piston capacitor.

The inner electrodes are moved by a precision micrometer drive. Length and diameter of the cylinders are chosen in such a way that $C_{pr.1}$ has a variable capacity of 24 $\mu\mu$F for a 50 mm. displacement and $C_{pr.2}$ has a variable capacity of 1.5 $\mu\mu$F for a 25 mm displacement. The air in the condensers is kept dry by a silicagel cartridge. A calibration with a frequency-deviation method showed $C_{pr.2}$ to be entirely linear over the whole range. Subsequently all mm. settings of C_{pr1} were calibrated against C_{pr2}, and a table giving the capacity of C_{pr1} for each mm. setting in terms of scale divisions of C_{pr2} could be composed. During the measurements only whole millimeter settings of C_{pr1} are used, between which interpolation is effected with C_{pr2}. In this way it is possible to measure capacity-differences with an accuracy of $\pm 0.5 \times 10^{-3}$ $\mu\mu$F.

II.B.1.3. *Subsidiary apparatus*

For the mixing of the frequencies of the two oscillators a pentode-valve, type 6 AK5, is used. The use of a normal mixer-tube, as used in receivers, presents difficulties because of considerable hum induction from the cathode into the anode circuit, when two signals are mixed to give an audible beat-frequency. Although this hum induction does not disturb the result of the measurement, it blurs the oscilloscope trace and prevents exact tuning of the measuring-oscillator. It was found that all normal

mixer-tubes of various makes showed this effect, and so mixing via first and third grid of a pentode was preferred. The measuring-oscillator is connected to the first grid and the fixed-oscillator, after insertion of a buffer-stage, to the third grid. Thus drawing of the two oscillators at low beat-frequencies is avoided. After a low-pass filter, which eliminates the sum-frequencies of the two oscillators, the difference- or beat-frequency is amplified and connected to the vertical deflection-plates of an oscilloscope-tube. A separate output-stage powers a small loudspeaker for a quick check on the tuning of the oscillators.

The horizontal deflection-plates of the oscilloscope tube are connected to a built-in low-frequency oscillator and amplifier. For this purpose a stable phase-shift oscillator [70] was chosen, with stabilisation by the bias-voltage [71, 72]. The frequency is variable from 300-2000 c/s, for variable-frequency measurements; during the normal measurements 500 c/s is always used. Switching facilities are incorporated to check the frequency of this oscillator externally or to use an external precision oscillator for accurate frequency-deviation measurements. A diagram of this part of the apparatus is presented in fig. II.B.V.

An electronically stabilised power supply provides stable anode voltages for the high- and low-frequency oscillators, besides unstabilised voltages for the rest of the apparatus.

This power-supply is constructed on the basis of well-known circuits [73, 74]. The heaters of the oscillator tubes are also stabilised. In this case a saturated-core pre-stabiliser was used, followed by an iron-hydrogen series tube and special current transformer. Thus an even better stability of the high frequency oscillators was reached, than was possible with batteries.

II.B.1.4. *Thermostat and connections to the measuring-cells*

An oil thermostat is incorporated in the instrument. Since the periodic switching of the heaters in the thermostat appeared to interfere with the accurate measurement of small capacities, the use of an electric regulator was dispensed with.

A dewar-vessel with additional heat-insulation on the outside was used instead. This only contains the measuring-cell, a glass centrifugal stirrer, an accurate thermometer and one heating-element. The silicone-oil in the dewar-vessel is heated to approximately the right temperature, after which the heater is connected to ground and an equilibrium temperature is established. Because of the big heat-inertia in the dewar-vessel, the temperature does not change by more than $0.01^{o}C$ during a measurement, A calibrated thermometer gives the exact measuring-temperature. Alongside the top of this thermostat a needle-contact of very low capacity is provided to switch the cell into circuit. The cell is fixed into a trapezium-shaped plate to provide accurate fitting into the top plate of the thermostat. These cells will be described in section II.B.2. On the panel of the instrument, near the pre-

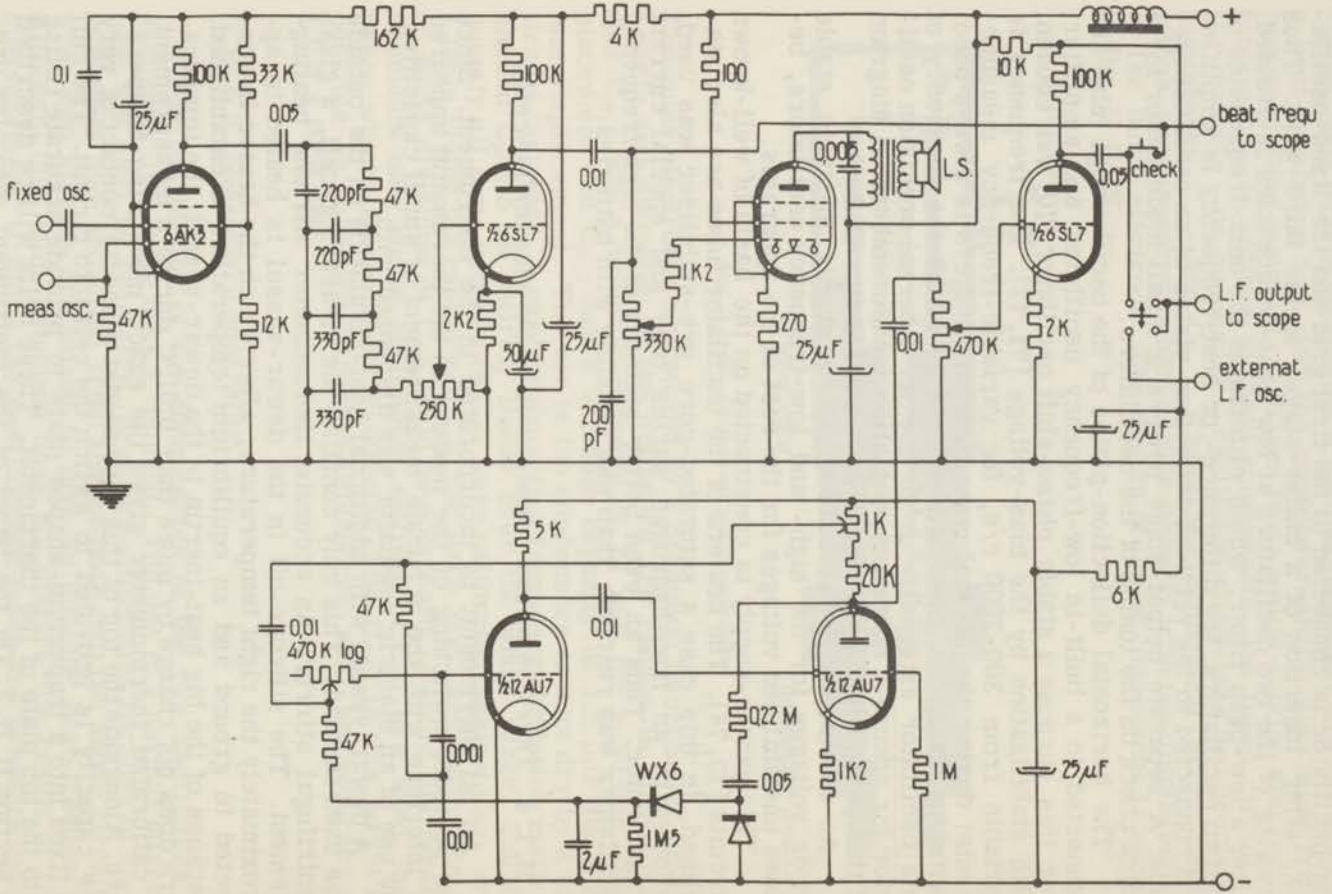

Fig. II.B.V. Additional circuits of the heterodyne method.

cision condensers an additional coaxial receptacle is fitted, for the connection of external measuring cells. This also takes the absolute cell, to be described below, that is used for the calibration of various other cells.

II.B.2. Measuring cells and accuracy

With the apparatus described capacity-measurements may be carried out over a range of 25 $\mu\mu$F with an accuracy of 0.01% $\pm$ 0.0005 $\mu\mu$F. Since the value of the unknown capacity is evaluated from the difference of two sets of readings on the precision-condensers, the relative accuracy will be dependent on the capacity of the unknown. The dimensions of the measuring cells are chosen in such a way that the best use is made of the range of the precision condensers.

The final accuracy of the permittivity values will be determined, however, by the accuracy to which the measuring cells can be calibrated. This leads to a pronounced difference between the absolute and the relative accuracy obtainable with this method. In the equation $C = C_{par.} + \varepsilon C_o$ for the capacity of the cell, filled with a liquid of relative permittivity ε, the value of C_o will not be constant for small cells. Besides other minor effects this is due to the fact that the fringing field of the cell-capacity comprises both the liquid in the cell and the glass walls. Thus the capacity due to the fringing field, and hence the value of C_o, will be dependent on the permittivity of the liquid. Since the value of the permittivity of the liquids to be measured is evaluated from the difference in capacity of the empty cell and the cell filled with liquid, the following equations apply:

$$\left.\begin{aligned} C_e &= C_{par.} + \varepsilon_0 C_0 \\ C_1 &= C_{par.} + \varepsilon C_{0\varepsilon} \end{aligned}\right\} \quad \Delta C = \varepsilon C_{0\varepsilon} - \varepsilon_0 C_0 \qquad \text{(II.B.2.1)}$$

The values of C_0 and of $C_{0\varepsilon}$ are dependent on permittivity, and must be determined by the measurement of a number of liquids of known permittivity. This sets a limit to the accuracy obtainable with the method, since reliable literature values are available only for a very limited number of liquids. Furthermore small discrepancies may result from differences in purity between the sample used for the calibration and the sample cited in the literature. In the permittivity-range from 2-2.5, which is of great importance for the determination of dipole moments from measurements on dilute solutions, cyclohexane, benzene and carbontetrachloride seem to be useful as calibrating liquids.

In order to eliminate the possibility of errors, due to impurities of the liquids as a result of the manufacturing process, the properties of these three compounds were carefully investigated. As a result cyclohexane and benzene were selected for the calibrations, carbontetrachloride being discarded for reasons described below:

Of the three compounds various samples from different manufacturers were purified according to standard procedures known in the literature (75,76). Finally the samples were carefully distilled and dried over a drying agent, after which their permittivities were determined over a temperature range of 20-50°C with a measuring cell described below. The measurements were repeated with a month's interval over a period of about half a year. The values of the density and refractive index were also checked against the literature values.

The values for cyclohexane were found to be the same for each sample and no variations with time could be detected. For benzene minor differences between the samples, amounting to about 5 units in the fourth decimal place, were found. The repeated measurements only check with the first series, if the samples are kept dry very carefully as can be seen from measurements of $\partial\epsilon/\partial T$. Since reliable values of the permittivity of cyclohexane and benzene were recently given by Hartshorn (63), these two compounds are very suitable for calibrations. For carbontetrachloride, recommended by several authors for the calibration of measuring cells, the permittivity values obtained for different samples deviated considerably. Furthermore the permittivity changes with time, unless the samples are kept very dry and light is excluded. Carbontetrachloride is purified in most cases by careful drying and distillation. For this investigation four p.a.samples were treated in this way. The results are given in table II.B.2.1. The permittivity values were obtained with a cell calibrated with benzene.

Table II.B.2.1. Measurements on CCl_4

Sample Manuf.	$\epsilon_{20°}$	$-\frac{\partial\epsilon}{\partial T}.10^3$	purification
I A. Hopkins-Williams p.a.	2.2374	1.98	drying and dist.
I B. "	2.2374	1.98	drying 7 days, dist.
II Schuchardt p.a.	2.2380	1.98	drying, dist.
III A. U.C.B. p.a.	2.2580	2.22	drying 24 hours, dist.
III B. U.C.B. p.a.	2.2510	2.08	drying 14 days
III C. U.C.B. p.a.	2.2436	2.16	drying, dist.
IV Merck p.a.	2.2372	1.975	drying, dist.

As can be seen from this table both prolonged drying and distillation are necessary. The differences between the samples must result from impurities that cannot be eliminated by this procedure. By the use of infrared spectra $CHCl_3$ and C_2HCl_3 were shown to be present in sample III C up to 5‰ and in sample II to 1.5‰ approximately.

Comparison of the measured values with the literature values for calibration purposes is hardly possible, since the origin and purity of the materials used, cannot be obtained in most cases, or the measuring accuracy is doubtful. Furthermore considerable differences exist between the various literature values as given in table II.B.2.2.

Table II.B.2.2. Literature values for CCl_4

Author	ϵ_{20}	$-\frac{\partial\epsilon}{\partial T}.10^3$	Reference
Davies	2.236	1.865	Phil.Mag.21.1008.1936
Cowley	2.234	2.05	J.Chem.Soc.1184.1936
Goss	2.2345	1.96	J.Chem.Soc.727.1935 I
Le Fêvre	2.2352	1.76	Trans.Farad.Soc.34.1127.1938
Rodebush	2.2355	2.00	J.Chem.Phys.8.889.1940
Miller'	2.2372	1.97	J.Am.Chem.Soc.64.117.1942
Clay,Dekker	2.2445	1.5	Physica X.768.1943
Mecke	2.2363	1.88	Z.Naturforschung 4a.182.1949 Angew.Phys.Chem.52.40.1948
Heston,Smyth	2.239	1.80	J.Am.Chem.Soc.72.99.1950
Treiber	2.2360	1.99	Monatshefte J.Chemie 81.627.1950 l.c. 82.32.1951

For higher permittivity values comparison with literature values for use in the calibrations of the cells becomes even more difficult. Therefore direct comparison of measurements on the same sample, both with an absolute cell and the cells to be calibrated was preferred.

In an absolute cell the capacity is directly proportional to the

permittivity of the liquid, without edge-effect corrections: $C=\varepsilon C_o$. With the cell described in section II.B.2.2. an accuracy of 0.2% was obtained over a wide range of permittivities.

Thus the absolute accuracy of the permittivity measurements will be limited to this value. Though for an absolute cell with a smaller permittivity range the accuracy may be improved to about 0.05%, no such cells were built, since for most purposes an absolute accuracy of 0.2% is sufficient. For applications requiring a very high precision, the relative accuracy is usually the main concern, as in the case of dipole moment determinations, where small variations in the permittivity with concentration or temperature must be measured. Hence the accuracy of the capacity-measurement is conclusive, resulting in a relative accuracy for the permittivity values of about 2 units in the fourth decimal place. Since the permittivity-values of our samples of benzene and cyclohexane, as measured with the low-frequency bridge and the absolute cell by this method, agreed with the values obtained by Hartshorn within the above limits, his values were used for the calibration of the small measuring-cells at these points. For higher permittivity-values the cells were calibrated with arbitrary liquids, first measured in the absolute cell.

II.B.2.1. Two small measuring-cells were constructed for the determination of dipole-moments and the accurate measurement of mixtures. The cells have a permittivity range of 1-3 and 1-10 respectively, with a liquid volume of 3.5 cc and 2 cc including the filling-tubes. The design of these cells is presented in fig.II.B.VI. They are a further development of the cells described in a former paper [38].
The cells are made from a special type of Jenaglass (16.III) that can be welded onto platinum. Two drawn platinum tubes, are coaxially welded onto glass tubes to form the two electrodes A and B. The inner electrode has a slightly larger diameter than the glass finger by which it is supported. The outer electrode has a slightly smaller diameter than the outer glass wall of the cell and is choosen a few millimeters longer than the inner electrode. These precautions reduce the edge-effect of the cell-capacity considerably, which results in a more linear relation between the permittivity of the liquid and the capacity of the cell. For filling the cell two glass capillaries are used, as shown in the fig. Connection to the electrodes is made with platinum wires, one leading through the central glass tube, to the needle contact on top of the cell. The three glass tubes, from which the cell is hanging in the thermostat, are clamped in a distyrene block, supported by the brass trapezium-shaped top plate of the cell. The outer electrode of the cell is connected to this plate, which fits exactly in the grounded top plate of the thermostat. The cells were extremely stable over a long period of time.

The capacity of this type of cell cannot be calculated accurately from its dimensions. Therefore the values of the cell-con-

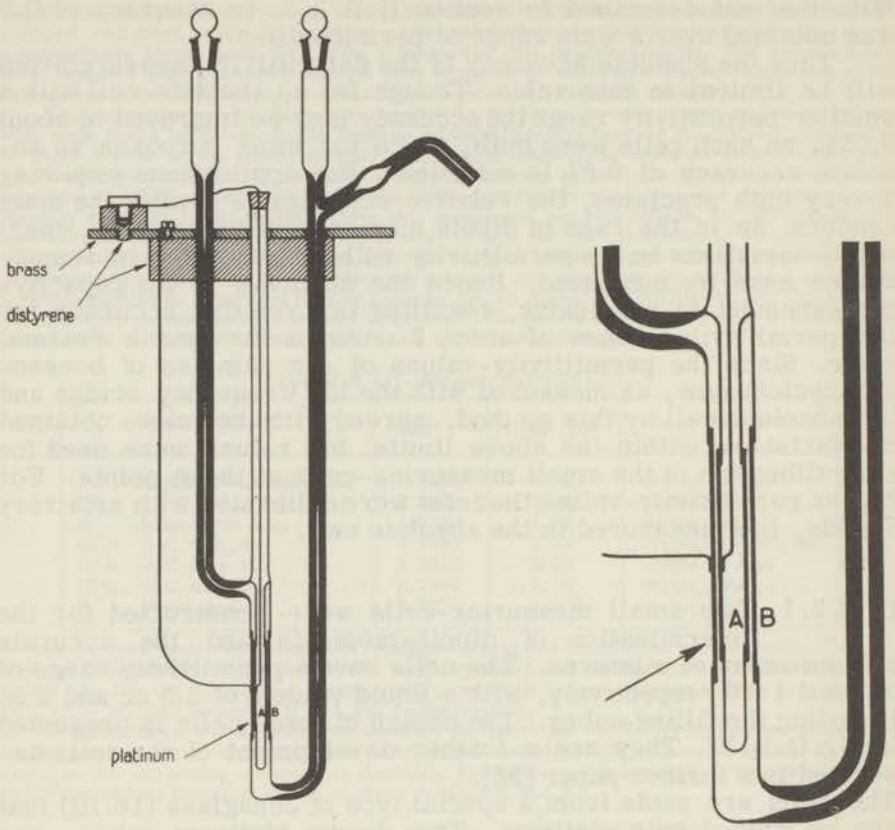

Fig. II.B.VI. Small measuring cell for liquids.

stants in relation to the permittivity of the liquid, were determined by the measurement of liquids of known permittivity according to equation II. B. 2. 1; written in a more convenient form

$$\Delta C = (\varepsilon - 1)(C'_o - \varepsilon C''_o) \qquad \text{(II. B. 2. 2)}$$

where C''_o is the part of the cell constant that varies with the permittivity of the liquid.

Besides the values of ε obtained with the absolute cell, the following values given by Hartshorn (H) were used:

Benzene $\varepsilon_{20} = 2.2836$ (H) $\frac{\partial \varepsilon}{\partial T} = -0.00190$

Cyclohexane $\varepsilon_{20} = 2.0250$ (H) $\frac{\partial \varepsilon}{\partial T} = -0.00155$

Since only relative values are concerned, the values of ΔC, C'_o and C''_o in terms of the micrometer readings are used directly, without converting them to $\mu\mu F$.

A. cell with permittivity range 1-10.
This cell was calibrated at 30° centrigrade with benzene, cyclohexane, carbontetrachloride, a number of mixtures of benzene and bromobenzene, and pure bromobenzene. The permittivity values obtained with the absolute cell were used together with the values given above for cyclohexane and benzene. The values obtained for the cell constants are:

cell A. $C'_o = 28.900$
$C''_o = 0.366$

The permittivity-values are best obtained from the measured ΔC-values by a few successive approximations. A few comparative results are given in table II. B. 2. 3.

Table II. B. 2. 3

	$(\varepsilon_{abs})\ 30^o$	$(\Delta C)_{meas}$	$\varepsilon_{cell\ A}$
C_6H_{12}	2.0095 (H)	28.420	2.0090
CCl_4	2.216	34.170	2.2165
C_6H_6	2.2646 (H)	35.515	2.2652
C_6H_6/C_6H_5Br	3.460	67.915	3.4580
C_6H_5Br	5.301	115.92	5.2997

B. cell with permittivity range 1-3.
This cell is generally used for the dipolemoment determinations. It was calibrated at four temperatures between 20 and 40°C with n. hexane, cyclohexane, carbontetrachloride, and benzene. It appeared that for this cell, which due to its dimensions has a far smaller edge-effect than cell A, one cell constant C_o can be used for the four liquids and a different value only has to be inserted for the air value. Thus a simpler calculation of the permittivity-values from the capacity-readings results:

$$\Delta C = \varepsilon C_o - \varepsilon_o C'_o \qquad \text{(II. B. 2. 3)}$$

The values of C_o and $\varepsilon_o C'_o$ were evaluated statistically from the measurements of the four liquids at four different temperatures. The resulting values are:

cell B. $C_o = 77.98$
$\varepsilon_o C'_o = 78.70.$

The permittivity values obtained with these values at 30° centrigrade, as compared with the standard values, are given in table II. B. 2. 4.
The two sets of values given for C_6H_{12} and C_6H_6 relate to two different samples measured with a few weeks interval.

Table II. B. 2. 4.

	(ε_{abs}) 30°	$(\Delta C)_{meas}$	$\varepsilon_{cell\ B}$
n. C_6H_{14}	1.8743	67.605	1.8762
C_6H_{12}	2.0095 (H)	78.010	2.0096
		78.035	2.0099
CCl_4	2.216	94.285	2.2183
C_6H_6	2.2646 (H)	97.895	2.2646
		97.877	2.2644

II. B. 2. 2. *Absolute cell*

The principle of an absolute cell is drawn in fig. II. B. VII.

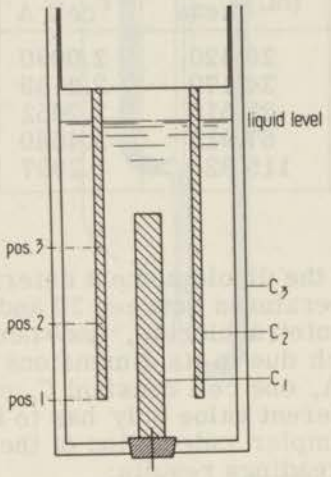

Fig. II.B.VII. Principle of an absolute cell.

Three cylindrical electrodes, C_1, C_2 and C_3 are mounted coaxially, as indicated. C_1 is placed on a quartz insulator in the bottom of C_3. C_2 and C_3 are connected together via the plunger on top of the cell.

The capacity of the cell will be given by the sum of the capacities of two coaxial condensers, C_1-C_2 and C_1-C_3, and their associated edge-effects. The edge-effects will consist of capacities from the top of C_1 to C_2 and from the lower side of C_2 to C_1. When C_2 is moved, e.g. from position 1 to position 2 or 3, the coaxial capacities will change, but the edge-effects remain the same. Thus the capacity change of the cell for a given displacement of C_2 can be calculated, starting from the well known equation for coaxial capacitors:

$$\Delta C = \frac{\Delta l}{2}\left(\frac{1}{\log_e r_2/r_1} - \frac{1}{\log_e r_3/r_1}\right) \qquad \text{(II. B. 2. 4)}$$

The same equation applies, with a multiplication factor ε, when the cell is filled with a liquid having a permittivity ε. Care must be taken that the cell is filled high enough and that C_2 in its lowest position is still far enough from the bottom of the cell so as not to disturb its normal edge-effect. These limits are best determined experimentally, by checks on the linearity of the cell. Furthermore the cell must be machiened very carefully to establish a really concentric movement of C_2 with respect to both C_1 and C_3. In our cell the outer diameter of C_1 is 5 mm and the inside diameters of C_2 and C_3 are 10 and 15 mm respectively.

The movement of C_2 is controlled by a micrometer with a range of 25 mm and an accuracy within 0.002 mm.

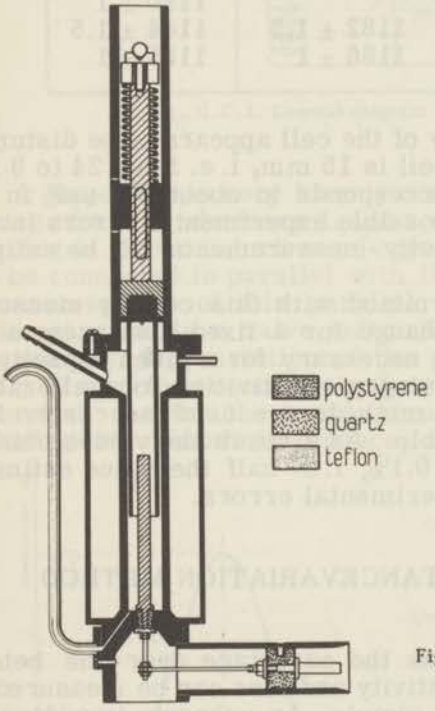

Fig. II.B.VIII. Details of an absolute measuring cell for liquids.

Further details of this cell are given in fig. II. B. VIII. The liquid volume of the cell is about 18 cm^3. The linearity of the cell was calibrated with a frequency-deviation method, by measuring the frequency shifts of the measuring oscillator for fixed increments of the C_2 micrometer over its whole range. This calibration was carried out with bromobenzene, that in consequence of its permittivity, gave convenient frequency shifts per mm. displacement of C_2. The cell-temperature was kept constant at $30 \pm 0.01^{\circ}$ centrigrade by means of a circulating thermostat.

The results of the calibrations, taken with 3 and 5 mm in-

crements are given in table II.B.2.5. The values for the 5 mm increments are multiplied by 3/5 for easy comparison with the values of the 3 mm increments. Three series were measured in each case; the deviations recorded give the extreme values of the measurements.

microm. readings		$\frac{3}{5}(\Delta f)_{5mm.}$	$(\Delta f)_{3mm.}$
25-20	24-21	1181 ± 1.5	1180 ± 2
	21-18		1179 ± 0.5
20-15	18-15	1180 ± 1	1179 ± 1.5
15-10	15-12	1179 ± 1	1179 ± 1
	12-9		1180 ± 1
10-5	9-6	1182 ± 1.5	1184 ± 1.5
5-0	6-3	1186 ± 1	1185 ± 1

At values below 9 the linearity of the cell appears to be disturbed. Thus the useful range of the cell is 15 mm, i.e. from 24 to 9 mm. on the micrometer. This corresponds to about 0.4 μμF in air. By considering the various possible experimental errors involved, the errors of the permittivity-measurements can be estimated as less than 0.2%.

Permittivities are determined with this cell by measuring the capacity- or frequency-change for a fixed displacement of C_2, or the displacement of C_2 necessary for a given capacity- or frequency-change. In determining permittivities for calibration-work on other cells all four methods are used successively to reduce errors as far as possible. As a result the values obtained appear to be reliable to about 0.1%, i.e. half the value estimated from the various possible experimental errors.

II.C. RESONANCE OR REACTANCEVARIATION METHOD (0.5 - 10 Mc/s)

The resonance-method has the advantage over the heterodyne-method that both permittivity and loss can be measured. In principle the method is very simple. An unknown impedance is connected in parallel with a tuned circuit consisting of a selfinductance and a precision condenser. From the shift of the resonant frequency or the capacity change necessary to restore the original frequency, and the change of the quality-factor Q of the tuned circuit, both capacity and loss tangent of the unknown impedance may be determined [77].

Consequently the method has found many applications, in various forms, though mainly for the measurement of coils for commercial purposes. In the literature several instruments are described for the measurement of the dielectric properties of materials with this method [78, 79, 80]. The best known of these

undoubtedly is the reactance-variation method described by Hartshorn [19]. In broad outline the instruments are constructed as indicated in fig. II.C.1.

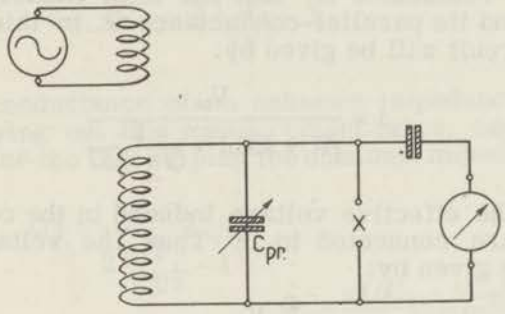

Fig. II.C.I. General diagram of a resonance method.

A generator is very loosely coupled to a resonantcircuit consisting of a selfinductance L and a calibrated condenser C_{pr}. The coupling is either inductive or capacitive. The unknown impedance can be connected in parallel with the condenser. To measure the resonant-voltage of this parallel combination an indicating instrument, usually a valve voltmeter, is connected to the circuit in some way. By variation of the generator frequency or the capacity around the resonance-value, two resonance-curves may be dilineated, one for the tuned circuit alone and one for the circuit including the unknown impedance, as indicated in fig. II.C.II.

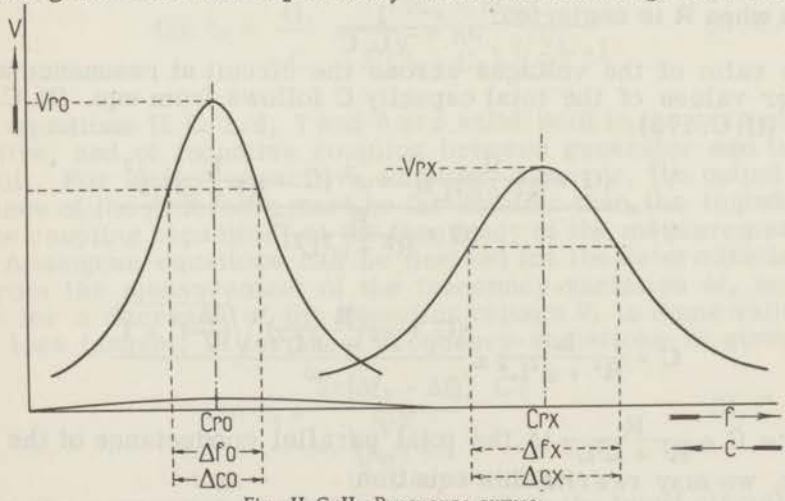

Fig. II.C.II. Resonance curves.

From these data both capacity and loss tangent of the unknown impedance may be evaluated.

II.C.1. Theoretical background of the resonance-method

Considering fig. II.C.I, we may assume that the inductance L has a series resistance R, that the total capacity in the tuned circuit is C and its parallel-conductance G. In this case the current in the circuit will be given by:

$$i = \frac{V_\infty}{(R + j\omega L) + \frac{1}{G + j\omega C}} \qquad \text{(II.C.1.1)}$$

where V_∞ is the effective voltage induced in the coil, if no other components are connected to it. Thus the voltage across the circuit will be given by:

$$V = \frac{i}{G + j\omega C} = \frac{V_\infty}{(R + j\omega L)(G + j\omega C) + 1}$$

or

$$V = \frac{V_\infty}{(R + j\omega L)} \frac{1}{G + \frac{R}{R^2 + \omega^2 L^2} + j\omega\left(C - \frac{L}{R^2 + \omega^2 L^2}\right)} \qquad \text{(II.C.1.2)}$$

For a certain frequency $\omega = \omega_R$ the voltage across the circuit will therefore reach a maximum, i.e. resonance will be established, when

$$C = \frac{L}{R^2 + \omega^2 L^2} = C_R \qquad \text{(II.C.1.3)}$$

The simple relation for a resonant circuit follows from this equation when R is neglected: $\omega_R = \frac{1}{\sqrt{L.C}}$

The ratio of the voltages across the circuit at resonance and at other values of the total capacity C follows from equ. (II.C.1.2) and (II.C.1.3):

$$\frac{V_r^2}{V^2} = \frac{\left(G + \frac{R}{R^2 + \omega^2 L^2}\right)^2 + \omega^2 \left(C - \frac{L}{R^2 + \omega^2 L^2}\right)^2}{\left(G + \frac{R}{R^2 + \omega^2 L^2}\right)^2}$$

or

$$C = \frac{L}{R^2 + \omega^2 L^2} \pm \frac{\left(G + \frac{R}{R^2 + \omega^2 L^2}\right)\sqrt{\left(\frac{V_r}{V}\right)^2 - 1}}{\omega}$$

Since $G + \frac{R}{R^2 + \omega^2 L^2}$ is the total parallel conductance of the circuit, we may rewrite this equation:

$$C = C_R \pm \frac{G_T \sqrt{\frac{V_r^2}{V^2} - 1}}{\omega} \qquad \text{(II.C.1.4)}$$

From two values of C, equidistant from C_r, for which the same voltage occurs (see fig. II. C. II), the total conductance is found:

$$G_T = \frac{\omega \Delta C}{2\sqrt{\frac{V_r^2}{V^2} - 1}} \qquad \text{(II. C. 1. 5)}$$

The parallel conductance of an unknown impedance can be evaluated by carrying out this measurement twice, once for the circuit and once for the circuit plus the unknown impedance:

$$G'_T = \frac{\omega \Delta C_0}{2\sqrt{\frac{V_r^2}{V^2} - 1}}$$

$$G_T = \frac{\omega \Delta C_x}{2\sqrt{\frac{V_r^2}{V^2} - 1}} \qquad G_x = \frac{\omega(\Delta C_x - \Delta C_0)}{2\sqrt{\frac{V_r^2}{V^2} - 1}} \qquad \text{(II. C. 1. 6)}$$

The value of the unknown capacity follows directly from the differences in C_R, when the unknown impedance is added to the circuit, parasitic impedances being left out of account:

$$C_x = C'_R - R_R \qquad \text{(II. C. 1. 7)}$$

The loss-tangent will then be given by:

$$\tan \delta_x = \frac{G_x}{\omega C_x} = \frac{(\Delta C_x - \Delta C_0)}{2(C'_R - C_R)\sqrt{\frac{V_r^2}{V^2} - 1}} \qquad \text{(II. C. 1. 8)}$$

The equations II. C. 1. 6, 7 and 8 are valid both in the case of capacitive, and of inductive coupling between generator and tuned circuit. For stiffer capacitive coupling, however, the output impedance of the generator must be far smaller than the impedance of the coupling capacitor at the frequency of the measurement.

Analogous equations can be derived for the determination of G_x from the measurement of the frequency-variation Δf, necessary for a decrease of the resonant voltage V_r to some value V. The loss tangent, in terms of frequency-variations is given by:

$$\tan \delta_x = \frac{2\pi(\Delta f_x - \Delta f_0)\ C_T}{\omega_r \sqrt{\frac{V_r^2}{V^2} - 1}\ C_x} \qquad \text{(II. C. 1. 9)}$$

Since the connection of a lossy capacitor to the tuned circuit results in a decrease of the resonant voltage, determination of the loss tangent is also possible from a measurement of the ratio of

the resonant voltage before and after the connection of the unknown impedance. This method is especially useful for the measurement of medium and high losses, since the resonance curve in this instance will be very flat, which leads to difficulties in determining the width of the curve at the voltage V. Moreover equ. II.C.1.8 loses its exact validity, when considerable loss is introduced in the circuit [81, 82].

If V_{ro} is the resonant voltage of the measuring-circuit alone and V_{rx} is the resulting resonant voltage, after connection of the unknown impedance, the ratio of these voltages follows directly from equ. II.C.1.2.

$$\frac{V_{ro}}{V_{rx}} = \frac{G + \frac{R}{R^2 + \omega^2 L^2}}{G - G_x + \frac{R}{R^2 + \omega^2 L^2}} = \frac{G_T}{G'_T} \qquad \text{(II.C.1.10)}$$

The value of $tg\delta_x$, after insertion of the values of G_T and G'_T given in equ. II.C.1.6, is given by:

$$tg\delta_x = \frac{(\frac{V_{ro}}{V_{rx}} - 1)\Delta C_o}{2C_x \sqrt{\frac{V_r^2}{V^2} - 1}} \qquad \text{(II.C.1.11)}$$

Thus the loss tangent of the unknown is directly proportional to the ratio of the two resonant voltages, after the properties of the measuring-circuit alone are determined by the capacity-variation method.

As was stated before, the influence of parasitic impedances was left out of account in the derivation of the above equations. Moreover any possible influence of the indicating instrument on the results was neglected. In section II.C.2 it will be shown that the indicating instrument is one of the main sources of error in resonance methods. The influence of other possible sources of error will also be discussed there.

II.C.2. Description of the apparatus

The apparatus was constructed according to the diagram shown in fig. II.C.III.
An accuracy of 0.2% for capacity- and 1% for loss-measurements was aimed at. This necessitates high stability of both generator and detector (indicating instrument) during the measurements. A commercial generator of high frequency- and output-stability drives the tuned circuit through a variable coupling capacitor of 1-10 $\mu\mu$F. In the tuned circuit the two capacitors C_1 and C_{prec} and the receptacle for the measuring cells are interconnected by short wires, to reduce the influence of parasitic series induc-

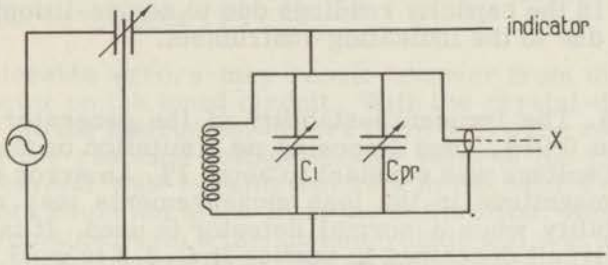

Fig. II.C.III. Circuit of the resonance method.

tance. C_1 has a variable capacity of 100 $\mu\mu$F, divided into 5000 scale divisions by means of a precision drive. This condenser serves the purpose of tuning the circuit to resonance and measuring the unknown capacities. The condenser C_{pr} is a piston-condenser of the type described in section II.B.1, with a variable capacity of 24 $\mu\mu$F over 5000 scale-divisions of a micrometer. With this condenser the widths of the resonance curves at a certain voltage, ΔC_o and ΔC_x, needed for the loss-measurements, are determined.

Both condensers were calibrated at a frequency of 10 000 c/s with the low frequency bridge after they were built into the instrument, by disconnecting the inductance L.

The inductances are made exchangeable. By using ten different inductances the circuit can be made to resonate at convenient settings of C_1, over the frequency-range of 0.5-20 Mc/s. The coils were wound from copper wire on grooved polythene cores, for high stability and low losses. They are connected into the circuit by silvered plugs and sockets.

Originally a crystal-diode with a sensitive μA-meter was used as indicating instrument because of its good frequency-characteristic. This detector was replaced by a special vacuum tube voltmeter for reasons given in section II.C.2.1.3. High stability of the circuit was reached by building all components together in a heavy brass enclosure, provided with a lid for the replacement of the coils and a drying agent to maintain low and constant humidity. Nevertheless the errors with the original circuit amounted to about 10% for the loss-measurements, depending on the value of the loss tangent and various other factors. Since these errors turned out to be inherent to the method, the various sources of error will be dealt with first.

II.C.2.1. *Possible sources of error*

a. errors due to instability of the generator.
b. errors in the capacity readings due to series-inductance.
c. errors due to the indicating-instrument.

II.C.2.1.a. The frequency-stability of the generator used, was better than 0.01%, thus imposing no limitation on the accuracy. The output voltage was constant to about 1%. An error of the same order of magnitude in the loss measurements may result from this instability when a normal detector is used. It is eliminated when the circuit described in section II.C.2.2 is used.

II.C.2.1.b. At high frequencies the effective capacity of the condensers rises above the value determined in the low-frequency calibration, as a result of the series inductance of the condensers and their connecting wires:

$$C_{eff} = \frac{C}{1 - \omega^2 L C} \qquad \text{(II.C.2.1)}$$

where C is the low frequency value of the capacity and L the total series inductance. The same equation applies to the capacity of the measuring cell, which has a series inductance L_x. The values of L and L_x may be determined, in the circuit by a method introduced by Field and Sinclair [83, 84] for high frequency bridges. This method will be considered in detail in section II.D.1.1. With the values of L and L_x thus obtained, the scale readings of C_1 and C_{prec} are corrected according to equation (II.C.2.1). Within the measuring accuracy the effective capacity of the unknown, found from the difference of two readings C_1' and C_1, will be given by:

$$(C_x)_{eff} = \frac{C_1' - C_1}{1 - \omega^2 L_c (C_1' + C_1)} \qquad \text{(II.C.2.3)}$$

the true value of C_x can then be evaluated from the equation:

$$C_x = \frac{(C_x)_{eff}}{1 + \omega^2 L_x (C_x)_{eff}} \qquad \text{(II.C.2.4)}$$

II.C.2.1.c. Errors in the readings of the indicating-instrument due to scale-deviations or variations of the characteristic of the detector with input-voltage can be eliminated to a large extent by careful calibration. If a crystal- or thermoionic-diode is used for the rectification of the high frequency voltage across the resonant circuit, the current in the μA-meter will be proportional to the square of the A.C. voltage at low input-voltages. This square-law characteristic will gradually change to a linear characteristic

at higher voltages (e.g. between 0.5 and 10 volts), but is frequency independent within a wide range of frequencies. The resultant error, after calibration, affects only the loss-measurements and may be reduced to about 1%.

Considerable errors may result however from the influence of the detector on the tuned circuit. With the crystal-diode originally used in the instrument errors up to 10% were recorded depending on the resonant voltage and the value of the loss tangent. Since the crystal was working entirely in the square-law region these errors could not arise from the calibration. Analogous results were obtained with a thermoionic diode and a grid-detector. Variations in the input impedance of the detector, and hence the loading of the resonant circuit, with input-voltage seemed to be the most obvious reason for the errors; for, if the loading of the tuned circuit varies when the resonance curve is delineated, wrong G_T values will be the result. Therefore the inherent losses of the circuit with the various detectors connected to it, were determined at one frequency with varying input voltage.

For these measurements a high frequency amplifier-voltmeter with constant and high input impedance was connected to the tuned circuit. With this voltmeter the inherent losses or Q-factors of the circuit, at ten resonant voltages ranging from 30 millivolts to 10 volts, were measured at a frequency of 1.5 Mc/s, when the various detectors were connected in turn. Thus possible variations in the input resistance of the detectors could be plotted against input voltage as variations of the Q-factor of the circuit, according to equation II.C.1.5.

$$Q = \frac{1}{\tan\delta} = \frac{\omega C_T}{G_T} = \frac{2C_T\sqrt{\frac{V_r^2}{V^2} - 1}}{\Delta C}$$

whereas the variations in the input capacity were given by the changes in C_T. A constant value of $Q = 160$ and C_T was found over the whole voltage-range for the tuned circuit and amplifier-voltmeter, when none of the other detectors was connected into circuit.

The following detectors were investigated in succession:

1. a germanium diode, type OA 56.
2. a germanium diode, type OA 72.
3. a thermoionic diode, RCA type 9006.
4. a grid-detector with a twin-triode, type 12 AU 7 (ampl. factor 20).
5. a grid-detector with a twin-triode, type 12 AT 7 (ampl. factor 60).
6. an "infinite"-impedance detector with a triode having an ampl. factor 100.

Since only simple standard-circuits were used, the diagrams of the circuits may be omitted here.

The variations of the Q-factor of the circuit for the various detectors are plotted in fig.II.C.IV. A few representative data for the input-capacity and input-resistance of detectors, calculated from the measurements are given in table II.C.2.1.

Detector 1			3		4		6	
V_{input} volts	C_i $\mu\mu F$	R_i Megohms	C_i	R_i	C_i	R_i	C_i	R_i
0.03	2.9	0.048	11.6	0.056	7.65	0.21		
0.1	2.3	0.086	11.6	0.072	7.45	0.20	4.0	1.77
0.3	1.9	0.11	11.4	0.13	7.3	0.20	4.0	1.77
1	1.5	0.13	11.3	0.19	7.3	0.19[5]	3.85	0.88
3	1.3	0.14	11.1	0.24	7.3	0.19[5]	3.80	0.53
10	1.25	0.066	11.1	0.24[5]			3.80	0.59

Table II.C.2.1.

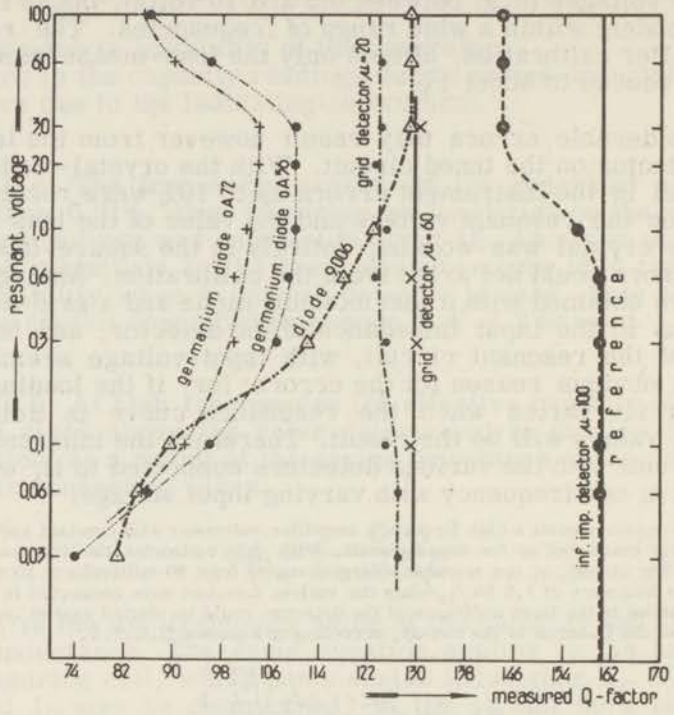

Fig. II.C.IV. Changes in the Q-factor with resonant voltage for various detectors.

It is evident from these results that the use of a germanium-diode is not permissible for this application, since the input-resistance is strongly dependent on the input voltage. The linear current-voltage characteristic of a thermoionic diode for voltages above 3-10 Volts is generally known. Since the alternating-current input-impedance of a diode is inversely proportional to the slope in the operating point (85), a simple calculation shows, that for voltages below 3 Volts the input resistance must fall considerably below the value usually given in text books (32, 86) i.e. $\frac{1}{2}R$ for series-diode circuits and $\frac{1}{3}R$ for parallel-diode circuits. In the voltage-range from zero to ten volts the loading of the circuit by the diode varies considerably, while the diode-characteristic gradually changes over from quadratic to linear. Moreover the input capacity of the circuit also changes to some extent.

The "infinite-impedance" detector has an almost constant input-impedance for voltages below 0,5 Volts and above 3 Volts. In the intermediate region the input-impedance decreases, while the detector-characteristic changes over from quadratic into linear. At low voltages the circuit is very insensitive.

With a grid-detector a reasonable accuracy may be obtained, if the electrode-voltages are chosen carefully and a valve with high mutual conductance is used. The detector-characteristic very gradually changes from quadratic to linear and is strongly dependent on the properties of the individual valve and its electrode-voltages, necessitating a calibration-curve and stabilisation of the supply-voltages. A circuit tested is reproduced in fig. II.C.V.

The input-capacity is virtually constant over the whole voltage range. The poor sensitivity of this circuit necessitates the use of a very sensitive currentmeter in the anode-circuit. As a result slight instabilities of the valve or the supply-voltages become very cumbersome.

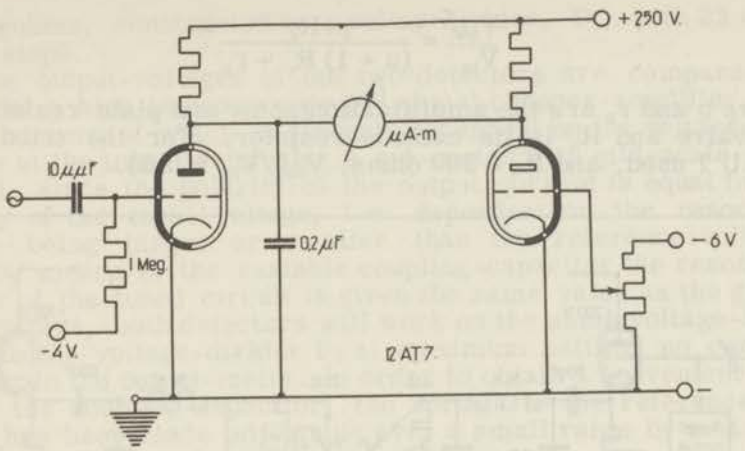

Fig. II.C.V. Circuit of a grid-detector.

It will be clear from the aforesaid that the variations in the impedance of the indicating-instrument with input-voltage, when the resonance-curve is delineated, may reduce the accuracy of the resonance-method considerably. It is for this reason that for most instruments based on this method a maximum accuracy of 5% is given for the loss-measurements.

Though a higher accuracy can be obtained by careful stabilisation and construction of a grid-detector [77], another circuit was used in our instrument. This circuit, described in section II.C.2.2, has a constant input-impedance and eliminates possible errors due to variations in the output voltage of the generator (see II.C.2.1.a). Since errors due to the calibration of the meter are also eliminated to a large extent, a better overall accuracy may be expected with this circuit.

II.C.2.2.

The circuit of this indicating instrument is drawn in fig. II.C.VI.
The voltage across the tuned circuit drives the grid of a cathode-follower. The output voltage of this stage, which essentially is an impedance transformer, is rectified by a germanium-diode and subsequently filtered. Thus a d.c. voltage proportional to the voltage across the tuned circuit will be developed across the load resistor R_L of 0.5 Megohm. Because of the high input-impedance of the cathode follower, the loading of the tuned circuit is negligeable, resulting in a high Q-factor of 210 at 1.5 Mc/s. The cathode output-voltage of this stage is directly proportional to the grid voltage according to [87, 88]:

$$\frac{V_{out}}{V_{in}} = \frac{\mu . R_c}{(\mu + 1) R_c + r_p},$$

where μ and r_p are the amplificationfactor and plate resistance of the valve and R_c is its cathode-resistor. For the triode, type 12 AU 7 used, and $R_c = 800$ ohms, $V_{out}/V_{in} \approx 0.65$.

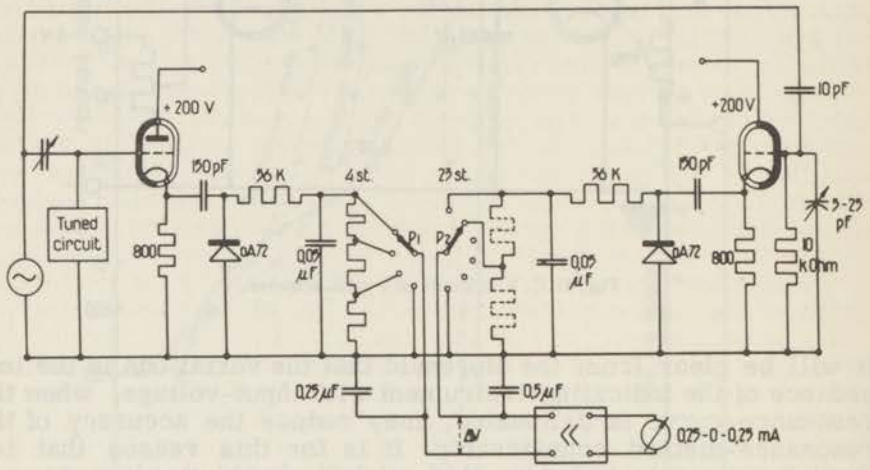

Fig. II.C.VI. Detector-circuit of the resonance-method, with twin triode 12 AU7 and matched diodes 0A72.

The output impedance is very low, i.e. according to the equation [87]:

$$R_o = \frac{1}{g_m + \frac{1}{R_c} + \frac{1}{r_p}} \approx \frac{10^3}{2.2 + 1.25 + 0.13} \approx 250 \text{ ohms},$$

where g_m is the mutual conductance of the triode. Thus variations of the impedance of the crystal-rectifier are of no consequence. The voltage calibration of the diode OA72 appeared to be linear above 300 millivolts, D.C. output, corresponding to a resonant voltage of 600 millivolts at the grid of the triode.

Below these voltages a calibration-curve must be used. With a resonant voltage of about 8 Volts, giving a D.C. output-voltage of 5 Volts, the maximum grid-swing of the input-circuit is reached, which results in deviations from linearity and added loading of the tuned circuit by the flow of grid current. Without reference to the calibration curve, the arrangement may therefore be used with resonant-voltages between 0.6 and 7.5 Volts.

To reduce the influence of variations in the output-voltage of the generator and to improve the accuracy of the meter-readings, the generator-output is simultaneously fed into a second or reference detector-circuit identical with the first one. The D.C.-output of this detector is also connected to a load resistor of

0.5 Megohms, constructed as a voltagedivider, P_2, with 22 calibrated steps.

The output-voltages of the two detectors are compared by means of a high-impedance ($\approx 10^9$ ohms) chopper-amplifier, the output current of which is linearly dependent on the voltage-difference at the input-terminals. A mA-meter with mid-scale zero is used, since the polarity of the output current is equal to the polarity of the input voltage, i.e. dependent on the resonant-voltage being larger or smaller than the reference-voltage. When by means of the variable coupling-capacitor the resonant-voltage of the tuned circuit is given the same value as the generator voltage, both detectors will work on the same voltage-level and with the voltage-divider P_2 at maximum setting, no current will flow in the output-meter. In order to obtain a convenient setting of the coupling-capacitor, the voltage to the reference detector has been made adjustable over a small range by means of a capacitive voltage divider.

Resonance curves may now be delineated by measuring the width of the curve between two points for which a zero detector-reading is obtained, at a given setting of the voltage divider P_2. Thus two points on the resonance curve are established, where the voltage across the circuit is a certain fraction of the resonant-voltage. From the ΔC values measured in this way, conductance or loss values may be evaluated with equ. II.C.1.6 or II.C.1.8. A number of values for the same loss tangent are easily obtained by taking the ΔC-readings for various settings of P_2, which gives a useful check on the precision of the measurements.

Variations in the generator ourput-voltage are of no consequence for the results, since the detector and reference-detector voltages are changed in the same way. When a zero detector-reading is established for an arbitrary setting of P_2, the generator output can be changed from 1 to 3 Volts without any detectable shift of the zero-reading. A voltage divider P_1 is incorporated to provide an internal check on the resonant voltage of the tuned circuit, when P_2 is set to zero (short circuited).

For the measurement of large loss tangents equation II.C.1.11 is used. After the measurement of the ΔC_o value for the tuned circuit alone, the ratio V_o/V_x of the two resonant-voltages, with and without the unknown impedance, is determined with P_2. Interpolation between two steps of P_2 is effected by means of the readings of the mA-meter in the detector output-circuit. A full-scale reading of 0.25 mA is obtained for a voltage-difference of 50 millivolts at the amplifier input, resulting in a sensitivity of about 1 millivolt for the determination of the ΔC-values and the ratio V_o/V_x. This sensitivity could not be obtained with a direct indicating-instrument e.g. a diode and galvanometer. Preliminary adjustments are facilitated by the use of a shunt-resistor across the mA-meter.

One point must be stressed here in connection with the use of linear detectors. Even with a linear detector, the ratio of the

measured D.C. voltages will only be equal to the ratio of the applied A.C. voltages, when the linear plot of D.C. versus A.C. voltages passes through the origin. Since all diodes have a quadratic characteristic at low voltages, this condition will not be fulfilled and considerable errors may result.

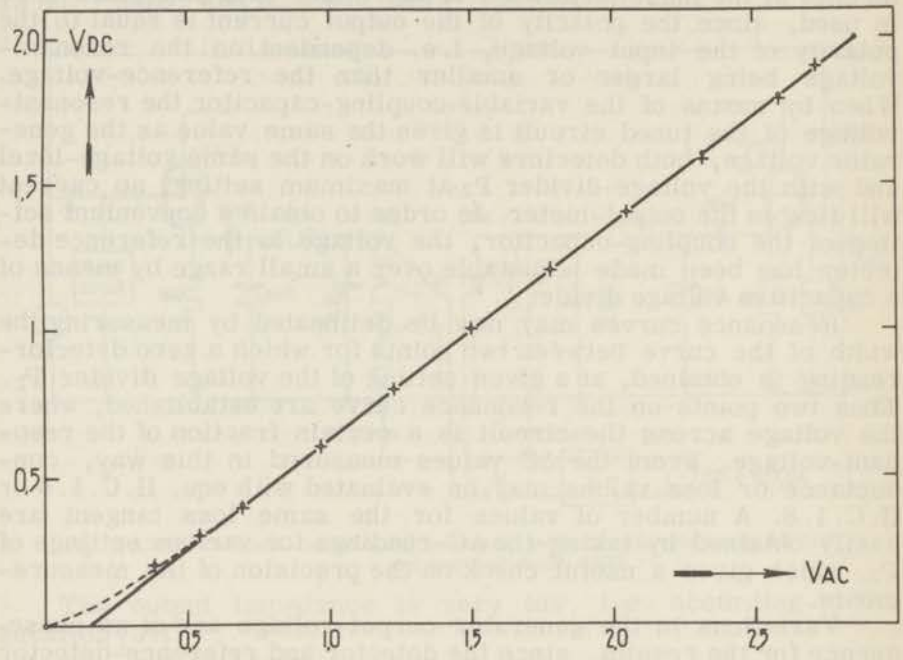

Fig. II.C.VII. Calibration curve of the cathode-follower detector.
+ calibration by voltage variation to the resonant circuit.
o calibration with the built-in voltage divider.

Fig. II. C. VII shows the calibration curve of the detector-circuit described above. The extrapolated linear part of this graph and the ordinate-axis intersect at a value of -0.111 Volt, while the slope of the line equals 0.736; these values were obtained by statistical evaluation of 25 measuring points. Thus the linear part of the detector-characteristic is given by:

$$V_{DC} = 0.736\ V_{AC} - 0.111 \qquad \text{(II. C. 2. 5)}$$

The ratio of the A. C. voltages across the tuned circuit will therefore be given by the ratio of the DC voltages increased by 0.111 Volt:

$$\left(\frac{V_{res}}{V}\right)_{AC} = \frac{(V_{res})_{DC} + 0.111}{V_{DC} + 0.111} \qquad \text{(II. C. 2. 6)}$$

II.C.3. Experimental procedure, and accuracy

II.C.3.1. By the choice of the appropriate self-inductance, the tuned circuit is made to resonate at the measuring frequency for a high value of C_1 (see fig. II.C.III). The output voltages of the detector and reference detector are both set to 2 Volts by means of the generator output control and the variable coupling capacitor.

For various settings of the voltage divider P_2 the widths of the resonance curve are measured with C_{prec}. With the ΔC_o-values obtained in connection with the voltage ratio's given by P_2, a number of values for the parallel conductance of the tuned circuit are evaluated by the use of equ. II.C.1.5, the correction given by equ. II.C.2.6 being taken into account:

$$G'_T = \frac{\omega \Delta C_o}{2\sqrt{\left(\frac{V_{res\ D.C.} + 0.111}{V_{D.C.} + 0.111}\right)^2 - 1}}, \qquad \text{(II.C.3.1)}$$

where V_{DC} equals 0.8, 0.75, 0.70..... $V_{res\ D.C.}$. From these values an average value of G'_T is calculated.

After connection of the unknown, e.g. a measuring cell, the circuit is made to resonate again by varying C_1. The effective capacity of the unknown is calculated with equ. II.C.2.3:

$$(C_x)_{eff} = \frac{C'_1 - C_1}{1 - \omega^2 L_c (C'_1 + C_1)} \qquad \text{(II.C.3.2)}$$

Since the top of the resonance curve is relatively flat, the exact value of C'_1 and C_1 is best obtained by bracketting with the detector. The true value of C_x is determined from $(C_x)_{eff}$ according to equ. II.C.2.4:

$$C_x = \frac{(C_x)_{eff}}{1 + \omega^2 L_x (C_x)_{eff}} \qquad \text{(II.C.3.3)}$$

where L_x is the series inductance of the unknown capacity. After the measurement of C_x the resonant voltage is restored to 2 Volts by means of the coupling capacitor and the value of the total parallel conductance of the circuit and the unknown is determined in the same way as G'_T:

$$G_T = \frac{\omega \Delta C_x}{2\sqrt{\left(\frac{V_{res\ DC} + 0.111}{V_{DC} + 0.111}\right)^2 - 1}} \qquad \text{(II.C.3.1a)}$$

The value of the loss tangent is calculated, from G'_T and G_T, according to equ. II.C.1.8:

$$\tan \delta_x = \frac{G_x}{\omega C_x} = \frac{G_T - G'_T}{\omega C_x} \qquad \text{(II.C.3.4)}$$

For the determination of high losses the measurement of the decrease of the resonant voltage may be used to advantage. First G'_T is determined as described, and subsequently the ratio of the resonant voltages of the circuit with and without the unknown. The loss tangent may then be evaluated, by combining the equations II.C.1.8 and II.C.1.10, from the equation

$$\tan \delta_x = \left\{ \frac{V_o + 0.111}{V_x + 0.111} - 1 \right\} \frac{G'_T}{\omega C_x} \qquad \text{(II.C.3.5)}$$

where V_o and V_x are the resonant voltages of the tuned circuit without – and with – the unknown respectively.

Theoretically the ΔC values, read from the precision condenser C_{pr}, must be corrected for the series inductance of this condenser, according to the equation:

$$(\Delta C)_{eff} = \frac{\Delta C_{prec}}{1 - \omega^2 L (C'_{prec} + C_{prec})}$$

Due to the fact that the capacities involved are small and L is kept low (~ 10^{-8}) by the use of a very short connection between C_{prec} and the terminals, these corrections are well within the experimental error of 1% allowed for the loss measurements and may be neglected. It may be necessary, however, to correct the $(G_x)_{eff}$ values obtained with the above equations for the series inductance L_x of the unknown according to the equation, derived in section II.D.1:

$$G_x = (G_x)_{eff} (1 - \omega^2 L_x C_x)^2 \qquad \text{(II.C.3.6)}$$

II.C.3.2. *Measuring cells and accuracy*

The measuring cell described in section II.A.3 is also used in this method for liquids of low permittivity.

For higher permittivities a set of commercial cells (W.T.W.) was used. The cells are chosen in such a way that for a given permittivity the best use is made of the scale of C_1. The condenser C_1 has a zero-capacity of 24.97 $\mu\mu$F and a variable capacity of 75 $\mu\mu$F, divided over 4000 scale-divisions. Since C_1 appeared to deviate from linearity, a calibration-table was composed, enabling capacity measurements to be made with an accuracy of 0.02 $\mu\mu$F. The capacity of the measuring-cells therefore has to be larger than 20 $\mu\mu$F for the required accuracy of 0.2%. The precision condenser C_{prec}, of the type shown in fig. II.B.IV, has a variable capacity of 21 $\mu\mu$F, divided into 2250 scale-parts.

C_{prec} can therefore be used for the measurement of small capacities and is further used for the determination of the ΔC-values, needed for the loss-measurements. The series inductance of this condenser and its connection is so small that it does not affect the loss-measurements, even at the highest frequency of

10 Mc/s. For the measuring-cell described in section II. A. 3 the same equations for the correction of the results apply, that are used for this cell in connection with the twin-T network described in section II.D. Only the value of L_x is different and equals 8.5×10^{-8} H in this case. Since the cell-constants of the W. T. W. - cells vary considerably with dielectric constant and the apparent series inductance, due to the construction of the cells, varies with frequency, graphs were composed for these cells, giving the permittivity of the liquid in terms of the measured cellcapacity at a number of fixed frequencies. The errors of the permittivity-measurements are thereby increased to 0.5%.

The accuracy of the loss-measurements is set both by the accuracy of the ΔC-determinations and the accuracy of the voltage ratio's. The accuracy of the voltage-divider and the input-sensitivity of the detector give rise to a possible error of 0.2% in the $\tan\delta$-values. Furthermore the value of -0.111 Volts, used in equ. II.C.3.1. e.a., resulting from the extrapolation of the detector-characteristic will only be accurate to about 2%. As a result the errors in the measurements of the loss tangent will vary from case to case and amount to 0.5-1%, when the reference voltage is 2 Volts and the voltage ratio's are limited to values above 0.35. Measurements on a number of networks with known loss tangent, at various frequencies, were carried out at voltage ratio's between 0.4 and 0.8. It appeared that the errors were less than 0.5% for all measurements.

II.D. Twin-T Bridge Network (0.5 - 30 Mc/s)

At frequencies above a few megacycles many difficulties are encountered in the use of ratio-, e.g. Schering-bridges. These are due, both to shielding problems and the enhanced influence of parasitic impedances, and basically arise from the fact that no common ground-point exists between generator and detector.

Parallel-T circuits and their conditions for zero transfer-admittance can be used to advantage for measurements at radio-frequencies, as was originally pointed out by Tuttle [50]. In these circuits both generator and null-detector have one common earth-connection and equations for zero transfer can be derived, giving the value of an unknown impedance in terms of the component values. Corrections are only necessary for the parasitic impedances of the condensers used and their connections. The basic circuit is drawn in fig. II.D.I.

Not only does the common ground eliminate the need for a shielded bridge transformer, but it renders innocuous many of the residual circuit capacities. The unknown impedance is measured by parallel substitution at the terminals of C_B. For the measurements a commercial parallel-T circuit, General Radio type 821-A, was used after extensive calibration, since the value of the corrections for the invididual circuit appeared to deviate considerably from the standard values.

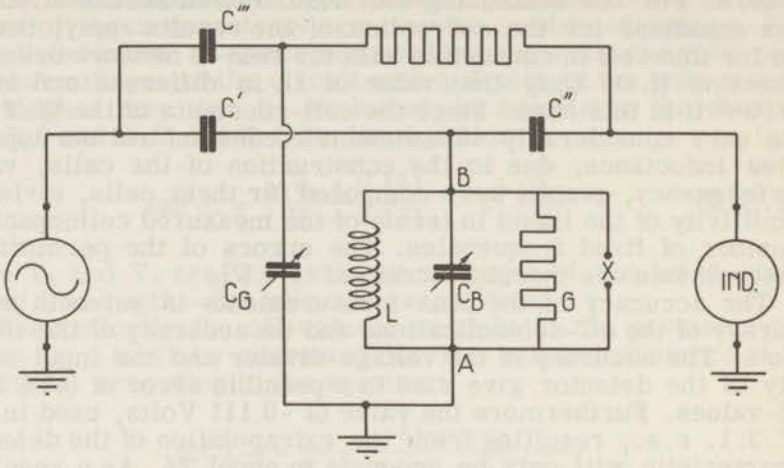

Fig. II.D.I. Basic Twin-T circuit.

II.D.I. *Equations for zero-transfer admittance and corrections*

Since a parallel-substitution method is used in the measurements, the equations will be given in terms of admittance, rather than impedance, for greater simplicity. According to Tuttle [50] and Sinclair [84], the equations for zero-transfer admittance, or balance conditions, for the circuit of fig. II.D.I may be written:

$$G_L - R\omega^2 C' C'' (1 + \frac{C_g}{C'''}) = 0 \qquad \text{(II.D.1.1)}$$

$$C_B + C' C'' (\frac{1}{C'} + \frac{1}{C'''} + \frac{1}{C''''}) - \frac{1}{\omega^2 L} = 0 \qquad \text{(II.D.1.2)}$$

An unknown admittance $Y_x = G_x + jB_x$ being connected in parallel with C_B, the values of G_x and B_x will be given by the differences in equ. II.D.1.1 and II.D.1.2 for the two cases:

$$G_x = \frac{R\omega^2 C' C''}{C''''} (C_{G2} - C_{G1}) \qquad \text{(II.D.1.3)}$$

$$B_x = \omega(C_{B_1} - C_{B_2}) \qquad \text{(II.D.1.4)}$$

Thus G_x and B_x may be evaluated directly from the differences in the readings of the two variable condensers C_G and C_B.

Many of the residual circuit capacities are made innocuous, since both one side of C_B and C_G, and one side of the unknown are connected to the common ground. Furthermore capacities from input- and output-side of the circuit to ground fall across generator and detector and cause no error. Capacities from the T-junctions to ground fall across the measuring condensers C_B and C_G

and affect the initial balance-conditions of the circuit. For measurements of an unknown admittance, however, they drop out in taking incremental readings. The influence of the residuals left, can best be grasped by considering the part of the measuring circuit between the points marked A and B in fig. II.D.I in greater detail. An equivalent circuit of the susceptance condenser C_B, the connection to the x-terminals and to the T-junction and the associated residual impedances, is given in fig. II.D.II.

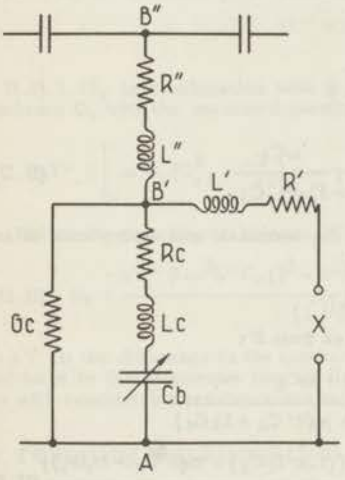

Fig. II.D.II. Equivalent network for the terminal part of the Twin-T circuit.

The inductance L and its conductance G_L in fig. II.D.I can be left out of account, since they do not enter the balance conditions II.D.1.3 and II.D.1.4. Within the Bridge R' and R'' are so small that their influence may be neglected. Correction for R' in a connection to the unknown may however be necessary. G_c is independent of the setting of C_B and drops out in taking difference readings. The value of L' is not determined separately, since it is in series with the inductance L_x of the connection to the unknown. The sum of L' and L_x is evaluated in the calibration of the measuring cells and referred to as L'_x. The other residuals L_c, R_c and L'' affect the measurements and must be determined individually.

L_c increases the effective capacity of the condenser C_B according to:

$$C_e = \frac{C}{1 - \omega^2 L_c C}$$

As a result the measured values of the unknown susceptance B_x are found too low and must be corrected:

$$B_x = \omega(C_{e1} - C_{e2}) = \frac{\omega(C_1 - C_2)}{1 - \omega^2 L_c(C_1 + C_2)} \qquad \text{(II.D.1.5)}$$

where C_1 and C_2 are the readings of C_B.

L'' does not affect the measurement of B_x, since parallel substitution is effected between A and B' (fig. II.D.II), but does affect the G_x determination, since effective conductances from B'' to A are measured with C_G.

An additional error in G_x results from the series resistance R_c of the susceptance condenser, since R_c introduces a conductance component G_c from B' to A, which depends on the setting of C_B. The values of these corrections will be calculated in terms of the equivalent circuit in fig. II.D.II.

The initial admittance between B' and A, no admittance being connected to the terminals, is given by:

$$Y'_c = G_c \frac{1}{(R_c + j\omega L_c + \frac{1}{j\omega c})}$$

$$= G_c + \frac{\omega^2 R_c C_1^2}{(1-\omega^2 L_c C_1)^2} + j \frac{\omega C_1}{1-\omega^2 L_c C_1} \qquad \text{(II.D.1.6)}$$

When an admittance $Y_x = G_x + j\omega C_x$ is connected to the terminals and susceptance balance is restored by decreasing the value of C_B from C_1 to C_2:

$$Y'_c = Y_c + (Y_x)_{eff}, \qquad \text{(II.D.1.7)}$$

where $(Y_x)_{eff}$ is the effective admittance of Y_x as seen from B':

$$(Y_x)_{eff} = \frac{G_x + j\omega C_x}{(1-\omega^2 L'_x C_x) + j\omega(R' C_x + L'_x G_x)}$$

or

$$(Y_x)_{eff} = \frac{(G_x + j\omega C_x)\{(1-\omega^2 L'_x C_x) - j\omega(R' C_x + L'_x G_x)\}}{(1-\omega^2 L'_x C_x)^2 + \omega^2 (R' C_x + L'_x G_x)^2} \qquad \text{(II.D.1.8)}$$

The second term of the denominator can be neglected, considering the maximum frequency used and the estimated values for R' and L'_x. By combining equ. II.D.1.6, II.D.1.7 and II.D.1.8 and separating the real and imaginary parts, the susceptance of the unknown admittance may be written:

$$\frac{C_1}{1-\omega^2 L_c C_1} - \frac{C_2}{1-\omega^2 L_c C_2} = \frac{C_x}{1-\omega^2 L'_x C_x} - \frac{G_x (R' C_x + L'_x G_x)}{(1-\omega^2 L'_x C_x)^2} \qquad \text{(II.D.1.9)}$$

When R' is kept sufficiently low, the term comprising G_x may be neglected. By the further introduction of effective values for the C_B readings, equ. II.D.1.9 is greatly simplified to:

$$\frac{C_1}{1-\omega^2 L_c C_1} = C_{e1}$$

$$\frac{C_2}{1-\omega^2 L_c C_2} = C_{e2}$$

$$C_x = \frac{C_{e1} - C_{e2}}{1+\omega^2 L'_x (C_{e1} - C_{e2})} \qquad \text{(II.D.1.10)}$$

Since susceptance balance is restored in this measurement, the difference in the conductance between B' and A, resulting from the connection of the unknown admittance, will be given by substraction of the conductances in equ. II.D.1.6 and II.D.1.7 - II.D.1.8:

$$\Delta Y' = -\omega^2 R_c (C_{e1}^2 - C_{e2}^2) + \frac{G_x}{1-\omega^2 L'_x C_x} + \frac{\omega^2 C_x (R' C_x + L'_x G_x)}{(1-\omega^2 L'_x C_x)^2}$$

or

$$\Delta Y' = -\omega^2 R_c (C_{e1}^2 - C_{e2}^2) + \frac{G_x}{(1-\omega^2 L'_x C_x)^2} + \frac{\omega^2 C_x^2 R'}{(1-\omega^2 L'_x C_x)^2} \qquad \text{(II.D.1.11)}$$

The circuit measures conductance, however, between the junction-point B'' and the ground-point A; so the admittance at B' has to be transformed through L'' and R'' to B''. If the admittance at B' is written $Y_{B'} = G_T + j\omega C_T$, the admittance at B'' is given by:

$$Y_{B''} = \frac{(G_T + j\omega C_T)\{(1-\omega^2 L'' C_T) - j\omega R'' C_T\}}{(1-\omega^2 L'' C_T)^2} \qquad \text{(II.D.1.12)}$$

In connection with the original balance-conditions and the fact that the total capacity C_T between B' and A is kept constant during the measurement, equ. II.D.1.12 results in a relation between the conductance change $\Delta Y'$ in B' and the conductance change $\Delta Y''$ and B'', which to a good approximation is given by:

$$\Delta Y'' = \Delta Y' \frac{1}{(1-\omega^2 L'' C_T)^2} \qquad \text{(II.D.1.13)}$$

Equ. II.D.1.13, in combination with II.D.1.11, leads to an equation relating the unknown conductance G_X with the measured quantities:

$$\Delta Y'' = \left[-\omega^2 R_c(C_{e1}^2 - C_{e2}^2) + \frac{G_x}{(1-\omega^2 L_x' C_x)} + \frac{\omega^2 R' C_x^2}{(1-\omega^2 L_x' C_x)^2}\right] \frac{1}{(1-\omega^2 L'' C_T)^2} \qquad \text{(II.D.1.14)}$$

Since, due to the susceptance balance, $C_T = C_{e1}$ in both cases, the value of G_X will be given by:

$$G_x = \frac{\Delta Y''(1-\omega^2 L'' C_{e1})^2 - \omega^2 R'(C_{e1} - C_{e2})^2 + \omega^2 R_c(C_{e1} - C_{e2})^2}{\{1 + \omega^2 L_x'(C_{e1} - C_{e2})\}^2} \qquad \text{(II.D.1.15)}$$

where $\Delta Y''$ is the difference in the conductance readings, as taken from C_G. In most cases the second term in the numerator may be left out of account, unless long connections to the unknown with considerable resistance are used.

The resulting equations for the evaluation of the measurements are:

$$C_x = \frac{C_{e1} - C_{e2}}{1 + \omega^2 L_x'(C_{e1} - C_{e2})} \qquad \text{(II.D.1.10)}$$

$$G_x = \frac{G''(1 - \omega^2 L'' C_{e1})^2 + \omega^2 R_c(C_{e1} - C_{e2})^2}{\{1 + \omega^2 L_x'(C_{e1} - C_{e2})\}^2} \qquad \text{(II.D.1.15)}$$

where $C_e = \frac{C}{1 - \omega^2 L_c C}$ and C_1, C_2 and G'' are obtained from scale-readings. The values of the residual parameters L_c, L_x', L'' and R_c must be determined by individual calibration.

II.D.1.1. *Determination of the residual parameters L_c, L_x', L'' and R_c.*

For the determination of the main residual parameter L_c a simple procedure can be derived from equ. II.D.1.5:

$$C_x = \frac{C_1 - C_2}{1 - \omega^2 L_c(C_1 + C_2)}$$

By measuring an arbitrary small capacitor at one frequency and various initial settings of the precision condenser C_B, a linear

relation between $(C_1 - C_2)$ and $(C_1 + C_2)$ results, from which L_c may be calculated, C_x being constant. Neither the value of L'_x, nor the exact value of C_x need to be known, since measurements are carried out at one frequency and the effective capacity of C_x is the same for all readings. The condenser-readings are first corrected for scale-errors by the use of a correction table, made up from a low frequency calibration.

The measurements were carried out at five frequencies, ten different initial settings of C_B being used at each frequency, for the evaluation of L_c. Three condensers, of 50, 75 and 100 $\mu\mu$F respectively, were measured by this procedure. Consistent results were obtained, the resulting L_c values at the various frequencies being:

Frequency	30	25	20	15	10	Mc/s
L_c.	5.8	5.1	4.6	4.5	4.5	10^{-9} Henry

Thus L_c appears to be dependent on frequency. This result is in contradiction with the corrections supplied by the manufacturers of the Twin-T circuit, but was confirmed by them in subsequent correspondence. The effect may be due to the distributed nature of inductance and capacitance in the variable capacitor and stray common impedances between various parts of the circuit.

The value of L'' can be determined with a similar procedure. If a fixed resistor with negligible parallel capacitance is connected to the circuit, a constant effective conductance G' must result between B' and A for any setting of C_B at one frequency. The values of G'', as obtained from difference readings on C_G, however will depend on the initial setting of C_B according to equ. II.D.1.13 or II.D.1.15, which may be written:

$$\frac{1}{\sqrt{G''}} = \frac{1}{\sqrt{G'}} - \omega^2 L'' \frac{1}{\sqrt{G'}} C_{e1}$$

By measuring an arbitrary resistor of e.g. 1000 Ohms at different initial settings of C_B the value of L'' can be evaluated from the linear relation between C_{e1} and $\frac{1}{\sqrt{G''}}$.

From measurements at 30, 25 and 20 Mc/s a virtually constant value for L'' was obtained:

$$L'' = (3.3 \pm 0.1) \times 10^{-9} \text{ Henry.}$$

The series resistance R_c of the susceptance condenser introduces an additional error in the G'' readings when the unknown admittance comprises both a conductive – and a capacitive – component, as can be seen from equ. II.D.1.14 or II.D.1.15. This error will be considerable when the capacitive part of the admittance is large as compared with the conductance. Therefore the conductance readings obtained in the measurements, necessary for the L_c determination are very useful here.

The G'' values from these measurements can be converted into G' or $\Delta Y'$ values with equ. II.D.1.13. Each of these $\Delta Y'$ values is the sum of a constant G'_x value and a variable $G_{cond.}$ value, due to R_c, according to equ. II.D.1.11:

$$\Delta Y' = -\omega^2 R_c (C_{e1} - C_{e2})(C_{e1} + C_{e2}) + G'_x.$$

When $\Delta Y'$ is plotted against $(C_{e1} + C_{e2})$ a straight line results with a slope equal to $-\omega^2 R_c (C_{e1} - C_{e2})$ and an intercept equal to G'_x.

Thus
$$R_c = \frac{-1}{\omega^2} \frac{\text{slope}}{(C_{e1} - C_{e2})}$$

The resultant value at 30 Mc/s was found to be $R_c = 0.018$ Ohm.

R_c varies directly as the square root of the frequency, inasmuch as skin-effect is complete at frequencies where any significant effect of R_c on the measurements can be detected.

$$R_{c'} = \sqrt{\frac{f}{3 \times 10^7}} \times 0.018 \text{ Ohms.}$$

The value of L'_x, the series inductance of the connection between the susceptance condenser C_B and the unknown admittance cannot be determined with a similar procedure. L'_x comprises the inductance of the bridge terminals and the inductance of the connection to the measuring cell. For our measurements the cell described in section II.A.3 was used, an adaptor being inserted between the coaxial cell connector and the bridge-terminals. The total series inductance of this connection between the internal cell-capacity and C_B was determined from a series of measurements of the air-filled cell and the cell filled with benzene and chlorobenzene, the capacity of the connector being taken into account. Since the accuracy of this method is lower than that of the low-frequency bridge, the separation of C_o and C'_o (equ. II.A.3.2) is not necessary and the capacity of the cell and connector may be written:

$$C = C_p + \varepsilon C_o \qquad \text{(II.D.1.16)}$$

Due to the series-inductance L'_x of the connection between the cell-capacity C_o and the bridge, the effective capacity will increase with frequency. It is difficult to apply a simple correction to C_p, the parallel-capacity of the connection, since C_p is distributed along L'_x, as may be seen from fig. II.D.III.
Where the major part of C_p is concentrated in the insulator of the cell, near the point where the capacity C_o is located, a good approximation is obtained by correcting the total capacity C for its series inductance L'_x. In this way a virtually constant value for L'_x was found from a series of measurements on benzene and chlorobenzene up to 25 Mc/s, the value being $L'_x = 3.4 \times 10^{-8}$ Henry. For the measurements on the empty cell a somewhat lower value was found, i.e. $L'_x = 3.0 \times 10^{-8}$ H. If for convenience, the value of 3.4×10^{-8} H is also used in this case, the error in C_{empty} amounts

to 0.6% at 25 Mc/s. Above 25 Mc/s the errors increase rapidly, but this was thought to be of no consequence, since above 25 Mc/s the method described in section II. E. may be used to advantage.

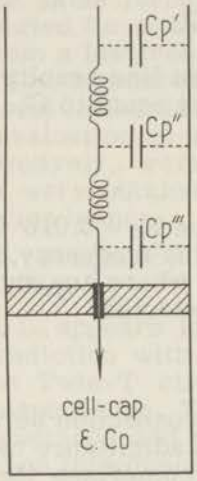

Fig. II.D.III. Series-inductance and parallel capacitance of the coaxial connector of the measuring cell.

Thus up to 25 Mc/s the properties of the measuring-cell, in terms of the calibration of the bridge and the connector used, may be summarized:

$$C = C_p + \varepsilon C_o \qquad \text{where } C_p = 11.0\ \mu\mu F.,\ C_o = 63.3\ \mu\mu F.$$

$$C = \frac{C_{eff}}{1 + \omega^2 L'_x C_{eff}} \qquad \text{where } L'_x = 3.4 \times 10^{-8} \text{ Henry.}$$

II.D.2. Experimental set-up

A block-diagram of the apparatus is given in fig. II.D.IV

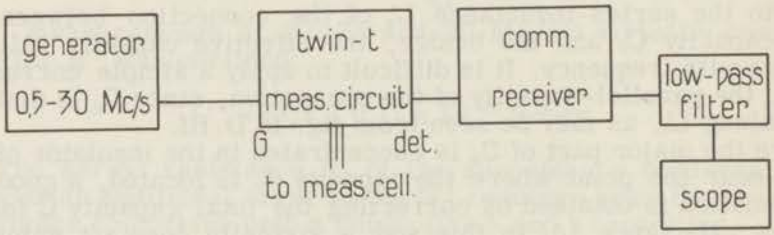

Fig. II.D.IV. Block-diagram of the Twin-T circuit and aux. apparatus.

The high-frequency voltage for the Twin-T bridge is supplied by a standard-generator with an output of 3 Volts and a frequency-

accuracy of 0.5%. A communications-receiver with a sensitivity of a few microvolts is used as null detector. Since accurate balancing of the Twin-T circuit is impossible when the generator-output is modulated, because of the strong frequency-dependence of the zero-transfer characteristic, the unmodulated signal is made audible in the detector-output by the use of a beat-frequency oscillator in the receiver. To obtain increased sensitivity for the null-detector the receiver output is connected to an oscilloscope, a low-pass filter being inserted for the reduction of noise produced by the receiver at high-gain settings. Extreme care must be taken to avoid couplings between the various parts at the high frequencies used. Double screened coaxial cable is used throughout and screening is maintained continuously from the Twin-T bridge to within the first stage of the receiver. In addition the bridge is surrounded by a metal enclosure as far as possible, while all earth-connections are made through one common ground-point near the detector terminals of the Twin-T circuit.

II.D.3. Experimental procedure and accuracy

For measurements on liquids the cell described in section II.A.3 is used. First the bridge is balanced without the cell, by means of the balance-controls, setting the conductance scale of the bridge to zero and the condenser C_B to a convenient value C_1. Subsequently the bridge is rebalanced after connection of the empty cell and readings are taken from the conductance- and capacity-scales. The same procedure is repeated for the cell filled with liquid.

Thus two conductance values $(G'')_{air}$ and $(G'')_{liquid}$ are obtained and two sets of readings for C_1 and C_2, one for the air-filled cell and one for the cell filled with liquid. The capacity readings are first corrected for scale-errors of C_B, by means of the low-frequency calibration chart and subsequently for errors due to L_c. The resulting C_{e1}, $(C_{e2})_{air}$ and $(C_{e2})_{liquid}$ values are used (in connection with the values of L'_x, L'' and R_c obtained from the calibrations) for the evaluation of C_x and G_x with equ. II.D.1.10 and equ. II.D.1.15.

From the two C_x and G_x values obtained the permittivity and loss tangent of the liquid can be calculated with the equations:

$$(C_x)_{air} = C_o + C_p \qquad (C_x)_{liqu.} = \varepsilon C_o + C_p$$

$$(\varepsilon - 1) = \frac{(C_x)_{liqu} - (C_x)_{air}}{C_o}$$

or

$$\varepsilon = \frac{(C_x)_{liqu} - C_p}{C_o}$$

and $(G_x)_{liqu} - (G_x)_{air} = G_x$

or $$\tan\delta = \frac{G_x}{\omega \varepsilon C_o}$$

Measurements on benzene and chlorobenzene at various frequencies are summarized in table II.D.I.

Table II.D.I
ε_{25} values for C_6H_6 and C_6H_5Cl

	Low-frequ. bridge	0.5	10	15	20	25 Mc/s
C_6H_6	2.273	2.28	2.27	2.26	2.26^5	2.28
C_6H_5Cl	5.62	5.62	5.61	5.61^5	5.63^5	5.61

It appears from these measurements that the errors in the permittivity values are less than 0.5% up to 25 Mc/s. The considerable amount of numerical work involved can be simplified by systematic lay-out of the computation, since many similar factors are involved. Further simplification results from the use of standard frequencies.

The accuracy of the capacity measurements is better than 0.4% for capacities above 100 $\mu\mu$F, since the scale reading of C_B is limited to 0.2 $\mu\mu$F and two readings are involved in the measurement of C_x; the final accuracy will be lower for smaller capacities. The accuracy of the conductance measurements cannot be simply estimated, because of the many factors involved. From the consistancy of the results in various measurements, the overall accuracy for G_x may be estimated as 1%. The error may be considerably higher, however, for low G_x values as compared with the C_x values, i.e. for low values of the loss tangent.

II.E. HIGH FREQUENCY SCHERING-BRIDGE (5 - 250 Mc/s)

At frequencies above 30 Mc/s, the maximum frequency for the measurements with the Twin-T bridge, accurate impedance measurements become increasingly difficult, due to the large corrections needed for even small residual inductances and other stray effects. Furthermore the distributed nature of inductance and capacitance cannot be left out of the picture anymore at frequencies above 50 or 100 Megacycles, unless special precautions are taken.

These difficulties will necessarily arise with any lumped-circuit technique used at these frequencies. On the other hand the use of coaxial measuring systems, as described in section II.F. for frequencies above 300 Megacycles, is hardly possible at lower frequencies, due to the excessive length of the systems and hence the large quantities of liquid required. As a result a high accuracy of permittivity and loss measurements cannot be expected in the frequency range from e.g. 50 to 250 Megacycles. An attempt was made to adapt a commercial high-frequency bridge, recently developed for the measurement of high-frequency components, to dielectric measurements and to increase the accuracy as far as possible by the use of calibrations and special measuring cells.

II.E.1. Description of the high-frequency bridge

With the bridge-circuit used (Boonton RX type 250 A), unknown capacities up to 20 $\mu\mu$F, having parallel resistances between 15 Ohm and 100 k Ohm, may be measured by a parallel substitution method across the built-in variable capacitor over a frequency range from 5-250 Mc/s. A block-diagram of the bridge and the auxiliary apparatus, which is completely self-contained is given in fig. II.E.I.

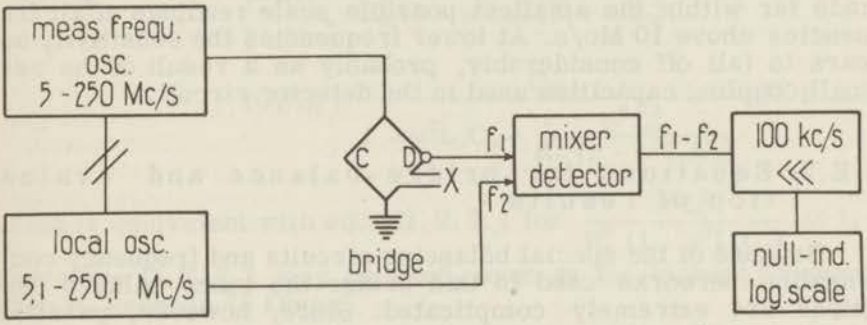

Fig. II.E.I. Block-diagram of high frequency Schering-bridge.

The use of a shielded-bridge transformer between the floating detector-terminals C-D of the bridge is avoided by the use of a special mixer-detector circuit, thus eliminating one of the main sources of error at high frequencies. The bridge-circuit without the associated balancing circuits is schematically drawn in fig. II.E.II.

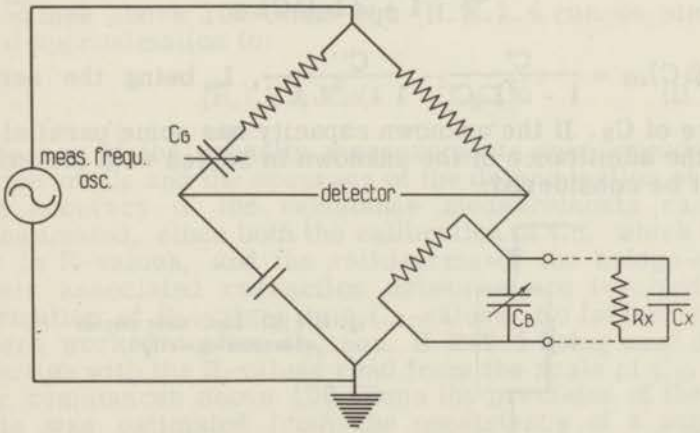

Fig. II.E.II. Schematic bridge circuit.

The whole bridge circuit is built into a small die-cast block, which also contains the mixer-detector stage. The two detector-terminals C-D are connected through very small capacities to the

grid of a triode, the cathode of which is modulated by the local oscillator at a frequency 100 kc/s above the measuring frequency. By subsequent filtering out of all but the 100 kc/s beat note in the anode circuit, the amplitude of which is proportional to the unbalance of the bridge, possible stray couplings are reduced to a minimum. The use of parallel substitution in the measurements reduces the shielding problems considerably. In preliminary tests the circuit residual impedance appeared to be very small.

The sensitivity of the detector enables capacity settings to be made far within the smallest possible scale readings at all frequencies above 10 Mc/s. At lower frequencies the sensitivity appears to fall off considerably, probably as a result of the very small coupling capacities used in the detector circuit.

II.E.2. Equations for bridge-balance and evaluation of results

Because of the special balancing circuits and frequency compensation networks used in this bridge the exact balance conditions are extremely complicated. Since, however, parallel substitution in one arm of the bridge is used for the capacity measurements, the normal equations for this method may be applied without loss of accuracy.

An unknown capacity is measured as the difference between two readings C' and C'' of the susceptance condenser C_B. Therefore according to the equations derived in section II.D, C_x is given by:

$$C_x = \frac{(\Delta C)_{eff}}{1 + \omega^2 L_x (\Delta C)_{eff}}, \qquad \text{(II.E.2.1)}$$

where $(\Delta C)_{eff} = \frac{C'}{1 - \omega^2 L_c C'} - \frac{C''}{1 - \omega^2 L_c C''}$, L_c being the series inductance of C_B. If the unknown capacity has some parallel resistance, the admittance of the unknown in series with the inductance L_x must be considered:

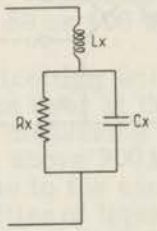

Fig. II.E.III. Equivalent circuit of measuring cell.

The admittance of the equivalent circuit of fig. II.E.III is given by:

$$Y = \frac{1}{j\omega L_x + \frac{R_x}{j\omega R_x C_x + 1}} = \frac{1 + j\omega R_x C_x}{R_x (1 - \omega^2 L_x C_x) + j\omega L_x} \qquad \text{(II. E. 2. 2)}$$

The real and imaginary parts of this equation are the effective values of capacity and parallel resistance at the bridge terminals:

$$(C_x)_{eff} = \frac{C_x R_x^2 (1 - \omega^2 L_x C_x)}{R_x^2 (1 - \omega^2 L_x C_x)^2 + \omega^2 L_x^2}$$

or

$$(C_x)_{eff} = \frac{C_x}{1 - \omega^2 L_x C_x + \frac{\omega^2 L_x^2}{R_x^2 (1 - \omega^2 L_x C_x)}} \qquad \text{(II. E. 2. 3)}$$

which is equivalent with equ. II. E. 2. 1 for $\frac{\omega^2 L_x^2}{R_x^2 (1 - \omega^2 L_x C_x)} \ll 1$.

Therefore II. E. 2. 1 may be used, even at the highest frequency when R_x exceeds 75 Ohms.

$$(G_x)_{eff} = \frac{R_x (1 - \omega^2 L_x C_x) + \omega^2 L_x C_x R_x}{R_x^2 (1 - \omega^2 L_x C_x)^2 + \omega^2 L_x^2} = \frac{1}{R_x (1 - \omega^2 L_x C_x)^2 + \frac{\omega^2 L_x^2}{R_x}}$$

or

$$(R_x)_{eff} = R_x (1 - \omega^2 L_x C_x)^2 + \frac{\omega^2 L_x^2}{R_x} \qquad \text{(II. E. 2. 4)}$$

For R_x values above 100 Ohms equ. II. E. 2. 4 can be simplified with good approximation to:

$$(R_x)_{eff} = R_x (1 - \omega^2 L_x C_x)^2 \qquad \text{(II. E. 2. 5)}$$

The accuracy of the capacity measurements only depends on the calibration of C_B and the accuracy of the determination of L_c and L_x. The accuracy of the resistance measurements cannot be simply estimated, since both the calibration of C_G, which is read directly in R-values, and the ratio-arms of the bridge-circuit, with their associated correction networks are involved in the transformation of R_x-values into C_G-values. No further corrections were worked out for R_x, equ. II. E. 2. 5 being used directly in connection with the R-values read from the scale of C_G.

For resistances above 100 Ohms the precision of the measurements was estimated from the consistency of a number of measurements on coaxial resistors. At frequencies below 100 Mc/s the errors will be less than 2%, increasing gradually at the higher frequencies to 3-4% at 250 Mc/s.

II.E.3. Corrections, measuring cells and accuracy

The accuracy of the capacity measurements entirely depends on the calibration of the scale of the measuring condenser C_B and the accuracy to which the series inductances L_c of C_B and L_x of the measuring cells can be evaluated. The scale-readings of C_B give the effective value of the unknown capacity C_x directly, initial balance being established with a separate balance-control while C_B is set to zero.

Since, because of the small range of C_B (0-20 $\mu\mu$F), this condenser cannot be calibrated with an external precision condenser another procedure had to be adopted. The original bridge terminals were replaced by a coaxial-connector, enabling reproducible measurements to be made on a small coaxial capacitor. As an initial check on the scale of C_B, a coaxial capacitor of 2.40 $\mu\mu$F was measured at different points of the C_B-scale by the use of the separate balance control. At a measuring frequency of 10 Mc/s errors in the capacity-values due to L_c may be neglected. Considerable differences were found in the capacity of the coaxial capacitor for the various C_B-settings. Since the deviations appeared to be cyclic to a certain extent, the errors are probably due to imperfections in the worm-drive of C_B. The resulting values were $C_x = 2.35 \pm 0.15$ $\mu\mu$F.

A better calibration of C_B is therefore of paramount importance. This was obtained by the following procedures:

a. the coaxial capacitor of 2.40 $\mu\mu$F was measured at 27 different initial settings of C_B. Thus integrated values of the capacity of C_B for a given part of the scale are obtained. To avoid errors due to backlash in the worm-drive of C_B the dial is always turned clockwise to the final setting.
b. a coacial capacitor of 9.04 $\mu\mu$F was measured in the same way at 4 different initial settings (0, 2.5, 5 and 7.5 $\mu\mu$F) of C_B.
c. at 37 points of the scale, the number of scale-divisions to the left and to the right of the minimum were determined which resulted in a fixed small detector reading. The values obtained are inversely proportional to the effective capacity per scale-division at the point of the scale where the shift is measured and give a rough idea of the shape of the correction-curve.

The values of the capacity per scale division, as measured by method c, were summed for each part of the scale involved in the measurements of the fixed coaxial capacitors. By comparing the 27 values for the coaxial capacitor thus calculated, with the values measured by procedure a, subsequent corrections could be applied to the capacities per scale-division by trial and error, till the best average value for the coaxial capacitor was obtained. The measurement sub b was used as a check on the final result.

The corrections on the readings of the C_B-scale were plotted in a curve giving the ΔC values for each setting of scale with respect to zero. By the use of this curve the capacities of the two coaxial capacitors were found to be:

	meas. values	true value
C_1	2.401 ± 0.015 μμF (27 values)	2.404 ± 0.005
C_2	9.07 ± 0.05 μμF (4 values)	9.04 ± 0.005

where the ± values give the maximum deviations from the average value.

II. E. 3. 1. *Measuring cells and corrections for series inductances*

At frequencies around 200 Mc/s, very small inductances begin to have a marked effect on the measured quantities and the connections between bridge-terminals and unknown must be kept as short as possible. Furthermore the capacity and size of the measuring cells must be kept small because of the distributed nature of capacity and inductance at very high frequencies. Therefore a small coaxial measuring-cell was constructed around the high bridge terminal, as shown in fig. II. E. IV.

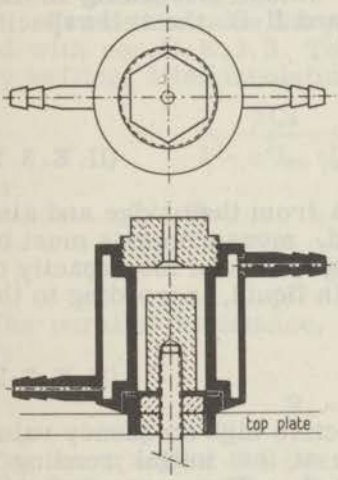

Fig. II.E.IV. Coaxial cell for measurements on liquids.

The lower part of the cell wall is screwed into the top plate of the bridge around the high terminal. A teflon insulator 0.7 mm thick is clamped on top of the terminal stub, by screwing the top part of the cell wall onto the lower part as indicated. The height of the cell, above the insulator is 20 mm. The cell wall is surrounded by a thermostating mantle. The cell is closed by a metal nut with a small filling hole. By the choice of the diameter of the inner conductor, which is kept 3 mm shorter than the cell wall, the cell-constant may be varied.

Three inner conductors are used for the measurements:

C_I	diam. 10.5 mm	ε-range 1 - 4
C_{II}	diam. 9 mm	ε-range 2 - 6
C_{III}	diam. 7.5 mm	ε-range 2.5 - 10

The series inductance of the precision condenser C_B was determined, according to the procedure described in section II.D.1.1 by measuring the capacity-changes produced by the insertion of the inner conductor for various initial settings of C_B. These measurements were carried out with the three inner conductors and at five different frequencies, i.e. 150, 175, 200, 225 and 250 Mc/s. L_c appeared to be very small. By statistical evaluation of the 150 measuring points, the best average value of L_c was found to be:

$$L_c = (2.5 \pm 0.05) \times 10^{-10} \text{ Henry.}$$

For the three measuring cells the cell constants and associated series-inductances L_x were determined by further calibration. Due to the geometry of the cell the cell-constants will vary somewhat with the permittivity of the liquid. It appeared, however, that within the ranges given above for each cell and the required accuracy of 1% the cell constants may be represented by two values, one air-value and one liquid value. According to the equation already used in section II.A. and II.B. the cell capacity will therefore be given by:

$$(C_x)_e = C_p + C_o'$$

$$(C_x)_{\text{liquid}} = C_p + \varepsilon C_o \qquad \text{(II.E.3.1)}$$

Since these cells cannot be disconnected from the bridge and also the inner conductor cannot be removed, measurements must be carried out by taking difference-readings between the capacity of the air-filled cell and the cell filled with liquid, according to the equation:

$$\Delta C_x = \varepsilon C_o - C_o' \qquad \text{(II.E.3.2)}$$

The equation (II.C.3.3) giving the effective high frequency value of C_x, cannot be applied to ΔC_x, since at the initial reading a capacity C_o' is already in series with L_x. The measured ΔC_x values at each frequency are therefore related to εC_o and C_o' by the equation:

$$(\Delta C_x)_{\text{eff}} = \frac{\varepsilon C_o}{1 - \omega^2 L_x \varepsilon C_o} - \frac{C_o'}{1 - \omega^2 L_x C_o'} \qquad \text{(II.E.3.3)}$$

For the three cells the values of C_o, C_o' and L_x were determined by measurements on liquids of known dielectric constant at various frequencies. At these high frequencies L_x varies somewhat with frequency as should be expected. The resulting values are given in table II.E.1.

Table II. E. 1

	C'_o	C_o	50	125	200	250 Mc/s
			$L_x x 10^9$ Henry			
Cell I	4.87	4.98	2.50	2.50	2.65	2.70
Cell II	2.90	2.93	2.70	2.70	2.75	3.05
Cell III	1.98	1.95	2.00	2.00	2.30	2.75

II. E. 3. 2. *Measuring procedure and accuracy*

With the air-filled cell in position the bridge is balanced at the measuring frequency, by means of the balance-controls and C_B. The initial reading C_1 of C_B is taken. After filling the measuring-cell with the liquid, balance is again established with C_B and R_p. The two readings C_1 and C_2 of C_B are corrected for scale-deviations and the series inductance L_c, the difference of the final values giving $(\Delta C_x)_{eff}$.

From this value the permittivity of the liquid can be evaluated with equ. II. E. 3. 3. This calculation can be greatly simplified, by writing, after tabulation of $(C'_o)_{eff}$ at various frequencies:

$$\frac{\varepsilon C_o}{1 - \omega^2 L_x \varepsilon C_o} = (\Delta C_x)_{eff} + (C'_o)_{eff} = C_T \,. \qquad \text{(II. E. 3. 4)}$$

or

$$\varepsilon C_o = \frac{C_T}{1 + \omega^2 L_x C_T} \qquad \text{(II. E. 3. 5)}$$

The parallel resistance, according to equ. II. E. 2. 5 will be given by:

$$R_x = \frac{R_p}{(1 - \omega^2 L_x \varepsilon C_o)^2} \qquad \text{(II. E. 3. 6)}$$

The accuracy of the permittivity measurements was checked by measuring a number of mixtures of cyclohexane, benzene and chlorobenzene, both with the low-frequency bridge described in section A and with this bridge. The results are given in table II. E. 2.

The errors in the permittivity measurements are well within 1% over the whole frequency range. The errors in the resistance measurements may amount to 3 or 4% at the high frequency side, as was pointed out in section II. E. 2.

Table II.E.2

	frequency 125	200	250 Mc/s	L.F. value
Cell I	2.009	2.012	2.010	2.0125
	2.276	2.275	2.276	2.277
	3.191	3.192	3.194	3.172
Cell II	2.00	2.009	2.013	2.0125
			2.005	
	2.264	2.255	2.272	2.277
	3.774	3.772	3.772	3.773
	5.56	5.578	5.60	5.565
Cell III	3.752	3.802	3.754	3.773
	5.547	5.572	5.575	5.565

II.F. COAXIAL MEASURING SYSTEMS USED FROM 300 - 5000 Mc/s

At frequencies above 250 Mc/s the use of the normal lumped-circuit techniques, described for the lower frequencies, is no longer practicable and a change to transmission line methods becomes necessary. Though it is possible to describe some of the measuring schemes for very high frequencies as extensions of lumped-circuit methods, the proper additions being made, a general description of the measuring schemes on the basis of Maxwell's equations is to be preferred.

In the frequency-range from 300 - 5000 Mc/s coaxial measuring systems are generally used. Because of the broadband properties, one system can be used in a wide frequency range, theoretically from frequency zero to infinity. At low frequencies the application is limited however by the length of line necessary for the measurements (at 300 Mc/s a measuring system of two wavelengths is already two meters long), whereas at high frequencies difficulties due to the exitation of unwanted modes arise, necessitating the substitution of a hollow wave guide of appropiate size.

II.F.1. Mathematical basis of the techniques of measurement

The principles of transmission line methods follow from the consideration of $\hat{\varepsilon}$ and $\hat{\mu}$ in the wave equations. The interpretation of Maxwell's wave equations, starting from the separation of the field vectors E and H, having been described extensively, both in textbooks [89-92] and in the literature [93-95], only a short survey of the formulae necessary for the description of the measurements will be given here.

We may assume that E and H are a function of x and t only, and obtain in this way the wave equations of the electromagnetic field:

$$\frac{\partial^2 E}{\partial x^2} - \hat{\varepsilon}\hat{\mu}\frac{\partial^2 E}{\partial t^2} = 0$$
$$\frac{\partial^2 H}{\partial x^2} - \hat{\varepsilon}\hat{\mu}\frac{\partial^2 H}{\partial t^2} = 0 \qquad \text{(II. F. 1. 1)}$$

The solution of these differential equations is a plane wave:

$$E = E_o\, e^{j\omega t - \gamma x}$$
$$H = H_o\, e^{j\omega t - \gamma x}$$

having a frequency $f = \frac{\omega}{2\pi}$ and advancing in the + x direction through space with a complex propagation factor:

$$\gamma = j\omega(\hat{\varepsilon}\hat{\mu})^{\frac{1}{2}} = \alpha + j\beta \qquad \text{(II. F. 1. 2)}$$

α being the attenuation factor and $\beta = \frac{2\pi}{\lambda}$ the phase factor of the wave.

In many formulae the index of absorption, i. e. the attenuation per radian is used:

$$k = \frac{\alpha\lambda}{2\pi} = \frac{\alpha}{\beta} \qquad \text{(II. F. 1. 2a)}$$

In the case of isotropic non magnetic dielectrics this leads to

$$-\gamma^2 = \omega^2(\varepsilon' - j\varepsilon'') \qquad \text{(II. F. 1. 3)}$$

ε' and ε'' will be referred to as the real and imaginary parts of the complex permittivity respectively.

The methods for measuring the complex propagation factor, and hence the complex permittivity can be divided into three groups:

1. standing wave methods
2. resonance methods
3. transmission, or travelling wave methods.

II. F. 1. 1. *Standing wave methods*

In the measuring systems the unknown impedance generally terminates a certain length of line and the wave in the line strikes the boundary at normal incidence. If the unknown impedance is different from the characteristic impedance of the line, the mismatch at the boundary will result in a reflection, and hence a standing wave pattern in the line. The amplitude and phase of the reflected wave are related to the real and imaginary parts of the unknown impedance.

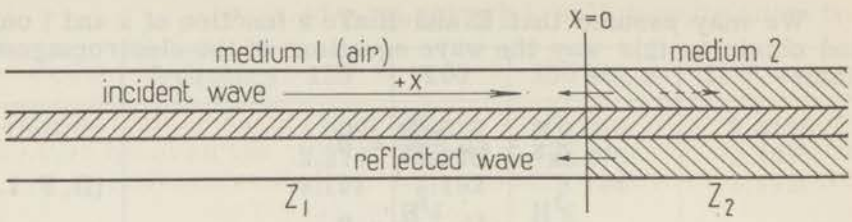

Fig. II.F.I. Coaxial line terminated by a specimen (medium 2) of infinite length.

In fig. II. F. I a coaxial line is drawn, terminated at one end by an unknown impedance, medium 2, of infinite length. If the incident wave E_y, H_z travelling in the + x direction strikes the boundary of medium 2 at x = 0, the reflected wave returning in the - x direction, will combine with it to yield a resulting field distribution:

$$E_{y1} = E_o\, e^{j\omega t-\gamma_1 x} + E_1\, e^{j\omega t+\gamma_1 x}$$
$$H_{z1} = H_o\, e^{j\omega t-\gamma_1 x} + H_1\, e^{j\omega t+\gamma_1 x} \qquad \text{(II. F. 1. 4)}$$

Introducing a reflection coefficient r as the ratio of the reflected and the incident wave and writing $Z = E_o/H_o$ (Z being the characteristic impedance of the air filled line), we can rewrite equation II. F. 1. 4 as:

$$E_{y1} = E_o\, e^{j\omega t}\,(e^{-\gamma_1 x} + r\, e^{\gamma_1 x})$$
$$H_{z1} = \frac{E_o}{Z}\, e^{j\omega t}\,(e^{-\gamma_1 x} - r\, e^{\gamma_1 x}) \qquad \text{(II. F. 1. 5)}$$

As medium 2 is of infinite length no reflection results from the wave continuing in medium 2 and

$$E_{y2} = E_2\, e^{j\omega t-\gamma_2 x}$$
$$H_{z2} = \frac{E_2}{Z_2}\, e^{j\omega t-\gamma_2 x} \qquad \text{(II. F. 1. 6)}$$

Instead of equation II. F. 1. 5 we also can write:

$$E_{y1} = E_o\, e^{j\omega t-\gamma_1 x}\,(1 + r_o\, e^{2\gamma_1 x}) \qquad \text{(II. F. 1. 7)}$$

In equation II. F. 1. 7 the first part is the incident wave, whereas the term in brackets gives rise to the standing wave pattern. Introducing polar coordinates:

$$x = \frac{\lambda}{2\pi}\,\Phi$$
$$r_o = e^{-2u} = e^{-2(\rho+j\varphi)} = \left|r_o\right| e^{-2j\varphi} \qquad \text{(II. F. 1. 8)}$$

and using equation II. F. 1. 2a this term becomes:

$$(1 + r_o\, e^{2\gamma_1 x}) = 1 + r_o\, e^{2\Phi\alpha/\beta}\, e^{2j(\Phi-\varphi)} \qquad \text{(II. F. 1. 9)}$$

The terminating impedance of medium 1, given by the ratio of the two field vectors at the boundary (x = 0), can be found by measuring the amplitude and phase of the reflection coefficient:

$$Z(0) = \frac{E(0)}{H(0)} = Z\,\frac{1 + r_o}{1 - r_o} \qquad \text{(II. F. 1. 10)}$$

The first minimum of E will be reached when (according to equation II. F. 1. 7 and II. F. 1. 9):

$$2\,\Phi_o = \pi + 2\varphi \qquad \text{(II. F. 1. 11)}$$

As in practice x is measured with a standing wave indicator, we convert this back to linear coordinates for the first minimum:

$$2\,\Phi_o = \frac{4\pi x_o}{\lambda} \qquad \text{(II. F. 1. 12)}$$

Now the phase angle of the reflection coefficient at the first minimum will be given by

$$2\varphi = \frac{4\pi x_o}{\lambda} - \pi \qquad \text{(II. F. 1. 13)}$$

The ratio of the electric and the magnetic fieldstrength at this minimum is:

$$E_{min}/H_{max} = Z\,\frac{1 - |r_o|\, e^{-2\alpha_1 x_o}}{1 + |r_o|\, e^{-2\alpha_1 x_o}} \qquad \text{(II. F. 1. 14)}$$

If the losses in the measuring line (medium 1) may be neglected, $\alpha_1 = 0$, $H_{max} = E_{max}/Z$ and equ. II. F. 1. 14 is simplified to

$$E_{min}/E_{max} = \frac{1 - |r_o|}{1 + |r_o|} \qquad \text{(II. F. 1. 15)}$$

By using equ. II. F. 1. 15 and II. F. 1. 13, the terminating impedance Z(0) can be evaluated.

For dielectric measurements this method can only be used with high-loss samples, however, because of the "infinite" length of medium 2 required. Only for high-loss samples will the amplitude of the wave in the sample decrease so rapidly, that a reasonably short cell can be used without disturbing reflection from the lower end of the cell.

Therefore a finite length of sample will generally be used, terminated again by another impedance (medium 3), as shown in fig. II. F. II.

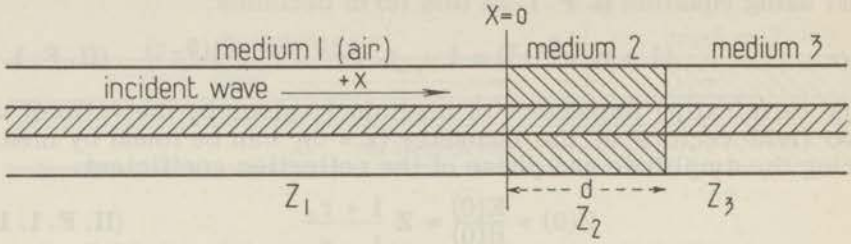

Fig. II.F.II. Coaxial line with specimen of thickness d, terminated by an impedance Z_3.

In most cases the terminating impedance will be a short-circuit, a metal plate backing the sample, but other terminations may be used. By setting $r_o = e^{-2u}$ (where $u = \rho + j\varphi$) in equation II.F.1.10, the terminating impedance Z(0) can be written:

$$Z(0) = Z\,\frac{1 + r_o}{1 - r_o} = Z \coth u \qquad \text{(II.F.1.16)}$$

For a voltage minimum in medium 1, the losses α_1 in the air-filled line being neglected, we derived:

$$s = \frac{E_{min}}{E_{max}} = \frac{1 - |r_o|}{1 + |r_o|} = \frac{1-e^{-2\rho}}{1+e^{-2\rho}} = \tanh\rho \qquad \text{(II.F.1.17)}$$

By combining equation II.F.1.16, II.F.1.17 and II.F.1.11, the desired expression, relating Z(0) with s and x, can be obtained:

$$Z(0) = Z\,\frac{s - j \tan\frac{2\pi x_o}{\lambda}}{1 - j\, s \tan\frac{2\pi x_o}{\lambda}} \qquad \text{(II.F.1.18)}$$

Thus the terminating impedance is evaluated experimentally by measurements of the standing wave pattern in medium 1. To obtain the properties of medium 2, however, we have to consider the situation at the boundary 2 - 3, located at x = +d. At this boundary a reflection coefficient r_{23} sets up a standing wave in medium 2, which in analogy with equ. II.F.1.5 and II.F.1.6 can be expressed as:

$$\begin{aligned} E_{y2} &= E_2\, e^{j\omega t}\left\{ e^{-\gamma_2(x-d)} + r_{23}\, e^{\gamma_2(x-d)} \right\} \\ H_{z2} &= \frac{E_2}{Z_2}\, e^{j\omega t}\left\{ e^{-\gamma_2(x-d)} - r_{23}\, e^{\gamma_2(x-d)} \right\} \end{aligned} \qquad \text{(II.F.1.19)}$$

The terminating impedance at x = 0, the boundary 1 - 2, is given by:

$$Z(0) = \frac{E_2(0)}{H_2(0)} = Z_2\,\frac{e^{\gamma_2 d} + r_{23}\, e^{-\gamma_2 d}}{e^{\gamma_2 d} - r_{23}\, e^{-\gamma_2 d}} \qquad \text{(II.F.1.20)}$$

Only three values of r_{23} are of practical interest for the measurements:

a. $r_{23} = 0$; in this case no reflection takes place at the boundary 2 - 3, i.e. the impedances of medium 2 and 3 are equal, and the situation is exactly the same as in the case of medium 2 having infinite length.

b. $r_{23} = -1$; total reflection takes place at the boundary. When medium 3 is a metal plate this condition is very well approximated. This gives the so called "short-circuit measurement" of medium 2 and the equation for the terminating impedance (equ. II. F. 1. 20) is simplified to:

$$Z(0) = Z_2 \tanh \gamma_2 d \qquad \text{(II. F. 1. 21)}$$

c. $r_{23} = +1$; again total reflection, but with opposite phase relationship, occurs at the boundary, when medium 3 forms an open circuit. This can be simulated by backing medium 2, with a short-circuited section of lossless line a quarter wavelength long, resulting in an open circuit at the boundary.
For this "open-circuit measurement" of mediun 2, equation II. F. 1. 20 is simplified to:

$$Z(0) = Z_2 \coth \gamma_2 d \qquad \text{(II. F. 1. 22)}$$

A combination of equation II. F. 1.18 with II. F. 1.21 leads to a well known expression, relating the propagation constant γ_2 of medium 2 with the measured quantities in a short-circuit measurement, used by most authors:

$$Z_2 \tanh \gamma_2 d = Z \frac{s - j \tan \frac{2\pi x_o}{\lambda}}{1 - j\, s \tan \frac{2\pi x_o}{\lambda}} \qquad \text{(II. F. 1. 23)}$$

For non magnetic dielectrics:

$$Z\, \gamma_1 = Z_2\, \gamma_2 \qquad \text{(II. F. 1. 23a)}$$

As medium 1 is lossfree, the propagation constant γ_1 equals $j \frac{2\pi}{\lambda}$ (equ. II. F. 1. 2a) and

$$\frac{\tanh \gamma_2 d}{\gamma_2 d} = -\frac{j\lambda}{2\pi d} \frac{s - j \tan \frac{2\pi x_o}{\lambda}}{1 - j\, s \tan \frac{2\pi x_o}{\lambda}} \qquad \text{(II. F. 1. 24)}$$

Several authors [96-98] have proposed charts for the solution of the transcendental function for γ_2. The preparation and use of the charts require a large amount of numerical work, and the accuracy is limited by the necessity for interpolating between the successive curves of the charts.

Cripwell and Sutherland (99) give a method of successive approximations for equ. II. F. 1. 24 which is very time consuming.

Furthermore the solution of the hyperbolic function is multivalued in both cases, necessitating knowledge of an approximate value of γ_2 beforehand.

Both von Hippel [21] and Krishna [100] have suggested methods to avoid these difficulties. For a short-circuit measurement and an open-circuit measurement on the same sample, equ. II. F. 1. 21 and II. F. 1. 22 apply.

$$\text{short-circuit:} \quad Z_s(0) = Z_2 \tanh \gamma_2 d$$
$$\text{open- circuit:} \quad Z_o(0) = Z_2 \coth \gamma_2 d$$

In both cases the standing wave pattern can be measured. Thus multiplying these two equations and using equ. II. F. 1. 18, we obtain:

$$Z_s(0)\, Z_o(0) = Z_2^2 = Z^2 \left\{ \frac{s - j \tan \frac{2\pi x_o}{\lambda}}{1 - j\, s \tan \frac{2\pi x_o}{\lambda}} \right\}_{\text{short}} \left\{ \frac{s - j \tan \frac{2\pi x_o}{\lambda}}{1 - j\, s \tan \frac{2\pi x_o}{\lambda}} \right\}_{\text{open}}$$

A direct relation between the complex permittivity and the data from the standing wave patterns is obtained by combining this equation with (II. F. 1. 3) and (II. F. 1. 23a):

$$\hat{\varepsilon} = \varepsilon' - j\varepsilon'' = \left\{ \frac{1 - j\, s \tan \frac{2\pi x_o}{\lambda}}{s - j \tan \frac{2\pi x_o}{\lambda}} \right\}_{\text{short}} \left\{ \frac{1 - j\, s \tan \frac{2\pi x_o}{\lambda}}{s - j \tan \frac{2\pi x_o}{\lambda}} \right\}_{\text{open}}$$

(II. F. 1. 25)

The limitations of this method will be discussed in section II. F. 2.

The method indicated by Krishna [100] is based on the short-circuit measurement of samples with thicknesses d, 2d etc. Setting the right hand side of equ. II. F. 1. 18 equal to x + j y we can write equ. II. F. 1. 24 for successive samples:

$$\frac{\tanh \gamma d_1}{\gamma d_1} = x_1 + j y_1$$

$$\frac{\tanh \gamma d_2}{\gamma d_2} = \frac{\tanh 2\gamma d_1}{2\gamma d_1} = x_2 + j y_2$$

This results in

$$\gamma d_1 = \left\{ \frac{(x_1 - x_2) + j(y_1 - y_2)}{(x_1 + j y_1)^2 (x_2 + j y_2)} \right\}^{\frac{1}{2}} \qquad \text{(II. F. 1. 26)}$$

Thus a direct relation between the complex permittivity and the measured quantities is obtained. As an elaboration of this method, Bos [101] derived a new equation, giving ε' and ε'' in terms of the measured quantities directly.

II. F. 1. 2. *Resonance methods*

In the frequency range under consideration the resonance methods can be devided into two groups:

A. Coaxial line resonators.

B. Reentrant cavities.

A. Coaxial line resonators

Like an L C resonant circuit, a part of coaxial line short-circuited at both sides, will have one main resonant frequency. From the shape of the resonance curve, the loss tangent of the circuit can be evaluated. Starting from the field equations in polar coordinates, Dunsmuir [94] derived the resonant frequencies, for the system drawn in fig. II. F. III, through application of the continuity requirements at the boundary surfaces:

$$\sqrt{\frac{\varepsilon_2}{\varepsilon_1}}\sqrt{\frac{\varepsilon_2}{\varepsilon_3}}\tan\beta_1 l_1 \tan\beta_2 l_2 \tan\beta_3 l_3 - \sqrt{\frac{\varepsilon_2}{\varepsilon_1}}\tan\beta_1 l_1 - \tan\beta_2 l_2 - \sqrt{\frac{\varepsilon_2}{\varepsilon_3}}\tan\beta_3 l_3 = 0 \qquad \text{(II. F. 1. 27)}$$

If a specimen having a permittivity ε_m is located at l_2, the further sections l_1 and l_3 being air filled, equ. II. F. 1. 27 reduces to:

$$\sqrt{\frac{\varepsilon_m}{\varepsilon_o}} = \cot\frac{\beta_s l_s}{2}\cot\frac{\beta_o l_o}{2} \qquad \text{(II. F. 1. 28)}$$

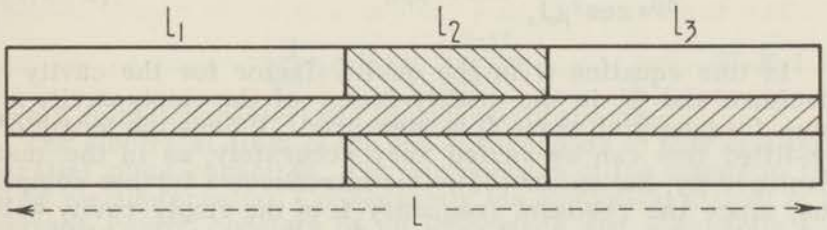

Fig. II.F.III. Coaxial resonator with specimen of thickness l_2.

For the case, shown in fig. II. F. IV, where the test specimen is located at one end of the coaxial resonator, equ. II. F. 1. 27 reduces to:

$$\sqrt{\frac{\varepsilon_m}{\varepsilon_o}} = -\tan\beta_s l_s \cot\beta_o l_o \qquad \text{(II. F. 1. 29)}$$

With the help of equ. II. F. 1. 2a. this equ. can be rewritten

$$\sqrt{\varepsilon_m} = -\tan\frac{2\pi\sqrt{\varepsilon_m}\,d}{\lambda}\cot\frac{2\pi(1-d)}{\lambda}$$

or

$$\frac{\tan\left(\frac{2\pi d}{\lambda}\sqrt{\varepsilon_m}\right)}{\frac{2\pi d}{\lambda}\sqrt{\varepsilon_m}} = -\frac{\lambda}{2\pi d \cot\frac{2\pi(1-d)}{\lambda}} \qquad \text{(II. F. 1. 30)}$$

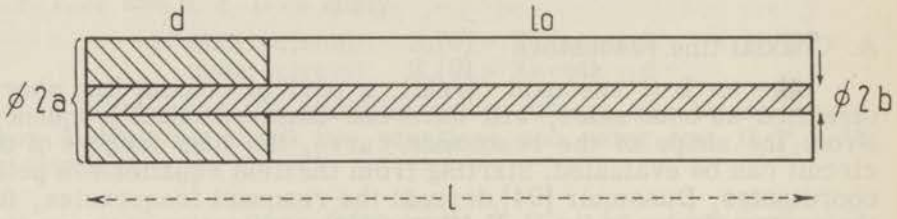

Fig. II.F.IV. Coaxial resonator terminated by a specimen of thickness d.

In this way a direct evaluation of the permittivity of loss-free specimens is possible with one resonant frequency determination and the use of $\frac{\tan x}{x}$ tables.

The equations for the loss tangent, $\tan\delta_m$, of low loss specimens, as derived by Dunsmuir are rather complicated for this case:

$$\tan\delta_m = \frac{l_s + \frac{\cos^2\beta_s l_s}{\cos^2\beta_o l_o} l_o}{l_s + \frac{1}{2\beta_o}\frac{\cos^2\beta_s l_s}{\cos^2\beta_o l_o}\sin 2\,\beta_o l_o} \left\{\frac{1}{Q} - \frac{1}{Q'}\right\} \qquad \text{(II. F. 1. 31)}$$

In this equation Q is the quality-factor for the cavity with specimen and Q' is the quality-factor of the empty cavity at the same frequency at which Q is measured. Unless the length of the air-filled line can be varied very accurately, as in the method developed by Eichacker [58], this introduces a further complication, since the resonant frequency f_o of the empty cavity will be higher than the resonant frequency f_s, after insertion of the specimen. Therefore the measured quality-factor Q_o of the empty cavity must be converted to Q' by a separate calculation [94].

The calculation of $\tan\delta_m$ from the measuring data is very time consuming, but yields accurate results for low-loss specimens that cannot be obtained from standing wave measurements. The method was extended by Huber [59, 102], using variable length resonators. Here at one frequency the thickness of the sample is varied till resonance is established, the other dimensions being kept constant. For this method Untermann's [103] scheme of computations to convert the resonance data into the dielectric data for the specimen was used.

B. Reentrant cavities

Another type of resonance method used at frequencies in the order of 1000 Mc/s is known as the reentrant cavity method. Originally introduced by Dakin and Works [104], the method was further developed by various authors [105-107, 56].

A reentrant cavity basically consists of a piece of coaxial line short-circuited on both sides and with a gap in the inner conductor, as shown in fig. II. F. V.

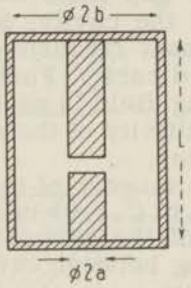

Fig. II.F.V. Re-entrant cavity.

To a first approximation the cavity may be regarded as a loss-free coaxial transmission line, short circuited at one end and loaded with a capacity C at the other end. Thus according to the foregoing equations, the resonant frequency of the system will be given by:

$$\frac{1}{2\pi fC} = Z \tan \frac{2\pi fl}{3x10^{10}}, \qquad \text{(II. F. 1. 33)}$$

where Z is the characteristic impedance of the line.

The electrical field in the gap corresponds to that existing in a parallel plate capacitor. The distribution of the magnetic field will be circumferential. Consequently the equivalent circuit of the reentrant cavity consists of an inductance and a capacity C in series. In terms of this equivalent circuit a far simpler representation of the properties of this cavity is possible than could be made on the basis of the field equations.

The frequency-range of the cavity is determined by its length and the possible variation in the capacity C. Roughly the same equations, as were derived for the reactance variation method in section II. C, apply in this case. If the resonance curve of the cavity is delineated by varying the capacity C the total conductance G_T of the circuit is given by:

$$G_T = \frac{\omega \Delta C}{2\sqrt{q-1}}, \qquad \text{(II. F. 1. 34)}$$

where ΔC is the width of the resonance curve for a given value of q, q being equal to V_r^2/V^2, where V_r and V are the resonant voltage and the voltage at which ΔC is measured respectively. The capacity C is varied by altering the width of the gap in the inner conductor with a micrometer drive. When a specimen is clamped in the gap the thickness and permittivity of this specimen determine the capacity C_s in the gap and hence the frequency at which the specimen is measured. The measuring-frequency can only be changed by varying the thickness of the specimen.

After removal of the specimen resonance is restored at the same frequency by narrowing the gap, till the same capacity is reached. As the width of the air gap fixes the capacity C, and hence the resonant frequency of the cavity, a calibration curve can be produced giving the resonant frequency, in terms of the micrometer readings for the gap, directly. Furthermore a capacity calibration of C and its fringing field is necessary for the accurate determination of the permittivity of the specimen from the two settings of the main micrometer.

The equation giving the loss tangent of the sample in terms of frequency-variations (see equ. II. C. 1. 9) cannot be used here, as a variation in the frequency of the generator may result in changes in the output, the coupling between cavity and generator, and the inherent losses of the cavity.

The loss-tangent of a specimen in the gap is given by:

$$\tan\delta_m = \frac{\Delta C_s - \Delta C_o}{2\, C_s \sqrt{q-1}} \qquad \text{(II. F. 1. 35)}$$

where ΔC_s and ΔC_o are the widths of the resonance curve with and without the specimen and C_s in the capacity of the specimen. As C_s cannot be varied when the specimen is placed in the gap, another way of tuning the cavity has to be found, or the additional equation (see II. C.) for the loss tangent must be used:

$$\tan\delta_m = \frac{\Delta C_o}{2\, C_s \sqrt{q-1}} \left(\sqrt{\frac{V_{or}^2}{V_{sr}^2} - 1}\right) \qquad \text{(II. F. 1. 36)}$$

The cavity can be tuned, without changing the gap, by introducing a vernier capacitor C_2. If this capacitor is connected in parallel with part of the line, as indicated in fig. II. F. VI, a very accurate ΔC setting over a small range is possible.

The impedance of the equivalent circuit of fig. II. F. VI is given by:

$$Z = \frac{L_1/C_1 + (L_2/C_1)\,\dfrac{1}{1 - \omega^2 L_2 C_2}}{j\left[\omega L_1 - \dfrac{1}{\omega C_1} + \dfrac{\omega L_2}{1 - \omega^2 L_2 C_2}\right]}$$

resulting in the resonance condition:

$$\frac{1}{\omega C_1} - \omega L_1 = \frac{\omega L_2}{1 - \omega^2 L_2 C_2} \qquad \text{(II. F. 1. 37)}$$

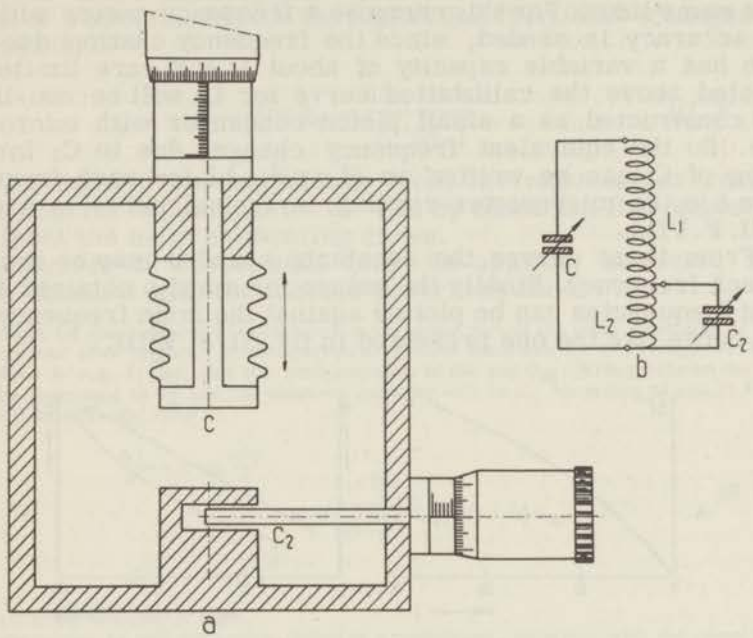

Fig. II.F.VI. a. Re-entrant cavity with vernier capacitor.
b. Equivalent circuit.

From this equation the ratio of ΔC_1 and ΔC_2 can be derived and hence the equivalent frequency shifts for ΔC_1 and ΔC_2:

$$\Delta C_2 = \frac{(1 - \omega^2 L_2 C_2)^2}{L_2^2 C_1^2 \omega^4} \Delta C_1 \approx \frac{(L_1 + L_2)^2}{L_2^2} (1 - \omega^2 L_2 C_2)^2 \Delta C_1$$

$$-\Delta C_1 = \left\{ \frac{2 \omega L_2 C_1^2}{(1 - \omega^2 L_2 C_2)^2} + 2 \omega L_1 C_1^2 \right\} \Delta\omega \qquad \text{(II. F. 1. 38)}$$

$$-\Delta C_2 = \left\{ \frac{2}{\omega^3 L_2} + \frac{2 L_1}{\omega^3 L_2^2} \cdot (1 - \omega^2 L_2 C_2)^2 \right. \Delta\omega$$

The right-hand side of the first equation is used to determine, approximately, the position of C_2 in the cavity for a desired ratio of $\Delta C_2 / \Delta C_1$. This ratio will be approximately equal to $(L_1 + L_2)^2 / L_2^2$ and dependent on frequency. As can be seen from the first and third equations, the calibration of C_2 both in capacity and equivalent frequency changes will be non-linear, in contradiction with the curves given by Reynolds [105]. The capacity C_2 therefore has to be calibrated at each measuring frequency separately.

Since the frequency of the cavity has to be calibrated for each setting of the gap, at a fixed setting of C_2, in any case, it is con-

venient to calibrate C_2 in terms of equivalent frequency changes at the same time. For this purpose a frequency-meter with very high accuracy is needed, since the frequency changes due to C_2, which has a variable capacity of about 1 $\mu\mu$F, are limited. As indicated above the calibration curve for C_2 will be non-linear. C_2 is constructed as a small piston-condenser with micrometer drive. So the equivalent frequency changes due to C_2 for each setting of C_1 can be written as $\Delta f = al^2 + bl$ for each frequency, where l is the micrometer-reading. A typical curve is shown in fig. II. F. VIIA.

From these curves the constants a and b may be evaluated for each frequency. Finally the values for a and b obtained at different frequencies can be plotted against the main frequency, giving a curve like the one presented in fig. II. F. VIIB.

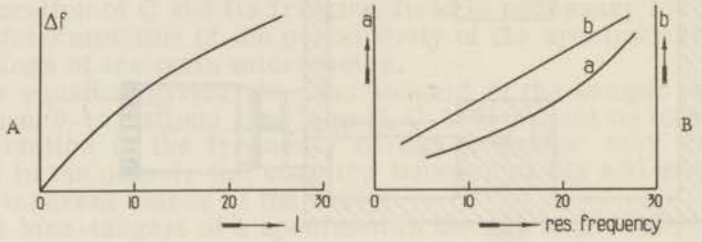

Fig. II.F.VII. Frequency-curves for the vernier capacitor C_2.

After these calibrations it is possible to evaluate the loss tangent of a specimen from the equivalent frequency changes with the equation:

$$\tan\delta_m = \frac{\Delta f_s - \Delta f_o}{f_r \sqrt{q-1}} \qquad \text{(II. F. 1. 39)}$$

where Δf_s and Δf_o are calculated from the micrometer readings of C_2 using the equation $\Delta f = al^2 + bl$ by inserting the values for a and b from the main calibrating curve.

A number of corrections must be applied, however, to the results obtained with the method described above:

a. correction for the increase of inductance in the upper part of the inner electrode, if the gap is decreased after removal of the specimen. Without specimen the total length of the inner conductor is e.g. l_1 cm, and the total capacity of the gap C_m. With specimen the length will be decreased to l_2 and the unknown capacity will be C. According to equ.II.F.1.33, C_m will be different from C:

$$\frac{1}{\omega C} = Z \tan\frac{\omega l_2}{c}$$

$$C = \frac{\tan\frac{\omega l_1}{c}}{\tan\frac{\omega l_2}{c}} C_m = (1+\alpha)\, C_m \qquad \text{(II.F.1.40)}$$

$$\frac{1}{\omega C_m} = Z \tan\frac{\omega l_1}{c}$$

where c is the velocity of light.
The magnitude of this correction, taken as a percentage, increases with the sample thickness and its permittivity.

b. edge correction.
Since the electrical field in the gap is comparable with that existing in a parallel plate capacitor, the normal corrections for the edge effect in a parallel plate capacitor can be applied. To a good approximation the field in the gap will be homogeneous and the edge effect will be given by Kirchhoffs equation (3):

$$C_e = \frac{r}{3,6\pi}\left[\log_e \frac{16\pi r\,(b+d)}{d^2} + \frac{b}{d}\log_e \frac{b+d}{b} - 1\right] \mu\mu F \qquad \text{(II.F.1.41)}$$

Thus:

$$C = C_1 + C_e = \left(\frac{O}{3,6\pi d} + C_e\right) \mu\mu F\,, \qquad \text{(II.F.1.42)}$$

where b is the thickness of the electrodes, d the width of the gap and r the radius of the inner conductor. The value of C_e will be different for the sample-in and sample-out setting of the main micrometer: sample-in: $C = C_s + C_{es}$

sample-out: $C_m = C_1 + C_e$ (II.F.1.43)

The capacity due to the sample is obtained by combining equ.II.F.1.43 with II.F.1.40:

$$C_s = (1+\alpha)\,(C_1 + C_e) - C_{es} \qquad \text{(II.F.1.44)}$$

The capacities C_1, C_e and C_{es} are determined from a low-frequency calibration.

c. correction for self-inductance of the specimen. At very high frequencies the field strength E in the centre of the specimen will be higher than the field strength E_1 at the edge, because of the distributed inductance of the specimen.

Here the description of a reentrant cavity in terms of lumped-circuit elements breaks down and an addition has to be made in terms of transmission line equations. As a result of the distributed inductance of the sample, the measured capacities appear to be greater than the true values and the apparent conductance is increased in the same ratio. Considering the

sample as a disc transmission line of relative permittivity ε, we may use Schelkunoff's (108) equations to evaluate the ratio between the true and apparent values of the capacities.

By analogy with the equations derived by Hollway (107), the apparent capacity of the sample with thickness d_s in the gap is given by:

$$C_s' = \frac{\pi r^2 \omega \sqrt{\varepsilon\mu}}{\omega\sqrt{\frac{\mu}{\varepsilon}}\, d_s} \left(1 + \frac{\omega^2 \mu\varepsilon\, r^2}{8c^2} + \frac{\omega^4 \mu^2 \varepsilon^2 r^4}{48c^4} \ldots\ldots\right) \simeq \frac{\pi r^2 \varepsilon}{d_s} \left(1 + \frac{\omega^2 \varepsilon r^2}{8c^2}\right)$$

or

$$C_s' \simeq C_s \left\{1 + \frac{\varepsilon}{2} \left(\frac{\pi r}{\lambda}\right)^2\right\} \qquad \text{(II.F.1.45)}$$

When the sample is removed and resonance is restored the air capacitance in the gap at the new spacing, has the higher apparent value:

$$C_1' \simeq C_1 \left\{1 + \frac{1}{2} \left(\frac{\pi r}{\lambda}\right)^2\right\} \qquad \text{(II.F.1.46)}$$

By substituting C_s' and C_1' for C_s and C_1 in equ.II.F.1.44 this correction can be accounted for and the capacity of the sample, C_s, in terms of the measured quantities will be given by:

$$C_s = (1 + \alpha)\left\{C_1\left(1 + \frac{\varepsilon - 1}{2} \frac{\pi^2 r^2}{\lambda^2}\right) + \left(C_e - \frac{C_{es}}{1 + \alpha}\right)\left(1 - \frac{\varepsilon}{2} \cdot \frac{\pi^2 r^2}{\lambda^2}\right)\right\} \qquad \text{(II.F.1.47)}$$

In this equation several approximations are used: the series development for C_s' and C_1' is broken off after the second term and the assumption is made that C_e, C_{es} and the value of $(1 + \alpha)$ are not affected by the modification of the field distribution.

Furthermore the value of C_s, and hence ε, has to be evaluated by successive approximations, since the value of the permittivity appearing in the correction-term is not known beforehand. From the consistency of the permittivity values obtained by measurements on different thicknesses of a non polar material the errors in the permittivity measurements are found to be less than 2%.

In the measurements with a reentrant cavity the corrections described above, in combination with the elaborate calibrations necessary for the capacities, for their edge-effects and for the equivalent frequency-shifts of the vernier capacitor C_2, lead to very time-consuming calculations for the dielectric properties of the samples.

If liquids are to be measured further complications result from the fact that the liquid must be contained in some kind of cup [56] or insulating ring around the lower part of the inner conductor. In the first case three measurements are necessary, one without the cup, one with the empty cup and one with cup and sample. In the second case corrections due to the modification of the edge-effects for various permittivities of the samples and different settings of the main capacitor, must be accounted for. Thus both methods involve an enormous amount of numerical work.

As a result the method is of very limited use. It will mainly be useful for the accurate measurement of low loss solids, where the fitting of the specimen in a coaxial resonator may impair the accuracy of the permittivity- and loss-measurements. The results obtained for some lowloss solids, with a reentrant cavity of the type shown in fig. II. F. VI, will be published in a separate paper.

II. F. 1. 3. *Travelling-wave methods*

Travelling-wave methods are based on the measurement of the rate of change of the amplitude and phase of a high-frequency electromagnetic wave propagated through a material. Several methods have been devised to measure the difference between the amplitude and phase of an incident wave with those of the wave after passing through a specimen of known length [109, 110, 60, 61]. This may be accomplished by transmitting the incident wave both through the specimen and through a series-network consisting of a calibrated constant loss phase-changer and constant phase attentuator, after which the two signals are recombined and the components of the network are varied in such a way, that the two signals balance each other. The readings of the phase-changer and attenuator give the phase-shift and attenuation of the specimen, from which the complex permittivity of the specimen can be evaluated when the length of the specimen is inserted into the equations.

For liquids it is also possible to measure the amplitude and phase of the incident wave at two points in the sample, e. g. A and B, a known distance apart. If $\gamma = \alpha + j\beta$ is the propagation constant of the material, the ratio of the absolute values of the electric vector at A to that at B is $e^{\alpha l}$ and the phase difference between A and B is βl, l being the distance from A to B. Hence if the amplitude ratio and phase difference between the two points are measured, α and β can be calculated, and hence ε' and ε''.

While the mathematical basis of these methods is relatively simple, the difficulties arise mainly on the experimental side, where an attenuator has to be constructed without noticeable phaseshift and a phase-shifter without any noticeable attenuation. In a careful design these difficulties can be overcome over a limited frequency-range, as was shown by Buchanan and Grant [61, 109].

The method is particularly useful for high loss materials, where the accuracy of the standing-wave methods is greatly reduced. For medium-loss materials the results obtained with standing-wave methods appear to be more reliable, since small differences in attenuation cannot be readily measured with travelling-wave methods.

II. F. 2. Description of the standing wave apparatus

The frequency range between 300 and 5000 Mc/s is covered by two instruments. For frequencies up to 2000 Mc/s a coaxial system with a slotted line as standing wave indicator is used (II. F. 2. 1); and in the frequency range from 1700 to 5000 Mc/s a non-slotted coaxial measuring system (II. F. 2. 2).

II. F. 2. 1. *Standing wave apparatus for frequencies from 300-2000 Mc/s*

In fig. II. F. VIII a block-diagram of the experimental set-up is drawn. A stable high frequency generator, followed by a 10 db. attenuator and low-pass filter supplies a high-frequency voltage of about 0.5 Volt to the coaxial line (characteristic impedance 50 Ohms). The attenuator is inserted to avoid reaction from the measuring system on the generator and the low-pass filter serves the purpose of eliminating possible higher harmonics of the generator frequency. A frequencymeter is loosely coupled to the generator for accurate frequency determinations.

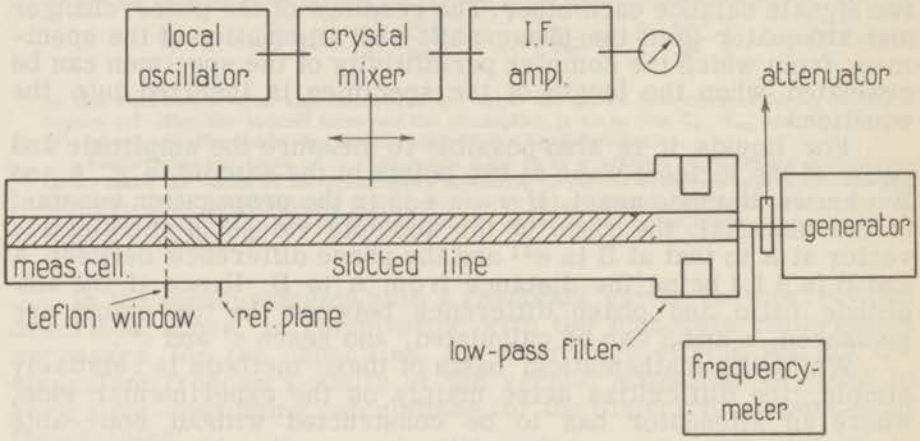

Fig. II.F.VIII. Block-diagram of the standing wave apparatus.

The standing wave pattern in the coaxial system resulting from the terminating impedance is measured by means of a slotted line (Rohde and Schwarz type LMD). The position of the antenna or probe, protruding through the slot, is measured to within 0.1 mm on a mm-scale, which gives the position of the antenna with respect to the reference plane directly. The voltage induced in the probe, proportional to the electric field strength in the line and the probe penetration, can be measured in several ways, e.g. by a crystal-diode and sensitive microammeter. This system has several disadvantages, particularly for the measurement of high standing wave ratio's. On account of the limited sensitivity of the system rather large probe penetrations must be used in the minimum of the standing wave pattern to obtain a sufficient reading on the meter. As a result errors may arise from probe-reflections and variations in the characteristic of the crystal over the large voltage-range between maximum and minimum in the standing wave pattern. A much higher sensitivity, with subsequent reduction of the probe penetration and higher accuracy can be achieved

by the use of a heterodyne-detector, consisting of a mixer crystal with local oscillator and an intermediate-frequency amplifier and meter. In our apparatus a Gen. Rad. amplifier was used with an I. F. frequency of 30 Mc/s and a band width of 0.7 Mc/s. The relative frequency drift of the two oscillators involved was found to be so small that very stable meter readings were obtained after a warming-up period of one hour. The input sensitivity of the system is about 2 microvolts over the whole frequency range. By the use of a calibrated attenuator in the input circuit of the I. F. amplifier, in combination with the linear voltage-characteristic of the mixer, standing wave ratio's can be measured with errors below 1%.

The actual errors in the measured standing wave ratio's may be somewhat larger, on account of small variations in the probe penetration with the displacement of the probe-carriage. Values of $E_{max}/E_{min} = S$ below 20 are measured directly, using the calibrated attenuator and meter of the I. F. amplifier.
For values of S in excess of 20 the double-minimum method [21] gives more accurate results. Here the width, Δx, of the curve around the minimum is measured at a voltage equal to $\sqrt{2}$ times the voltage in the minimum. The inverse standing wave ratio may then be evaluated with the equation:

$$E_{min}/E_{max} = s_m = \frac{\sin \frac{\pi \Delta x}{\lambda}}{\sqrt{1 + \sin^2 \frac{\pi \Delta x}{\lambda}}} \qquad \text{(II. F. 2. 1)}$$

For very high standing wave ratio's the accuracy is limited. This is due to the fact that neither small Δx values nor very small values of the voltage in the minimum can be accurately determined.

Measuring cells were constructed from pieces of coaxial line with the same diameters as the slotted line. They are short-circuited on one side by a metal disc and have a very thin teflon window on the other side. The connection to the slotted line is made by a short piece of the same coaxial line with precision flanges. Fig. II. F. XI gives a full-scale drawing of one of the cells. Since the inner conductor of the slotted line is fixed in this case, a spring loaded inner conductor is used in the connector, instead of the fixed one used at higher frequencies. Cells were constructed for liquid lengths of 3, 5, 7.5, 10, 15 and 20 centimetres. The length of the connector between the reference plane (flange) of the slotted line and the teflon window of the cell, must be determined separately.

First some measurements were carried out on a loss-free sample, i. e. benzene. For loss-free materials equ. II. F. 1. 24 is simplified to:

$$\tan \left(\frac{2\pi}{\lambda} d \sqrt{\varepsilon}\right) = - \sqrt{\varepsilon} \tan \frac{2\pi}{\lambda} (1 + \Delta), \qquad \text{(II. F. 2. 2)}$$

where ε and d are the relative permittivity and thickness of the sample (cell length), l is the length of the line between the reference plane and the first minimum in the standing wave pattern and Δ is the length of the connector. Thus $(l + \Delta) = x_o$ is the distance from the first minimum to the entrance-plane of the cell.

From the measurements on the empty cells, the cell lengths being known accurately, no consistant value for the length of the connector could be found with varying cell-length and frequency; the values for Δ were 3.40 ± 0.14 cm's. By inserting the medium value of $\Delta = 3.40$ in the measurements on benzene, differences in the permittivity values up to 7.5% were found for cell-lengths above 10 cm and even larger differences for the shorter cells. By inserting the value of Δ obtained for the empty cell at a given frequency and cell-length into the measurements on benzene, the same differences were found. These differences can be accounted for by considering the parasitic reflections in the measuring system and the differences between the wavelengths measured with the standing wave indicator and those calculated from the frequency measurements. The wavelength in the coaxial system will be somewhat shorter than the wavelength calculated from the frequency measurements with the equation $f = 3x10^{10}/\lambda(cm)$. This is due to the fact that the propagation velocity of electric waves in air is smaller than $3x10^{10}$ cm/sec and to losses, roughness etc of the coaxial line. From a number of measurements a constant correction factor was obtained over the whole frequency range:

$$f = \frac{3x10^{10}}{\lambda(cm)} \times 0.9985 \qquad \text{(II. F. 2. 3)}$$

Since the errors in the frequency measurements (0.003%) are considerably lower than those in the wavelength measurements, the values of λ obtained from the frequency measurements with equ. II. F. 2. 3 are used in the calculations. In the absence of parasitic reflections in the measuring system, the positions of the minima on the slotted line, terminated by an empty shortcircuited cell, will be given by:

$$d + x_o = d + l + \Delta = n\lambda/2 \qquad \text{(II. F. 2. 4)}$$

If parasitic reflections occur, e.g. at the end of the slot in the standing wave indicator and the window and connector of the cell, equ. II. F. 2. 4 no longer applies. Considering the piece of line, where the parasitic reflections arise, as a four-terminal network [92, 111], one finds that $d + x_o$ may be larger or smaller than $n\lambda/2$:

$$d + \Delta + l \pm \delta l = n\lambda/2 \qquad \text{(II. F. 2. 5)}$$

Furthermore with increasing d, the difference ∂l appears to vary periodically with a period of $\frac{1}{2}\lambda$. Since a correction is required

on the readings of the standing wave indicator, the differences ∂l are best plotted in terms of l instead of d. By measuring a number of empty cells of different length and by comparing the measured values of ∂l with standard sinecurves of different amplitude and a period equal to $\frac{1}{2}\lambda$, a correction curve can be obtained for the readings of the standing wave indicator at each measuring-frequency. These measurements were carried out over the whole frequency range with increments of 100 Mc/s and calibration curves were composed. The curve obtained for 900 Mc/s is shown in fig. II.F.IX.

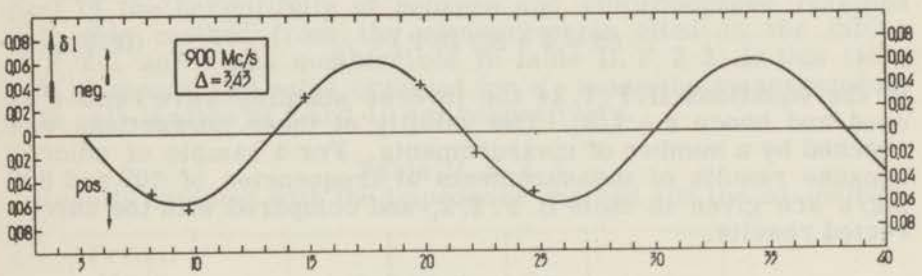

Fig. II.F.IX. Correction curve for the readings of the standing wave indicator.

When these corrections are applied to the measurements on the empty cells, a constant value of $\Delta = 3.43 \pm 0.005$ is found. From the measurements on benzene a virtually constant value of the permittivity is obtained, as may be seen from table II.F.2.1, where the corrected values are compared with the uncorrected results.

Table II.F.2.1
Measurements of the relative permittivity of benzene, T = 21°C.

frequ. Mc/s	cell length							
	5 cm		7.5 cm		10 cm		15 cm	
	uncorr.	corr.	uncorr.	corr.	uncorr.	corr.	uncorr.	corr.
400			2.40	2.29	2.32	2.28	2.28	2.29
500	2.45	2.29	2.31	2.27	2.28	2.28	2.27	2.29
600	2.37	2.28	2.30	2.29	2.29	2.29	2.30	2.29
700	2.34	2.28	2.28	2.29	2.27	2.28	2.30	2.285
800	2.30	2.27	2.27	2.29	2.26	2.28	2.31	2.28
900	2.28	2.28	2.26	2.28	2.27	2.28	2.30	2.29

The effective voltage standing wave ratio S, which is directly porportional to the parasitic reflections, can be calculated from the above correction curves with the equation [112]:

$$S = 1 + \frac{4\,\pi\,(\partial\, l)_{max}}{\lambda}$$

From our measurements a virtually constant value is calculated,

viz. $S = 1.024 \pm 0.003$. Thus the parasitic reflections can be estimated as 1.2%. The values of the standing wave ratio's may be corrected with the same correction curves. Here too the value of the measured ratio $S_m = E_{max}/E_{min}$ may be smaller or larger than the actual value S_a:

$$S_a = S_m \pm \Delta S \qquad \text{(II. F. 2. 6)}$$

Owing to phase difference the value of ΔS must be determined from the ∂ l curve at a point 90^o, or in the correction curve $-1/8\,\lambda$ from the point where the ∂ l correction for x_o is applied:

$$\Delta S = 4\,\pi\,S_m\,(\partial\, l')_{-\lambda/8} \qquad \text{(II. F. 2. 7)}$$

In the equations II. F. 1. 24 the inverse standing wave ratio s is used and hence $s = 1/S_a$. The validity of these corrections was checked by a number of measurements. For a sample of chlorobenzene results of measurements at frequencies of 700 and 900 Mc/s are given in table II. F. 2. 2, and compared with the uncorrected results.

Table II. F. 2. 2

Measurements of the complex permittivity of chlorobenzene, $T = 22^oC$.

frequ. Mc/s		Cell length					
		7.5 cm		10 cm		15 cm	
		ε'	ε''	ε'	ε''	ε'	ε''
700	uncorr.	(5.57)	(0.179)	5.62	0.165	5.60	0.160
	corr.	(5.61)	(0.164)	5.63	0.158	5.64	0.162
900	uncorr.	5.62	0.207	5.63	0.197	5.58	0.193
	corr.	5.61	0.203	5.62	0.197	5.63	0.201

For the evaluation of the results the charts given by Poley [98] for the solution of equ. II. F. 1. 24 were used. It must be emphasized here that the choice of the cell-length is rather critical, particularly at the higher frequencies, if accurate results are required. On the one hand the values of the tangents must be in the medium part of the curve for obvious reasons and on the other hand the impedance values must be such that a good interpolation in the charts is possible. If an approximate value of ε' and ε'' is known beforehand the appropriate cell-lengths can be arrived at by simple calculations.

Various attempts were made to apply the method indicated by von Hippel [21] (see equ. II. F. 1. 25) and Krishna [100] (see equ. II. F. 1. 26) to our measurements. The method of von Hippel necessitates the use of a variable length short-circuited line and

cells with two windows. It was found that owing to imperfections of the variable short circuit and to the difficulty of setting its length to exactly a quarter or a half wavelength behind the rear cell-window, no reliable results could be obtained.

The method of Krishna for the evaluation of results on cells with lengths of d and 2d could directly be applied in our case, since cells of appropriate length were available. The results, however, are very disappointing for no obvious reason. If two cells are chosen in such a way that good results are obtained with the normal impedance-measurement used above, the results of the 2d-method may be entirely different. A few values of the real part of the permittivity of benzene and chlorobenzene obtained with this method from the measurements cited in the tables II. F. 2. 1 and 2 are summarized in table II. F. 2. 3. In this table ε 5/10 means the value obtained for ε', using the measurements with cell-lengths of 5 and 10 cm respectively.

Table II. F. 2. 3
Results obtained with the impedance-method and the 2d-method.

Frequ. Mc/s	ε'	ε5/10	ε7.5/15	ε'	ε7.5/15
400	2.29		2.42		
600	2.29	2.31	2.25		
700	2.28	2.28	2.30	5.63	5.18
900	2.28	2.27	2.27	5.62	5.40

The reason for these discrepancies may lie in the fact, that in the 2d-method two sets of experimental data, each with a limited accuracy, are essentially substracted from each other, though this is not evident in equ. II. F. 1. 26. Therefore this method will be further investigated and in our measurements the equ. II. F. 1. 24 will be used.

From the consistency of various measuring results and comparison with other values, the errors in the measured values between 300 and 2000 Mc/s can be estimated as 0.5% for the real part and 1 - 1.5% for the imaginary part of the complex permittivity.

II. F. 2. 2. *Standing wave apparatus for frequencies from 1700 to 5000 Mc/s*

For this frequency range a non-slotted coaxial system developed by Eichacker [58] is used in connection with measuring cells of the same type as described in the foregoing section. The coaxial system (Rohde and Schwarz type LMC) is drawn schematically in fig. II. F. X.

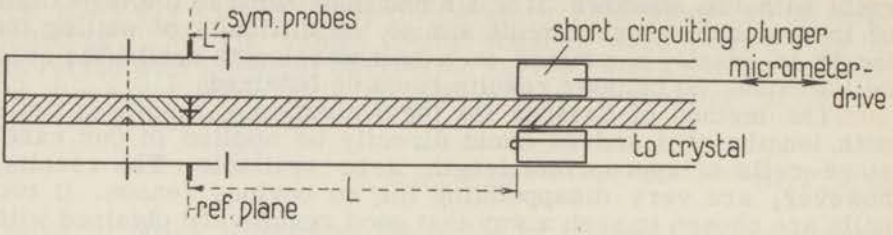

Fig. II.F.X. Diagram of a non-slotted coaxial measuring system.

The measuring system consists of a coaxial line, shortcircuited at one side by a variable shortcircuiting plunger or piston; the position of the effective shortcircuit can be accurately read with respect to the reference plane. Two small probes are inserted symetrically into the line near the reference plane, whereas a coupling loop protrudes through the piston; the penetrations of both the two probes and the coupling loop are variable. By the use of two probes opposite each other the errors that could arise from small dislocations of the inner conductor are considerably reduced.

The unknown impedance, viz. the measuring-cell, is connected to this system at the flange in the reference plane and the inner conductor of the line is supported by the piston and the measuring-cell only; thus spurious reflections of supporting studs are eliminated.

The two probes are tuned to the generator frequency by means of a tunable coaxial resonator. A klystron tube with wide range electronic tuning is used as generator, with square wave amplitude modulation via the reflector voltage at a frequency of 1000 c/s. The high-frequency voltage induced in the coupling loop is measured by means of an aperiodic coaxialdiode. The demodulated signal is amplified in a 1000 c/s selective amplifier and read on a meter, calibrated in connection with the diode.

This measuring system has several interesting features. Since the standing wave indicator is of the non-slotted type, errors due to parasitic reflections from the slot and variations in the probe penetration are eliminated. Moreover the system may be treated in two different ways, depending on the loss tangent of the unknown impedance.

In the case of low losses the system can be described in terms of a resonant system, when the shortcircuited cells described in the foregoing section are used, and accurate determinations of ε' and ε'' are possible by delineation of the resonance curves using the equations II. F. 1. 30 and 31. The Q-factors can be determined by line-length variation around the resonance position. In most cases, however, a simpler evaluation of ε' and ε'' is possible. Since it can be shown that the length of the line for resonance is equivalent to x_o in the standing wave method and the width of the resonance curve between the half power points is

equal to Δx in equ. II. F. 2. 1, all relations for calculating ε' and ε'' in the standing wave methods apply equally well to this system for low losses. Thus equ. II. F. 1. 24 may again be used. Owing to the fact that the above line-length variation method can only be used for the measurement of low losses, this equation may, however, be simplified considerably.

For loss free samples equ. II. F. 1. 24 simplifies to (see II. F. 2. 2):

$$\tan\left(\frac{2\pi d\sqrt{\varepsilon'_m}}{\lambda}\right) = -\sqrt{\varepsilon'_m}\tan\frac{2\pi x_o}{\lambda} \qquad \text{(II. F. 2. 8)}$$

Here ε'_m is given by x_o independently of s. The same equation results, if the real parts of both sides of equ. II. F. 1. 24 are equated for low loss [113]. The relation connecting the loss of the sample with the width Δx of the resonance curve is obtained by equating the imaginary parts:

$$\tan\delta_m = \frac{\Delta x}{d}\,\frac{1+\tan^2\frac{2\pi x_o}{\lambda}}{1+\tan^2\frac{2\pi d\sqrt{\varepsilon}}{\lambda} - \frac{\tan\frac{2\pi d\sqrt{\varepsilon}}{\lambda}}{\frac{2\pi d\sqrt{\varepsilon}}{\lambda}}} \qquad \text{(II. F. 2. 9)}$$

Equation II. F. 2. 8 is easily solved by the use of $\frac{\tan x}{x}$ tables. The values of Δx must be corrected for the inherent loss of the measuring system, represented by Δx_o, for the empty system under the same conditions. If an error of 1% is allowed in ε'_m, these simplified equations may be used for $\tan\delta$ values below 0.1, with ε'' below $0.2/n$, where n is the number of wavelengths in the sample. The Δx values are measured with a micrometer fitted on the piston, which can be read to within 0.005 mm. Thus the accuracy of the ε'' determinations mainly depends on the calibrating accuracy of the diode and meter and may be estimated as $1\frac{1}{2}\%$. It was found that the losses in the measuring system increased by factors of 3 to 4 after connection of one of the shortcircuited measuring cells. It was found that this increase was due to the transition between the inner conductors of the line and the cell. Since the inner conductor of this measuring line can be shifted over a small range, the spring-loaded inner conductors of the cell connectors could be replaced by fixed ones. Details of the construction of the measuring cells are shown in fig. II. F. XI.
A small locating-pin is inserted for support and alignment of the inner conductor of the measuring line.
After the connection of the cell flange, the inner conductor of the line is pressed onto the inner conductor of the cell connector. Thus stable inherent losses of the line and cell were obtained, resulting in Δx_o values of about 0.01 cm at 3000 Mc/s.

The length of the cell connectors was measured at various frequencies and found to be 3.40 ± 0.01 cm for all cells. Results of some measurements on benzene, which has no noticeable loss in this frequency range, are given in table II. F. 2. 4.

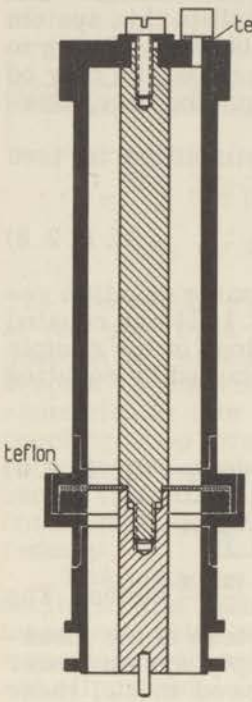

Fig. II.F.XI. Coaxial measuring cell for liquids, with connector.

Table II.F.2.4
Measurements of the relative permittivity of benzene, T = 22°C.

Frequ. Mc/s	Cell length		
	3 cm	5 cm	7.5 cm
3000	2.29	(2.25)	2.29
4000	2.28	(x)	(x)
5000	(2.30)	2.28	2.28

The values in brackets refer to measurements, for which the values of the tangents (see equ. II. F. 2. 8) were such that no accurate evaluation of ε' could be expected. For the points marked (x) even approximate evaluation was impossible for the same reason. Here again the importance of the choice of appropriate cell-lengths is clearly shown.

For samples with medium to high losses the above simplifications no longer apply. In this case the system can again be described in terms of a standing wave method. The voltage induced in the coupling loop is proportional to the current in the short-circuiting plane of the piston:

$$i_s = \frac{E_o}{Z_o} (1 - r_s)\, e^{-\gamma(L-L')}\, \frac{1 + r_x e^{-2\gamma L'}}{1 - r_s r_x e^{-2\gamma L}} \qquad \text{(II. F. 2. 10)}$$

where r_x and r_s are the reflection coefficients of the unknown impedance and the piston respectively. For small r_x values the losses in the coaxial line may be neglected and the reflection coefficient, $|r_s|$, of the piston may be taken equal to unity in good approximation. With the displacement of the piston (L variable) voltage maxima and minima will occur in the ratio:

$$s = \frac{E_{min}}{E_{max}} = \sqrt{\frac{1 - 2\,|r_x|\,|r_s|}{1 + 2\,|r_x|\,|r_s|}} = \sqrt{\frac{1 - 2\,|r_x|}{1 + 2\,|r_x|}} \qquad \text{(II. F. 2. 11)}$$

Owing to the fact that the position of the piston, L_{max}, for which the maximum value of E is obtained, is identical with x_o for the slotted standing wave indicator, the phase angle of r_x can be evaluated from L_{max}. Since the phase angle 2φ of the reflection coefficient r_s equals 180^o, the phase angle of $r_x = |r_x|\, e^{-2j\varphi x}$ (see equ. II. F. 1. 8) is given by the equation (see equ. II. F. 1. 13):

$$2\varphi_x = \frac{4\pi L_{max}}{\lambda} - \pi \qquad \text{(II. F. 2. 12)}$$

The measured values of L_{max} and s may also be used directly for the evaluation of ε' and ε'' from equ. II. F. 1. 24. In this equation only x_o must be replaced by L_{max}, which is the sum of the length of the cell connector and the length, l_{max}, of the measuring line between the reference plane and the first maximum:

$$x_o = L_{max} = l_{max} + \Delta$$

The accuracy of the measurements in this frequency range depends on various factors. Due to a lack of reliable comparative results, the final accuracy of the methods must be estimated from the consistency of the results, both in the frequency range covered and in connection with the results on the same materials in other frequency ranges. The accuracy of the ε' values for low loss samples only depends on the accuracy of the x_o determinations (equ. II. F. 2. 8). With the choice of appropriate cell lengths and a possible error of $\pm$ 0.01 cm in x_o, the error in the permittivity values is about 0. 5%. The accuracy of the ε'' values (equ. II. F. 2. 9), is dependent on the loss of the sample, the inherent losses of the coaxial system and the accuracy of the measurement of the half-power points. With an error of 1% in the relative power measurements, the errors in the ε'' values cannot be lower than about 1.5%. For very low losses the errors will rapidly increase owing to the smallest increments in Δx that can be accurately determined, in connection with the inherent losses of the system. Thus the errors in ε'' must be estimated in each case, in relation to the measured Δx-values.

For $\varepsilon''/\varepsilon'$ values > 0.1 the real and imaginary parts of the complex permittivity must be evaluated from equation II. F. 1. 24. The accuracy of the results is not only determined by the errors

in the measurements of x_o and s, but also by the errors arising from the interpolation in the charts for the solution of the hyperbolic functions. Since it is hardly possible to calculate the final accuracy from the various sources of error, owing to the many steps involved in the evaluation of the ε' and ε'' values, the final accuracy can best be estimated from the consistency of the results and comparison with results obtained at other frequencies. From the various measurements available, the errors in ε' were found to be lower than 1% in all cases, whereas the errors in ε'' increased from about $1\frac{1}{2}$% for $\varepsilon'' > 0.35$ to about 3% for $\varepsilon'' < 0.2$.

II. F. 3. Description of the resonance methods

The resonance method used in the frequency range from 1700 - 5000 Mc/s has been described in the foregoing section in connection with the standing wave method. In the frequency range from 300 - 1000 Mc/s fixed length cavities are used. A small probe protrudes through the wall of the cavity at a distance of $\frac{2n+1}{4}\lambda$ from the short circuiting flange with the coupling-loop. The sample to be investigated is filled into the cavity till resonance is established, after which the thickness of the liquid sample is measured with a kathetometer. On account of the location of the probe the measured voltage is directly proportional to the losses in the sample in the case of low losses. By measuring the difference of the resonant voltages for the sample and for a loss free sample of roughly the same permittivity, the loss tangent of the sample may be evaluated again with equ. II. F. 2. 9 using the relation:

$$\Delta x = \left[\frac{(E_{res})_o}{(E_{res})_s} - 1\right] \Delta x_o$$

which follows from an approximation of equ. II.F.2.1 for $\frac{\pi \Delta x}{\lambda} < 0.1$. The value of Δx_o for a lossfree sample is determined from a separate calibration. The values of the real part of the permittivity are evaluated from equ. II. F. 2. 8. These resonators are mainly used for preliminary measurements to determine the appropriate frequency range for the determination of dipole moments with equ. I. 12, from the onset of the relaxation curve. The errors in the ε' values are about 1%, whereas the errors in the ε'' values vary from 2 to 5%, depending on the various factors mentioned in section II. F. 2. 2.

Chapter III

DIELECTRIC MEASUREMENTS ON LIQUIDS

Dielectric measurements at various frequencies were carried out on chlorobenzene (solved in benzene and undiluted), bromobenzene (undiluted) and benzophenone (solved in benzene).

Chlorobenzene, bromobenzene and benzene (all compounds Merck-Darmstadt p. a. grade) were purified by distillation through a column filled with glass-rings, after drying over phosphorus-pentoxide for several days. This column is surrounded by a vacuum mantle and a small air-cooler is used on top to obtain a larger reflux-ratio. The distillations were carried out with a reflux-ratio of about twenty to one. The samples were kept over phosphorus-pentoxide. Shortly before the measurements the samples to be used were redistilled.

Benzophenone (Merck-Darmstadt, m. p. 48) was purified by vacuum-distillation, after which the solutions in benzene, required for the measurements, were prepared without delay. The purity of the benzene sample was checked by means of gas-liquid chromatography. Only minor traces of impurities, probably aliphatic hydrocarbons, could be detected. The purity of the other samples was checked by the measurement of their boiling- or melting-points, densities and refractive indices, which were found to be in close agreement with the standard values.

From the dielectric measurements on these samples permanent dipole moments were evaluated with methods starting both from low-frequency and high-frequency data. Furthermore the relaxation time at 22° centigrade was calculated, both for the diluted solutions and the undiluted polar liquids. The measurements confirmed the known fact [123, 124, 122], that the dielectric behaviour at room temperature of the compounds and solutions under investigation, can be described in terms of one relaxation time only.

III. 1. Measurements on C_6H_5Cl

For the determination of the permanent dipole moment of C_6H_5Cl from measurements on dilute solutions in benzene, ten different concentrations were used, the molar fraction x ranging from 0.005 to 0.03.

For these solutions the low-frequency permittivity, the density d and the refractive index for the sodium-D line, n_D, were measured at three temperatures (25, 35 and 45° centigrade).

For the density measurements Aubry pyknometers with a volume of ca. 10 c.c. were used, as described by Scholte [114]. The measurements of the refractive index were carried out with a Bausch and Lomb precision Abbe-refractometer. The results of these measurements are given in the tables III.1.1, III.1.2 and III.1.3.

Table III.1.1. Solutions of C_6H_5Cl in C_6H_6, T = 298°K

Sample	x	ε_s	d_4	n_D
C_6H_6	0	2.2746	0.87324	1.49790
1	0.004852	2.2918	0.87452	1.49798
2	0.008338	2.3040	0.87543	1.49803
3	0.011070	2.3136	0.87610	1.49803
4	0.011974	2.3168	0.87636	1.49808
5	0.015052	2.3272	0.87718	1.49817
6	0.017614	2.3364	0.87785	1.49832
7	0.020933	2.3489	0.87868	1.49836
8	0.021803	2.3515	0.87891	1.49841
9	0.024736	2.3625	0.87970	1.49850
10	0.028111	2.3743	0.88052	1.49856
C_6H_5Cl	1	5.625	1.1011	1.52159

Table III.1.2. Solutions of C_6H_5Cl in C_6H_6, T = 308°K

Sample	x	ε_s	d_4	n_D
C_6H_6	0	2.2552	0.86260	1.49169
1	0.004852	2.2719	0.86384	1.49177
2	0.008338	2.2839	0.86472	1.49189
3	0.011070	2.2925	0.86540	1.49199
4	0.011974	2.2971	0.86564	1.49199
5	0.015052	2.3058	0.86646	1.49224
6	0.017614	2.3148	0.86713	1.49229
7	0.020933	2.3263	0.86804	1.49238
8	0.021803	2.3274	0.86823	1.49249
9	0.024736	2.3394	0.86900	1.49258
10	0.028111	2.3508	0.86987	1.49268
C_6H_5Cl	1	5.467	1.09034	1.51686

Table III. 1. 3. Solutions of C_6H_5Cl in C_6H_6, T = 318°K

Sample	x	ε_s	d_4	n_D
C_6H_6	0	2.2369	0.85196	1.4857
1	0.004852	2.2529	0.85315	1.4860
2	0.008338	2.2642	0.85414	1.4861
3	0.011070	2.2735	0.85478	1.4861
4	0.011974	2.2760	0.85501	1.4864
5	0.015052	2.2851	0.85591	1.4861
6	0.017614	2.2927	0.85652	1.4863
7	0.020933	2.3039	0.85732	1.4866
8	0.021803	2.3065	0.86758	1.4865
9	0.024736	2.3166	0.85827	1.4867
10	0.028111	2.3279	0.85914	1.4868
C_6H_5Cl	1	5.316	1.07932	1.5119

Three different methods for the calculation of the dipole moments from these data were compared:

a. The method of Halverstadt and Kumler [30] is based on the original Debye equation. In this method the dipole moment is evaluated with the equation:

$$\mu = 0.01281 \sqrt{({}_0P_2 - R_D)\,T}, \qquad \text{(III. 1. 1)}$$

where $${}_0P_2 = \frac{\varepsilon_0-1}{\varepsilon_0+2}\left\{M_2\frac{1}{d_0} + M_1\left(\frac{d\left(\frac{1}{d}\right)}{dx}\right)_0\right\} + 3\,\frac{1}{d_0}\,M_1\frac{\left(\frac{d\varepsilon}{dx_2}\right)_0}{(\varepsilon_0+2)^2}$$

and $R_D = \dfrac{n_D^2-1}{n_D^2+2}\,\dfrac{M}{d}$, refers to the pure polar compound.

The suffices 1 and 2 refer to solvent and solute respectively and the suffix 0 refers to the extrapolated values of the quantities for infinite dilution. It must be mentioned here that no discrepancy was found between the value of ε_0, as extrapolated from the solutions and the value of ε_0 measured for the pure solvent, in contradiction with the results of Halverstadt and Kumler, Kwestroo [114] and Cohen-Fernandes [115].

b. The method of Böttcher and Scholte [116] is based on the Onsager-Böttcher equation. In differential form the equation may be written:

$$p = \frac{(\varepsilon_0-1)(2\varepsilon_0+1)}{12\pi\varepsilon_0 N_A}\,\frac{M_0}{d_0}\left[\frac{M_1}{M_0} + \frac{2\,\varepsilon^2{}_0+1}{\varepsilon_0(\varepsilon_0-1)(2\,\varepsilon_0+1)}\left(\frac{d\,\varepsilon}{dx}\right)_0 - \frac{1}{d_0}\left(\frac{dd}{dx}\right)_0\right] \qquad \text{(III. 1. 2)}$$

$$p = \frac{\alpha_1}{1-f_1\alpha_1} + \frac{\mu^2}{3kT(1-f_1\alpha_1)^2},$$

where $f_1 = \frac{1}{r_1^3} \frac{2\varepsilon_0-2}{2\varepsilon_0+1}$ and the suffices 0 and 1 refer to solvent and solute respectively. Furthermore the values of α_1 and r obtained by Scholte from measurements on the pure polar compound were used:

$$r = 3.24 \text{ Å} \quad \alpha_1 = 12.7 \text{ Å}^3.$$

c. The third method was introduced by Scholte [116, 135], starting from equation III. 1. 2. Here the shape of the molecule and the anisotropy of the polarisability in different directions is taken into account:

$$p = \frac{\alpha_1}{1-f_1\alpha_1} + \frac{2\varepsilon_0+1}{3\{\varepsilon_0+(1-\varepsilon_0)A_\mu\}} \frac{\mu^2}{3kT(1-f_\mu\alpha_\mu)^2}, \qquad \text{(III. 1. 3)}$$

where $$f_\mu = \frac{1}{r^3} \frac{3A_\mu(1-A_\mu)(\varepsilon_0-1)}{\varepsilon_0+(1-\varepsilon_0)A_\mu}.$$

The following values obtained by Scholte were used:

$$A_\mu = 0.197 \qquad \alpha_i = 12.7 \text{ Å}^3$$
$$r = 3.24 \text{ Å} \qquad \alpha_\mu = 14.3 \text{ Å}^3$$

The results of the calculations are given in table III. 1. 4.

Table III. 1. 4. Dipole moment of C_6H_5Cl in Debye units from measurements on dilute solutions

Calc. with equ.	T(°K) 298	308	318
III. 1. 1	1.58^7	1.58^9	1.58^9
III. 1. 2	1.57^7	1.57^5	1.57^1
III. 1. 3	1.74^1	1.73^6	1.73^0

The values of the dipole moment, as obtained with equ. III.1.1 and III.1.2 appear to be constant and reproducable to a few units in the third decimal place; they are considerably lower, however, than the values obtained from measurements in the vapour state.

Hurdis and Smyth	1942 [117]	μ_{vapour} =	1.72
Moore and Hobbs	1949 [118]		1.70
Groves and Sugden	1934 [119]		1.69
Le Fèvre and Russell	1936 [120]		1.69
Davar	1939 [121]		1.69

The literature values given for dilute solutions and undiluted C_6H_5Cl are considerably lower than the values obtained for the vapour (see table III. 1. 8). This fact was confirmed by the results given in table III. 1. 4.

Moreover the dipole moment of C_6H_5Cl was determined from measurements of the loss factor of solutions of C_6H_5Cl in benzene at high frequencies. For these measurements the coaxial system described in section II. F. 2. 2 was used at 3000 and 5000 Mc/s. The equations II. F. 2. 8 and II. F. 2. 9 were used for the evaluation of ε' and ε'' from the measured quantities. From these data the value of the dipole moment may be calculated, using equ. I. 12. In this equation the difference between ε_s and ε_∞ is neglected and both ε_s and ε_∞ are taken equal to ε_0, the permittivity of the solvent. Equ. I. 12 is derived from the equation:

$$\frac{3\varepsilon''}{(\varepsilon_s+2)(\varepsilon_\infty+2)} = \frac{4}{3}\pi N \frac{\mu^2}{3kT} \frac{\omega\tau}{1+\omega^2\tau^2}$$

Since the difference between ε_0 of the solvent and ε_∞ of the solutions is very small, a better approximation is obtained by changing equ. I. 12 to:

$$\varepsilon'' = (\varepsilon_s+2)(\varepsilon_0+2)\frac{4\pi N\mu^2}{27\,kT}\frac{\omega\tau}{1+\omega^2\tau^2}, \qquad \text{(III. 1. 4)}$$

where ε_s is the low frequency permittivity of the solution and N is the number of polar particles per unit volume. The results of the measurements are given in table III. 1. 5.

Table III. 1. 5. High frequency measurements on solutions of C_6H_5Cl in C_6H_6.
$T = 296^0K$. $\varepsilon_0 = 2.28$.

Frequ.	meas.	Solution I	II	III
	x	0.01009	0.01992	0.03958
	ε_s	2.3172	2.3519	2.4202
3000 Mc/s	ε'	2.321	2.348	2.417
	ε''	0.0044	0.0108	0.0202
5000 Mc/s	ε'	2.312	2.343	2.399
	ε''	0.0088	0.0160	0.0322

By plotting ε'' vs. x linear plots are obtained for each frequency as shown in fig. III.1.I. In drawing the lines, the decrease of the accuracy of ε'' for values of $\varepsilon'' < 0.01$, owing to the inherent losses of the measuring system must be taken into account. From the ratio of the ε'' values for the two frequencies at a given concentration, an approximate value of the relaxation time may be evaluated. Since both frequencies are well below the relaxation frequency, an accurate evaluation of τ from the ratio of the two values of $\omega\tau/1+\omega^2\tau^2$ is impossible. The approximate value obtained, $\tau = (7.5 \pm 0.3) \times 10^{-12}$, is in agreement with the value of 7.5×10^{-12} by Whiffen and Thompson [122]. By introducing this value of τ and the measured values of ε_s and ε'', into equation

III. 1. 4, the following values of the dipole moment are calculated:

3000 Mc/s $\mu = 1.60^2$ D.
5000 Mc/s $\mu = 1.58^5$ D.

These results are in good agreement with the values obtained from the low frequency measurements.

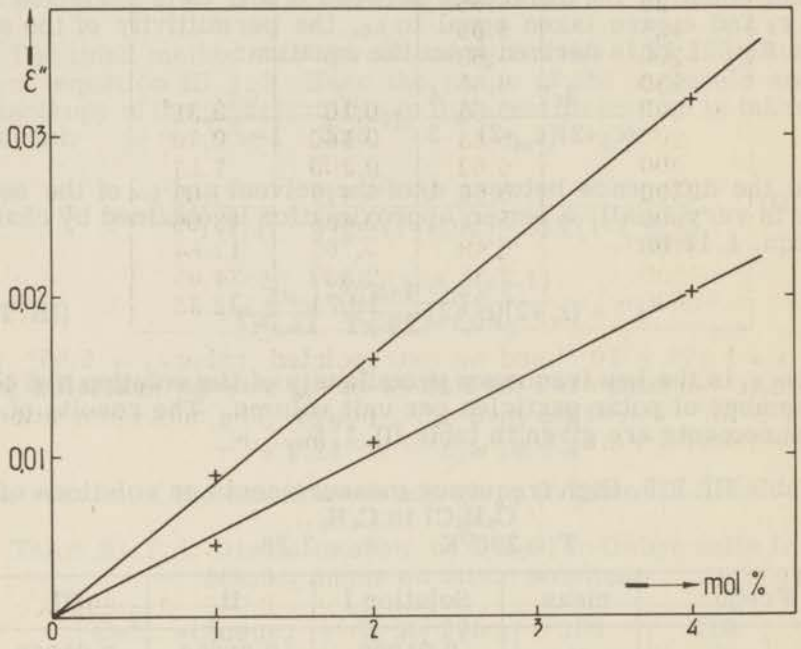

Fig. III.1.I. Loss-factor of solutions of C_6H_5Cl in C_6H_6 at 3000 and 5000 Mc/s

From measurements on the undiluted polar liquid both the dipole moment and the relaxation time of chlorobenzene were evaluated. The results of the measurements at various frequencies are given in Table III. 1. 6.
From these data, and those obtained by Bos at 10 000 Mc/s, the relaxation time was evaluated using the linear Cole-plot (equ. I. 5):

$$\varepsilon' = -\omega\varepsilon'' \tau + \varepsilon_s .$$

The resulting value $\tau = 1.17^3 \times 10^{-11}$ at 295°K, is slightly different from the values obtained by Poley [123] and Smyth [124]:

C_6H_5Cl,	Smyth	T = 298°K	$\tau = 1.03 \times 10^{-11}$
	Poley	295°K	$\tau = 1.18$
	Own meas.	295°K	$\tau = 1.17^3$

Table III. 1. 6. Measurements on C_6H_5Cl, liquid, T = 295°K.

Frequ. Mc/s	ε'	ε''	$\omega\varepsilon'' \times 10^{-9}$
0.1	5.671		
10	5.66		
20	5.68		
25	5.65		
125	5.65		
200	5.68		
250	5.65		
500	5.65	0.10	0.31^4
700	5.63	0.160	0.70^6
900	5.62	0.200	1.13^4
2000	5.56	0.449	5.65^7
3000	5.49	0.688	13.06
3700	5.48	0.765	17.84
4500	5.35	0.865	24.45
5000	5.27	1.024	32.33

With $\tau = 1.173 \times 10^{-11}$ and an extrapolated value $\varepsilon_s = 5.65^5$ for the static permittivity, the values of ε_∞ may be evaluated with equ. I. 3 for each of the measured points. The maximum value of ε'' is obtained from ε_s and ε_∞ with the equation:

$$(\varepsilon'')_{max} = \frac{\varepsilon_s - \varepsilon_\infty}{2}$$

The resulting values are:

$$\varepsilon_s = 5.655 \pm 0.005$$
$$\varepsilon_\infty = 2.475 \pm 0.005 \quad T = 295^oK$$
$$(\varepsilon'')_{max} = 1.59 \pm 0.005$$

A semicircular Cole-Cole plot based on these values fits all the measured points within the measuring accuracy, as shown in fig. III. 1. II. From these data the dipole moment of chlorobenzene in the pure dipole liquid may be calculated with the Debye-equation I. 8 or the Onsager-Böttcher-equation I. 9, by inserting ε_∞ instead of n^2_∞. The values of the dipole moment, thus obtained, are considerably lower than the values obtained from measurements on dilute solutions. If, as suggested by Böttcher [20], n^2_D is used instead of n^2_∞ or ε_∞, the calculated values are somewhat higher, but still lower than those obtained from measurements on dilute solutions. The values calculated from our measurements are given in table III. 1. 7.

From this table it follows that the values of permanent dipole moments obtained from measurements on the pure liquid differ considerably from those obtained from measurements on dilute solutions, in particular if in equation I. 8 and I. 9 ε_∞ is not replaced by n^2_D. Some values of the dipole moment of C_6H_5Cl obtained by other authors are given in table III. 1. 8.

Table III. 1. 7. Dipole moment of C_6H_5Cl

measurements on:				
	dilute solutions		pure liquid	
calc. with	Debye	Onsager-Böttcher	Onsager-Böttcher	Debye
n_D^2	1.58[7]	1.57[7]	1.46	1.22
ε_∞			1.38	1.17
ε''	1.59			

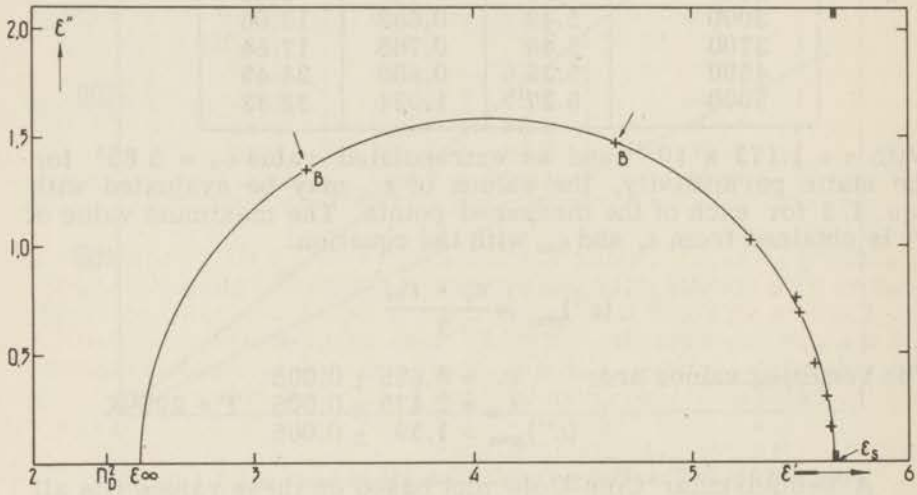

Fig. III.1.II. Semicircular Cole-Cole plot for C_6H_5Cl, T = 295°K.

Table III. 1. 8. Literature values of the dipole moment of C_6H_5Cl

author		dilute solutions	pure liquid
Smyth-Morgan [126]	1927		1.52
Smyth [125]	1928	1.61	1.22
Le Fèvre-Russell [120]	1936	1.59	
Müller-Sack [127]	1930	1.57	
Fischer [128]	1939	1.56	
Ketelaar [129]	1940	1.54	
Davis [130]	1943	1.53	
Spinrad [131]	1946	1.60	
Littlejohn [149]	1953	1.58	

III. 2. Measurements on C_6H_5Br

The permanent dipole moment and the relaxation time of bromobenzene were determined from measurements on the undiluted polar liquid. The results of the measurements at various frequencies are given in table III. 1. 9.

Table III. 1. 9. Measurements on C_6H_5Br, liquid, T = 295°K

Frequ. Mc/s	ε'	ε''	$\omega\varepsilon'' \times 10^{-9}$
0.1	5.419		
10	5.42		
25	5.40		
125	5.42		
200	5.41		
400	5.35	0.119	0.299
600	5.37	0.191	0.720
800	5.36	0.246	1.24
900	5.35	0.267	1.51
1000	5.34	0.307	1.93
3000	5.13	0.967	18.35
5000	4.74	1.16	36.6

By plotting ε' vs. $\omega\varepsilon''$, using the data given in table III. 1. 9 in combination with results obtained by Bos [44] at 10 000 Mc/s ($\varepsilon' = 3.98$, $\varepsilon'' = 1.43$), a straight line is obtained (linear Cole-plot, equ. I. 5) with a slope $-\tau$, equal to -1.74×10^{-11} and an intercept $\varepsilon_s = 5.407$. The relaxation time of C_6H_5Br, thus obtained is slightly higher than the relaxation time given by Smyth [137] and Poley [123].

Relaxation time of C_6H_5Br, undiluted:

Smyth (1952)	T = 298°K	$= 1.70 \times 10^{-11}$
Poley (1955)	295	1.72
own meas.	295	1.74

With this value of the relaxation time, the values of ε_∞ and $(\varepsilon'')_{max}$ were calculated from the ε' values at various frequencies:

Bromobenzene: $\varepsilon_\infty = 2.59 \pm 0.02$

$\varepsilon_s = 5.407$ T = 295°K

$(\varepsilon'')_{max} = 1.41 \pm 0.01$

A semicircular Cole-Cole plot based on these values corresponds with all measured points within the measuring accuracy. The permanent dipole moment of C_6H_5Br was evaluated from the values of ε_s, ε_∞ and n_D^2 in the same way, as described for C_6H_5Cl. The resultant values of the dipole moment are given in table III. 1. 10, together with the values obtained by other authors.

Table III. 1. 10. Dipole moment of C_6H_5Br, T ~ 295°K

a. own meas.	Measurements on: pure liquid		solutions in C_6H_6	vapour
calc. with	n_D^2	ε_∞		
equ. I. 8	1.18	1.13		
equ. I. 9	1.37^5	1.30		
b. litt. values				
Das-Roy [139]	1.41		1.53	
Williams [140]			1.51	
Bergmann [141]			1.49	
Müller [127]			1.52	
Daily [142]			1.70	
Tiganik [143]			1.53	
Le Fèvre [144]			1.55	
Otto [145]			1.55	
Trautteur [146]			1.48	
Littlejohn [149]			1.56	
Höjendahl [147]				1.56
Groves [148]				1.71
Hurdis [117]				1.77 (460°K)

III. 3. Measurements on $C_{13}H_{10}O$

The permanent dipole moment of benzophenone was determined both from low-frequency and high-frequency measurements on dilute solutions, in the same way as described for chlorobenzene.

The results of the low-frequency measurements are given in table III. 1. 11.

Table III. 1. 11. Solutions of $C_{13}H_{10}O$ in C_6H_6, T = 298°K

sample	x	ε_s	d_4	n_D^2
0	0	2.2781	0.84305	2.24251
1	0.00953	2.4094	0.87715	2.24857
2	0.02032	2.5514	0.88197	2.25540
3	0.02933	2.6712	0.88613	2.26117
4	0.04034	2.8222	0.89083	2.26819

From these results the value of the dipole moment of benzophenone was evaluated with the method of Halverstadt and Kumler:

$$\mu = 2.978 \pm 0.003$$

The high-frequency measurements were carried out at frequencies of 3000 and 5000 Mc/s. The results are given in table III.1.12.

Since deviations from the linear increase of ε'' occurred at molar fractions above 0.03, which was also noticed for ε_s in the low-frequency measurements, only the samples 1, 2 and 3 were used.

Table III.1.12. High frequency measurements on solutions of $C_{13}H_{10}O$ in C_6H_6

$T = 296^oK$ $\varepsilon_0 = 2.28$				
Frequ.	meas.	solution 1	2	3
	x	0.00953	0.02032	0.02933
	ε_s	2.4094	2.5514	2.6712
3000 Mc/s	ε'	2.402	2.506	2.606
	ε''	0.045	0.0928	0.138
5000 Mc/s	ε'	2.365	2.458	2.540
	ε''	0.057	0.123	0.180

Linear plots of ε'' vs. x are obtained from these results. From the ratio of the ε'' values for the two frequencies at a given value of x, the value of the relaxation time may be evaluated. Since the relaxation time of benzophenone is much larger than that of C_6H_5Cl, a more accurate evaluation is possible in this case. The value obtained from our measurements is in good agreement with that determined by Whiffen and Thompson:

Whiffen and Thompson [122] $T = 294^oK$ $\tau = 2.2 \times 10^{-11}$
Jackson and Powles [132] $T = 292^oK$ $\tau = 1.64 \times 10^{-11}$
own meas. $T = 296^oK$ $\tau = 2.2 \times 10^{-11}$

By introducing this value of τ and the measured value of ε_s in equ. III.1.4 the dipole moments were calculated both from the individual values of ε'' for the three samples and from the values of ε'' read from the best line through the three measured points. The resultant values of the dipole moment are given in table III.1.13. Some values obtained by other authors are given in table III.1.14.

Table III.1.13. Dipole moment of $C_{13}H_{10}O$ in C_6H_6 obtained from high-frequency measurements

sample	5000 Mc/s		3000 Mc/s	
	point	line	point	line
1	2.98	3.01	3.04	3.00
2	2.94	2.97	2.96	2.99
3	2.96	2.96	2.97	2.98
medium value	2.96	2.98	2.99	2.99
low frequency value 2.978.				

Table III. 1. 14. Literature values of the dipole moment of $C_{13}H_{10}O$, solved in benzene

author	
Estermann [133] (1928)	μ = 2.50
Donle [134] (1930)	2.95 ± 0.03
Fuchs-Donle [135] (1933)	3.00 ± 0.02
Granier [136] (1946)	2.95

For the accurate determination of relaxation times the frequency range from 50 c/s to 5000 Mc/s is insufficient in many cases and additional data at higher frequencies, e.g. up to 30 000 Mc/s, are of paramount importance.

SAMENVATTING

In dit proefschrift wordt een overzicht gegeven van een onderzoek betreffende de experimentele bepaling van de diëlectrische eigenschappen van vloeistoffen in afhankelijkheid van de frequentie van een uitwendig electrisch veld.

Dit onderzoek was in de eerste plaats gericht op het samenstellen van meetapparatuur, geschikt voor nauwkeurige diëlectrische metingen in een continu frequentiegebied van 50 Hertz tot 5000 MegaHertz. Daar alle bekende meetmethoden slechts in een deel van dit frequentiegebied bruikbaar zijn, werd de keuze der apparatuur als volgt bepaald:

Een gewijzigde Schering-brug voor frequenties van 50 Hz tot 350 kHz.

Een apparaat volgens de heterodyne-methode voor zeer nauwkeurige metingen bij frequenties van 1 tot 2,5 MHz.

Apparatuur gebaseerd op de resonantie-methode voor frequenties van 0,5 tot 10 MHz.

Een „Twin-T" meetbrug voor frequenties van 0,5 tot 25 MHz.

Een hoogfrequent meetbrug voor frequenties van 5 tot 250 MHz.

Resonantie apparatuur voor metingen aan stoffen met geringe verliezen bij frequenties van 300 tot 5000 MHz.

Apparatuur volgens de staande-golf methode, met coaxiale golfgeleiders, voor frequenties tussen 300 en 5000 MHz.

Bijzondere aandacht werd besteed aan de constructie en de ijking der benodigde meetcellen. Een aantal metingen werd verricht aan zuivere polaire vloeistoffen en verdunde oplossingen van deze stoffen in een niet-polair oplosmiddel, teneinde een indruk te geven van de met de genoemde apparatuur te bereiken resultaten.

In het eerste hoofdstuk wordt een samenvatting gegeven van de gebruikelijke formules voor de beschrijving van het diëlectrische gedrag van vloeistoffen, terwijl tevens de betrekkingen worden afgeleid tussen de macroscopische materiaalgrootheden en de uit metingen te verkrijgen gegevens. Na een kort overzicht van de historische ontwikkeling der meetmethoden, worden de eisen besproken, welke aan meetapparaten voor het diëlectrische onderzoek in de verschillende frequentiegebieden dienen te worden gesteld.

In het tweede hoofdstuk worden de, voor het frequentiegebied van 50 Hertz tot 5000 MegaHertz, ontwikkelde apparaten en meetmethoden beschreven. Hierbij wordt tevens een overzicht gegeven van de metingen welke werden verricht in verband met de keuze van de ijkvloeistoffen, de ijking van de apparaten en meetcellen en de bepaling van de uiteindelijk bereikte nauwkeurigheid der metingen.

In het derde hoofdstuk worden de met de beschreven apparatuur uitgevoerde metingen aan chloorbenzeen (onverdund en in verdunde oplossing), broombenzeen (onverdund) en benzophenon (in verdunde oplossing) behandeld.

REFERENCES

1. J. Schrama, Thesis Leyden September 1957.
2. J. C. Maxwell, El. and Magn. I. Berlin 1883.
3. G. R. Kirchhoff, Ges. Abh. Leipzig 1882, S. 112.
4. Fl. Ratz, Z. Phys. Chemie 19. 94. 1896.
5. E. Cohen, L. Arons, Wied. Ann. 28. 454. 1886
   33. 23. 1888.
6. Ch. B. Thwing, Z. Phys. Chem. 14. 286. 1894.
7. W. Nernst, Z. Phys. Chem. 14. 622. 1894.
8. C. E. Linebarger, Z. Phys. Chem. 20. 131. 1896.
9. J. C. Philip, Z. Phys. Chem. 24. 18. 1897.
10. A. Campbell, Proc. Roy. Soc. A 78. 196. 1906.
11. R. W. Swenson and R. H. Cole, J. Chem. Phys. 22. 284. 1954.
12. P. Drude, Z. Phys. Chem. 23. 267. 1897.
13. W. Möbius, Ann. d. Physik Leipzig 62. 293. 1918.
14. L. Hartshorn, D. A. Oliver, Proc. Roy. Soc. A 123. 644. 1929.
15. P. Debye, Phys. Z. 13. 97. 1912.
16. C. P. Smyth and S. O. Morgan, J. Am. Chem. Soc. 49. 1030. 1927.
17. J. Errera, Physik. Z. 27. 764. 1926
    29. 609. 1928.
18. L. E. Sutton, Proc. Roy. Soc. A 135. 668. 1931.
19. L. Hartshorn, W. H. Ward, J. Inst. elect. Engrs. 79. 597. 1936.
20. C. J. F. Böttcher, Theory of electric polarisation, Elsevier Publ. Comp. 1952.
21. A. R. von Hippel, Dielectrics and waves. John Wiley, New York 1954.
22. H. Fröhlich, Theory of dielectrics, Oxford 1949.
23. K. S. Cole and R. H. Cole, J. Chem. Phys. 9. 341. 1941.
24. R. H. Cole, J. Chem. Phys. 23. 492. 1955.
25. R. M. Fuoss and J. G. Kirkwood, J. Am. Chem. Soc. 63. 385. (1941).
26. L. C. v. d. Marel, J. van den Broek and C. J. Gorter, Physica 23. 361. 1957.
27. D. W. Davidson and R. H. Cole, J. Chem. Phys. 18. 1417. 1950.
28. G. Hedestrand, Z. Physik. Chemie B. 2. 428. 1929.
29. P. Cohen Henriquez, Thesis Delft 1935.
30. I. F. Halverstadt and W. D. Kumler, J. Am. Chem. Soc. 64. 2988 1942.
31. E. A. Guggenheim, Trans. Farad. Soc. 47. 573. 1951.
32. F. Kohlrausch, Praktische Physik Band II Rosenberg, New York 1947.
33. W. Jackson and J. G. Powles, Trans. Farad. Soc. 42A. 101. 1946.
34. W. Kwestroo, Thesis Leiden 1954.

35. J.W. Smith, Electric dipole moments, Butterworths 1955.
36. J.S. Dryden and R.J. Meakins, Rev. of pure and appl. Chem. 7. 15. 1957.
37. P. Debye, Physik. Z. 35. 101. 1934.
38. F.C. de Vos, Rec. Trav. Chim. 69. 1157. 1950.
39. Th. G. Scholte and F.C. de Vos, Rec. Trav. Chim. 72. 625. 1953.
40. K. Slevogt, Dechema Hauptversammlung, 11. 7. 1950.
41. K. Slevogt u. P. Dörffel, Tabak Zeitung 66. Jahrg. 15. 1956.
42. P. Duvernoy, Brauwelt Heft 20. 1952.
43. W. Deeg u. O. Huber, Berichte der dt. Keram. Ges. 32. Heft 9. 261. 1955.
44. F.F. Bos, Thesis Leiden to be published.
45. K.S. Cole and R.H. Cole, J. Chem. Phys. 10. 98. 1942.
46. D.W. Davidson, R.P. Auty and R.H. Cole, Rev. Sci. Instr. 22. 678. 1951.
47. G. Mole, Symp. Precision Electr. Meas. 1954. Nat. Phys. Lab. 1955.
48. H. Schering, Zeits. f. Inst. Vol. 40. 124. 1920.
49. B. Hague, A.C. bridge methods, Pitman London 1946.
50. W.N. Tuttle, Proc. I.R.E. 28. 23. 1940.
51. R.H. Cole and P.M. Gross, Rev. Sci. Instr. 20. 252. 1949.
52. H.A.M. Clark and P.B. Vanderlyn, Proc. I.E.E. 96 III. 189. 1949.
53. J. Stranathan, Rev. Sci. Instr. 5. 334. 1934.
54. J.C. van Vessem, Thesis Utrecht 1947.
55. D. Woods, Symp. Precision Electr. Meas. 1954. Nat. Phys. Lab. 1955.
56. J.V.L. Parry, Proc. I.E.E. 98 III. 303. 1951.
57. A. Lebrun, Thèses Lille 1953.
58. R. Eichacker, Rohde und Schwarz Mitt. no. 4. 250. 1953.
59. O. Huber, Z.f. Angew. Physik VI. 9. 1954.
60. T.J. Buchanan, I.E.E. Monograph 49. 1952.
61. T.J. Buchanan and E.H. Grant, Brit. J. Appl. Phys. 6. 64. 1955.
62. F.E. Terman and J.M. Pettit, Electronic Measurements MacGrawHill 1952.
63. L. Hartshorn, Proc. Phys. Soc. B. LXVIII. 422. 1955.
64. J. Timmermans, Physico Chem. Constants of Pure organic compounds, Elsevier 1950.
65. H.R. Reich, Theory and application of electrontubes, MacGraw-Hill 1944.
66. S. Seely, Electronic Engineering, MacGrawHill 1956.
67. M. Gevers, Philips Res. reports 1. 361. 1946.
68. J.K. Clapp, Proc. I.R.E. 42. 1295. 1954.
69. J.M. Schulman, Electronics 29. no. 9. 230. 1956.
70. J. Mc. Sowerby, Wireless World 1949 no. 9. p. 346.
71. K.C. Johnson, Wireless World 1948 no. 3. p. 82.
72. Howard Booth, Wireless World 1949 no. 3. p. 111.
73. H.J. Lindenhovius en H. Rinia, Phil. Techn. Tijdschr. 6. 54. 1941.

74. M. G. Scroggie, Wireless World 1948 p. 373. 415. 453.
75. M. Pestemer, Angew. Chem. 63. 118. 1951.
76. R. Mecke und K. Rosswog, Zeits. für Elektrochem. 60. 47. 1956.
77. L. Hartshorn, Radiofrequency measurements by bridge- and resonance methods, Chapman and Hall 1940.
78. L. G. Groves and S. Sugden, J. Chem. Soc. 1934 II. p. 1094.
79. M. Claude Abgrall, Compt. Rend. Aca. Sci. 237. 1650. 1953.
80. J. Wyman, Phys. Rev. 35. 326. 1930.
81. A. J. Lyon, Wireless Engineer 32. 107. 1955.
82. O. Zinke, Hochfrequenz messtechnik, Hirzel Zürich 1946.
83. R. F. Field and O. B. Sinclair, Proc. I. R. E. 24. 255. 1936.
84. D. B. Sinclair, Proc. I. R. E. 28. 311. 1940.
85. O. Zinke, l. c. p. 62. 77.
86. E. G. Spreadbury, Electronic measurements and measuring instruments, Constable London 1954.
87. Vacuum tube amplifiers, M. I. T. Radiation lab. Series no. 18 Sec. 11. 7. MacGrawHill 1948.
88. F. Langford-Smith. Radiotron designer's handbook R. C. A. 1954.
89. J. C. Slater, Microwave Transmission, McGrawHill 1942.
90. A. B. Bronwell and R. E. Beam, Theory and application of microwaves, McGrawHill 1947.
91. L. G. H. Huxley, Wave guides, Cambridge Univ. Press 1947.
92. H. H. Meinke und F. W. Gundlach, Taschenbuch der Hochfrequenztechniek Springer-Verlag 1956.
93. S. Roberts and A. R. von Hippel, J. Appl. Phys. 17. 610 1946.
94. F. Horner e. a. J. I. E. E. 93. III. 53. 1946.
95. E. H. Grant, Thesis Univ. of London 1956.
96. S. Roberts and A. R. von Hippel, Phys. Rev. 57. 1056. 1940.
97. J. Benoit, Ann. Telecomm. 4. 27. 1949.
98. J. Ph. Poley, Appl. Sci. Res. 4 B. 173 1954.
99. F. J. Cripwell and G. B. B. M. Sutherland, Trans. Farad. Soc. 42A. 149. 1946.
100. K. V. Gopala Krishna, Trans. Farad. Soc. 52. 110. 1956.
101. F. F. Bos, private communication, to be published.
102. O. Huber, Naturwissenschaften 38. 181. 1951.
103. G. Untermann, Z. angew. Phys. 2. 233. 1950.
104. C. N. Works, T. W. Dakin, F. W. Boggs, Proc. I. R. E. 33. 245 1945. Trans. Am. I. E. E. 63. 1092. 1948.
105. S. J. Reynolds, Gen. El. Rev. 50. 34. 1947.
106. C. N. Works, J. Appl. Phys. 18. 605. 1947.
107. D. L. Hollway and G. J. A. Cassidy, Proc. I. E. E. 99. III. 364 1952.
108. S. A. Schelkunoff, Electromagnetic waves, v. Nostrand Comp. 1947.
109. T. J. Buchanan, Proc. I. E. E. 99 III. 61. 1952.
110. G. H. Haggis, Thesis Univ. of London 1951.
111. A. Weissfloch, Schaltungstheorie und Mesztechnik des dm. - und cm. -wellengebietes, Birkhäuser Bazel 1954.
112. M. Wind and H. Rapaport, Handbook of microwave measurements, Distr. : Interscience Publ. 1955.

113. T.W.Dakin and C.N.Works, J.Appl.Phys. 18. 789. 1947.
114. W.Kwestroo, Thesis Leiden 1954.
115. P.Cohen-Fernandes, Thesis Leiden 1957.
116. Th.G.Scholte, Thesis Leiden 1950.
117. E.C.Hurdis and C.P.Smyth, J.Am.Chem.Soc. 64. 2212. 1942.
118. E.M.Moore and M.E.Hobbs, J.Am.Chem.Soc. 71. 411. 1949.
119. L.G.Groves and S.Sugden, J.Chem.Soc. p.696. 1934.
120. R.J.W.Le Fèvre and P.Russell, J.Chem.Soc. p.491.1936.
121. D.J.Davar, Current Sci. 8. 414. 1939.
122. D.H.Whiffen and H.W.Thompson, Trans.Farad.Soc. 42A. 114. 1946.
123. J.Ph.Poley, Thesis Delft 1955.
124. E.J.Hennelly, W.M.Heston and C.P.Smyth, J.Am.Chem. Soc. 70. 4102. 1948.
125. C.P.Smyth, S.O.Morgan and J.C.Boyce, J.Am.Chem.Soc. 50. 1547.1928.
126. C.P.Smyth, S.O.Morgan, J.Am.Chem.Soc. 49. 1030 1927.
127. H.Müller und H.Sack, Physik.Z. 31. 815. 1930.
128. E.Fischer, Physik.Z. 40. 331. 1939.
129. J.A.A.Ketelaar, Rec.Trav.chim. 59. 757.1940.
130. R.Davis, H.S.Bridge and W.J.Svirbely, J.Am.Chem.Soc. 65. 857.1943.
131. B.I.Spinrad, J.Am.Chem.Soc. 68. 617. 1946.
132. W.Jackson and J.G.Powles, Trans.Farad.Soc.42A.101.1946.
133. I.Estermann, Z.Physik.Chem. B.1. 134. 1928.
134. H.L.Donle und G.Volkert, Z.Physik.Chem. B.8. 60. 1930.
135. O.Fucks und H.L.Donle, Z.Physik.Chem. B.22.1.1933.
136. J.Granier, C.r.acad.Sci. 223. 893.1946.
137. F.H.Branin and C.P.Smyth, J.Chem.Phys. 20.1121.1952.
138. Th.G.Scholte, Physica XV. 437. 1949.
139. L.M.Das, S.C.Roy, Ind.J.Phys. 5. 441. 1930.
140. J.W.Williams, J.Am.Chem.Soc. 50. 2350.1928.
141. E.Bergmann e.a., Z.Phys.Chem. B10. 106. 1930.
142. C.R.Daily, Phys.Rev. 34. 548. 1929.
143. L.Tiganik, Z.Phys.Chem. B13. 425. 1931.
144. C.G.Le Fèvre, R.J.W.Le Fèvre, J.Chem.Soc. p.1130 1936.
145. M.M.Otto, H.H.Wenzke, Ind.Eng.Chem.Anal.Ed. 6. 187. 1934.
146. P.Trautteur, Nuovo cimento 14. 265. 1937.
147. K.Höjendahl, Phys.Z. 30. 391. 1929.
148. L.G.Groves, S.Sugden, J.Chem.Soc. p.971.1935.
149. A.C.Littlejohn and J.W.Smith, J.Chem.Soc. p.2456.1953.

Op verzoek van de Faculteit der Wis- en Natuurkunde volgen hier enige persoonlijke gegevens.

Na het behalen van het einddiploma Gymnasium-β in 1942, was het mij, tengevolge van de oorlogsomstandigheden, eerst in Juli 1945 mogelijk een aanvang te maken met de studie te Leiden, Het candidaatsexamen F in de faculteit der Wis- en Natuurkunde legde ik af in Juli 1947.

In Juli 1951 werd het doctoraalexamen afgelegd, met hoofdrichting physische scheikunde (Hoogleraar Dr. C. J. F. Böttcher) en bijvak experimentele natuurkunde (Hoogleraren Dr. C. J. Gorter en Dr. H. A. Kramers).

Na het vervullen van een assistentschap bij de Physische Scheikunde in de jaren 1947 en 1948, werd mij door de Nederlandse Organisatie voor Zuiver Wetenschappelijk Onderzoek gedurende drie jaren een toelage toegekend voor de voortzetting van onderzoekingen op diëlectrisch gebied aan bovengenoemde afdeling. Hierop volgde in 1952 mijn benoeming tot conservator bij de afdeling Physische Scheikunde, in de rang van wetenschappelijk ambtenaar. Sinds 1948 was ik belast met de administratie en instrumentatie van deze afdeling (na 1953 van de afgesplitste afdeling Physische Scheikunde II). Daarnaast werkte ik onder leiding van Prof. Dr. C. J. F. Böttcher aan het in dit proefschrift beschreven onderzoek.

Bij deze afsluiting van mijn studie is het mij een groot voorrecht een woord van dank te kunnen richten tot al diegenen die mij daarbij terzijde hebben gestaan. In het bijzonder wil ik mijn vader voor alles wat hij heeft gedaan om mijn opleiding mogelijk te maken, hartelijk danken.

Veel dank ben ik verschuldigd aan mijn collega's in het laboratorium en het technisch personeel, voor de medewerking die zij mij steeds zo bereidwillig hebben verleend en de prettige samenwerking, die ik met hen heb mogen hebben.

Voorts wil ik een woord van dank richten tot de Nederlandse Organisatie voor Zuiver Wetenschappelijk Onderzoek, die mij door het verlenen van toelagen niet alleen de voortzetting van het wetenschappelijk onderzoek, doch tevens een intensief contact met onderzoekers in het buitenland heeft mogelijk gemaakt.

Aan Prof. Dr. R. H. Cole (Brown University, Providence, U. S. A.), Dr. John Lamb (University of London, Imperial College) en Dr. K. Slevogt (Universität München) betuig ik mijn erkentelijkheid voor de vele waardevolle en stimulerende discussies over het onderwerp van dit proefschrift en tevens aan Dr. Geoffrey Haggis (University of Edinburgh) voor de bereidwilligheid waarmede hij hoofdstuk II taalkundig heeft gecorrigeerd.